CVEN 4511/5511: Introduction to Finite Element Analysis

by

Richard A. Regueiro
Professor
Department of Civil, Environmental, and Architectural Engineering
University of Colorado Boulder
1111 Engineering Dr.
428 UCB, ECOT 441
Boulder, CO 80309-0428

University of Colorado Boulder
Fall 2024

Contents

List of Figures

This page intentionally left blank.

Chapter 1

Introduction

1.1 Background on the Finite Element Method (FEM)

1.1.1 What is the Finite Element Method (FEM)?

Possible answers from various perspectives:

- Mathematician: variational, numerical method to solve a partial differential equation (PDE) or system of coupled PDEs (linear or nonlinear)
- Engineer: computational method to analyze various design scenarios in order to reduce wasteful prototyping and to understand potential failure scenarios
- Scientist: computational method to better understand physical processes in the observable world
- Physician: computer software to analyze various surgical and prosthetic implantation strategies in order to optimize a surgerys effectiveness

1.1.2 Why conduct Finite Element Analysis (FEA)?

Possible answers:

- To model continuous solid body problems, using plate, shell, or continuum finite elements.
- Beside solids, to solve other field problems, such as fluid flow, heat transfer, and the coupling of various field problems (e.g., solid-fluid interaction, solid-thermomechanical deformation, chemo-electrical, solid-fluid porous flow and deformation).
- To solve nonlinear problems computationally, with complex geometries, that would otherwise be impossible with analytical or other numerical methods.
- To make as few assumptions as possible with regard to boundary conditions, potential failure modes, etc.

1.1.3 Strengths and Weaknesses of FEM

Strengths:

1. Arbitrary element size, shape, and interpolation: quadrilaterals, triangles versus squares/rectangles in finite difference; linear, quadratic, or other polynomial shape function
2. Variational: reduced order of PDE and required continuity; integral formulation allows embedded discontinuities (phase transitions, cracks, shock fronts,)
3. Element-based: formulate general finite element that is then assembled for various geometries and boundary conditions
4. Lagrangian representation: resolve interface conditions (contact)

Weaknesses:

1. Arbitrary element size, shape, and interpolation: it can be difficult to mesh complex geometries
2. Lagrangian representation: it is difficult to resolve interface conditions (contact); for large deformations, need re-meshing to avoid high aspect ratio elements; not always well-suited for fluid mechanics, hence the need for Eulerian formulations, or *particle methods* like ...

1.1.4 How to conduct a Finite Element Analysis (FEA)

We will try our own, but here is the general outline:

1. Build a model:
   (a) create the geometry
   (b) add material properties and boundary conditions
   (c) create the solution type (e.g., elastostatics, heat transfer, ...)
   (d) select element type, and generate a mesh
2. Solve the problem for the "field" variable (e.g., displacement, temperature, ...):
   (a) possibly choose solution parameters
   (b) check for convergence (if solving nonlinearly; or if using an iterative linear equation solver such as conjugate gradient)
3. Evaluate the results (e.g., stress, heat flux, ...):
   (a) plot variables of interest for making design decision

(b) check quality of analysis versus known analytical solutions (verification) and/or experimental results (validation)

1.2 How This Course is Taught

- Covers the mathematical foundations, basics of FEM, in detail on the "board" and in notes
- Covers both theory and application, but emphasize theory and understanding of FEA
- You may feel there is too much math in this course, but it is balanced with practical FEA using Abaqus, and a project that allows further analysis using Abaqus or another software of your choosing, or programming your own FEA code
- Also, CVEN 5511 will have additional problems on problem sets and exams; grading also different from CVEN 4511
- If you just want to learn to run FEA, and not the theory behind it, then you will likely learn more from a software training course than from this course.

For a limited discussion of the procedure of **verification and validation (V&V)**, refer to Oberkampf et al. [2004], Babuska and Oden [2004], Schwer [2007]:

- **verification:** we check if the nonlinear governing equations are implemented correctly in our finite element (FE) code. This typically involves a combination of comparison to an analytical solution (if one exists) and/or to a separate numerical implementation (such as in Python); we also consider time step and mesh size refinement (temporal and spatial convergence). In CVEN 5511, we will do verification to some degree.

- **validation:** we check that the nonlinear governing equations are the correct ones to solve; i.e., are the physics of the problem being represented correctly in the model? This involves prediction of blind experimental data. Validation could be partly accomplished through your project, but for true validation, this is beyond the scope of the course. **Calibration** is a technique to estimate parameters from experimental data, and is not to be mistaken for **validation**, although it is the first step toward validation. If you have experimental data, you will likely conduct a calibration-exercise.

This page intentionally left blank.

Chapter 2

Linear FEM for Axially-Loaded Bar

For the 1D linear FEM, we assume linearity in the form of small strain, linear elasticity. We take an axially-loaded bar as our example problem [Pinsky, 2001]. Topics covered in remaining sections include the following:

(1) formulate differential form and apply boundary conditions (BCs) to give Strong Form (S) of elastostatic bar;

(2) formulate variational, Weak Form (W);

(3) formulate discrete, Galerkin Form (G);

(4) formulate Finite Element (FE), Matrix form;

(5) introduce natural coordinates, and isoparametric formulation;

(6) element assembly to obtain Global Matrix form;

(7) numerical integration using Gaussian quadrature;

(8) convergence of FEM (compatibility and completeness), and introduce Bernoulli-Euler beam;

(9) elastodynamics: modal analysis, Newmark's method for time integration.

2.1 Differential equation and Strong Form (S)

2.1.1 Linearity assumptions

Our linearity assumptions are the following:

(1) Assume linear elasticity: Hooke's law $\sigma = E\epsilon$, where σ is the axial stress (Pa), E the modulus of elasticity (Pa), ϵ the axial strain (m/m).

(2) Assume small deformations: (refer to Fig.2.1) where Cauchy stress $\sigma = F/A$, nominal stress $P = F/A_0$, strain increment $d\epsilon = dL/L$, deformed length $L = L_0 + u$, and total axial strain $\epsilon = \int_{L_0}^{L} dL/L = ln(L/L_0) = ln(1 + u/L_0)$. Assume a series expansion: $ln(1 + u/L_0) = \frac{u}{L_0} - \frac{1}{2}\left(\frac{u}{L_0}\right)^2 + \frac{1}{3}\left(\frac{u}{L_0}\right)^3 -$ h.o.t.'s, where if u is small, $\frac{u}{L_0} \ll 1 \implies \epsilon = ln(1 + u/L_0) \approx \frac{u}{L_0}$, and if area $A \approx A_0$, then we have the **small strain assumption**: $\epsilon \approx u/L_0$, $\sigma \approx F/A_0$, and we write $\epsilon = du/dx$ as our small strain as the spatial derivative of the axial displacement u.

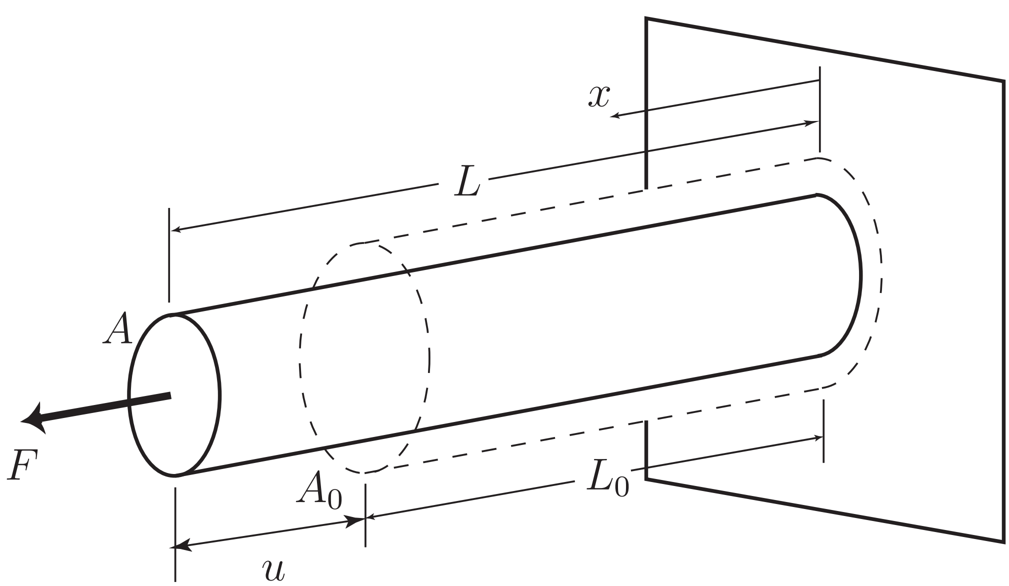

Figure 2.1. Axially-loaded bar assuming small deformations.

2.1.2 Differential equation and Strong Form (S)

We can derive the differential equation for balance of linear momentum of elastostatics. Refer to Fig.2.2 for the 1D bar with applied loads and BCs, where we have a concentrated force F at $x = L$ (N), distributed force $f(x)$ along bar (N/m), and displacement g at $x = 0$ (m).

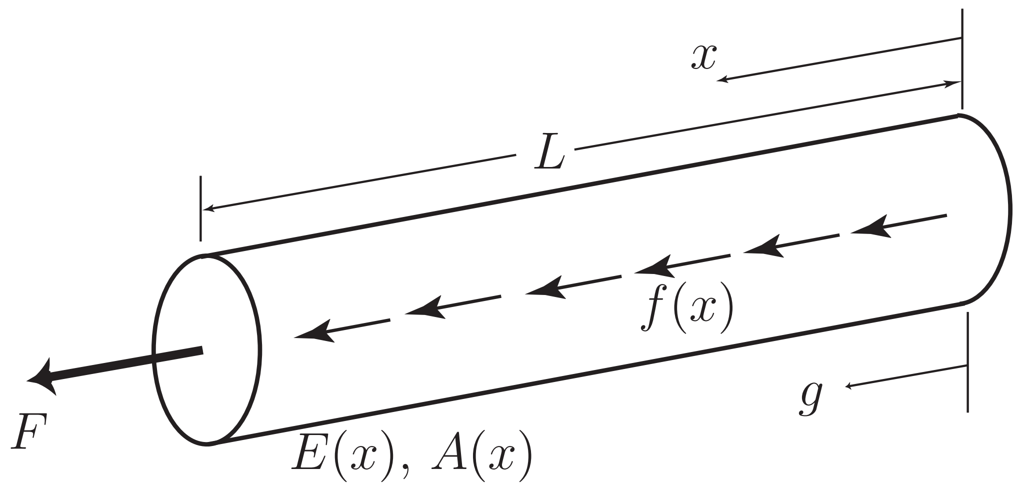

Figure 2.2. Axially-loaded bar with BCs.

We consider an axial displacement $u(x)$ of differential line segment dx at x, with internal axial force $N(x)$ in Fig.2.3.

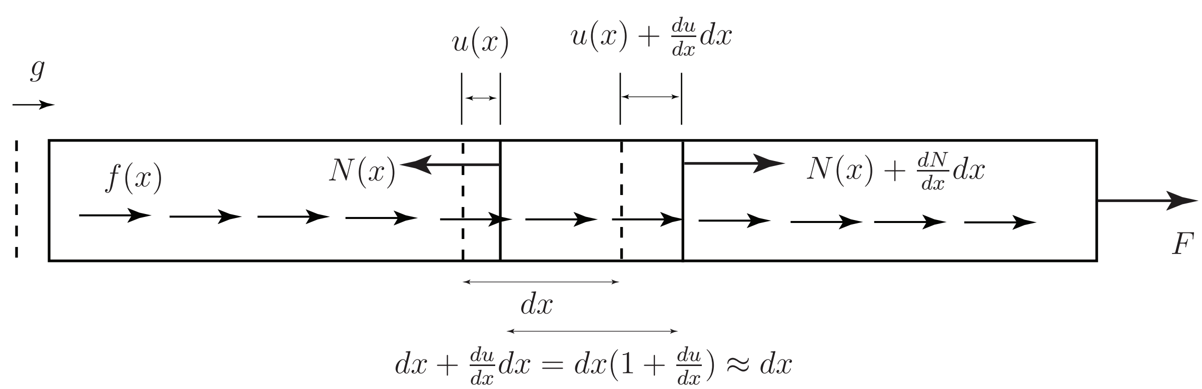

Figure 2.3. Differential line segment dx of axially-loaded bar.

Summing the forces leads to **balance of linear momentum for a static axially loaded**

bar:

$$\sum_{\to +} F_x = 0 \implies -N(x) + N(x) + \frac{dN(x)}{dx}dx + f(x)dx = 0 \quad (2.1)$$

$$-\frac{dN(x)}{dx} = f(x) \quad (2.2)$$

Recall the **small strain definition of stress and strain**:

$$\sigma(x) = \frac{N(x)}{A(x)} = E(x)\epsilon(x) \quad (2.3)$$

$$\epsilon(x) = \frac{du(x)}{dx} \quad (2.4)$$

$$\implies N(x) = EA(x)\frac{du(x)}{dx} \quad (2.5)$$

Thus, the **differential equation** can be written as (assuming linear elasticity, $\sigma = Edu/dx$):

$$-\frac{d}{dx}\left(EA(x)\frac{du}{dx}\right) = f(x) \quad x \in \Omega = (0, L) \quad (2.6)$$

where $x \in \Omega$ reads "x in the domain of Ω", $x \in \Omega = (0, L)$ means $0 < x < L$, and $x \in \bar{\Omega} = [0, L]$ means $0 \leq x \leq L$. We write the BCs as **force BC** at $x = L$, such that $N(L) = F$ or $\left(EA\frac{du}{dx}\right)_L = F$, and **displacement BC** at $x = 0$, such that $u(0) = g$. If BCs are properly prescribed, then the PDE (ODE here) is well-posed, such that there is a unique solution.

Given the **differential equation and BCs**, we may state the **Strong Form (S)** as:

$$(S)\begin{cases} \text{Find } u(x) : \bar{\Omega} \mapsto \mathbb{R}, \quad \bar{\Omega} = [0, L], \quad \text{such that} \\ -\frac{d}{dx}\left(EA(x)\frac{du}{dx}\right) = f(x) \qquad x \in \Omega \\ \left(EA\frac{du}{dx}\right)_L = F \qquad x = L \\ u(0) = g \qquad x = 0 \end{cases} \quad (2.7)$$

where $u(x) : \bar{\Omega} \mapsto \mathbb{R}$ reads "with x in $\bar{\Omega}$, u maps to the real number line $\mathbb{R}$", distributed axial force $f(x)$ is a body force, concentrated force F is a *natural*, or Neumann, BC, and prescribed displacement g is an *essential*, or Dirichlet, BC.

2.2 Variational equation and Weak Form (W)

From the Strong Form, we apply the **Method of Weighted Residuals** to formulate the **Weak (or variational) Form (W)**. "Weak" implies that the balance equation is not satisfied pointwise, but in an integral average sense. We can show equivalence between Weak and Strong forms for smooth functions (i.e., nothing lost by Weak form, assuming smoothness of functions); refer to Hughes [1987]. When we discretize the domain Ω for the Galerkin form (i.e., $\Omega^h \subset \Omega$), approximations (meshes) are generated. We assume an arbitrary weighting function $w(x)$, which can be thought of as a "variation" of displacement $u(x) \Longrightarrow w(x) = \delta u(x)$, where $\delta(\bullet)$ is the variation operator from variational calculus (refer to Lanczos [1949], Washizu [1982]), or you can think of it as a virtual displacement. We **apply the Method of Weighted Residuals to the differential equation** (not satisfied pointwise, but in an integral, average sense) such that,

$$\int_0^L w(x) \left[\frac{d}{dx} \left(EA(x) \frac{du}{dx} \right) + f(x) \right] dx = 0 \tag{2.8}$$

where we **integrate by parts using the chain rule** as $\frac{d(ab)}{dx} = \frac{da}{dx} b + \frac{db}{dx} a$, and **apply the Divergence theorem in 1D** such that $\int_0^L \frac{dG}{dx} dx = G|_0^L = G(L) - G(0)$. We apply the chain rule as $\frac{d}{dx}\left[w(x) EA(x) \frac{du}{dx}\right] = \frac{dw(x)}{dx}\left[EA(x)\frac{du}{dx}\right] + w(x) \frac{d}{dx}\left[EA(x)\frac{du}{dx}\right]$. We substitute into the weighted residual and apply the Divergence theorem as,

$$\left(wEA \frac{du}{dx} \right)_0^L - \int_0^L \frac{dw}{dx} EA \frac{du}{dx} dx + \int_0^L wf dx = 0 \tag{2.9}$$

Note on notation: we sometimes simplify $du/dx = u_{,x}$. Recall BCs $u(0) = g$ and $\left(EA\frac{du}{dx}\right)_L = F$, and note that the variation of a known field (or constant) is zero: $\Longrightarrow w(0) = \delta u(0) = \delta g = 0$. Then the variational, or integral form, results as,

$$\underbrace{\int_0^L \left(\frac{dw}{dx}EA\frac{du}{dx}\right)dx}_{related\ to\ internal\ strain\ energy} = \underbrace{\int_0^L wf dx + w(L)F}_{related\ to\ energy\ of\ external\ loads} \tag{2.10}$$

The Weak Form (W) can then be stated as,

$$(W)\begin{cases} \text{Find } u(x) \in \mathscr{S} = \{u : \Omega \mapsto \mathbb{R}, u \in H^1, u(0) = g\}, \text{such that} \\ \int_0^L \left(\frac{dw}{dx}EA\frac{du}{dx}\right)dx = \int_0^L wf dx + w(L)F \\ \text{holds } \forall w(x) \in \mathscr{V} = \{w : \Omega \mapsto \mathbb{R}, w \in H^1, w(0) = 0\} \end{cases} \tag{2.11}$$

where $\forall$ reads "for all," $\mathscr{S}$ is the space of admissible trial functions, $\mathscr{V}$ is the space of weighting functions, H^1 is the first Sobolev space, such that the H^1 norm is finite: i.e., $\|u\|_1 = \left(\int_0^L (u^2 + u_{,x}^2)dx\right)^{1/2} < \infty$, $\|u\|_1$ is called the "natural" norm, $u \in H^1$ essentially states that the first spatial derivative $u_{,x}$ CANNOT be a Dirac-Delta function, but can be a Heaviside function (i.e., discontinuous).

We consider here an alternate method for formulating the variational equation: the **Principle of Minimum Potential Energy (PMPE) for Elasticity**; *limitation: this variational principle is only applicable to those physical systems that lend themselves to a "functional" or "potential energy" representation; e.g., certain multiphysics problems do not generally lend themselves to such representation.* We define a potential energy $\Pi(u)$ in terms of internal strain energy $U(u)$ and potential energy of loads $V(u)$ as (see Lanczos [1949]),

$$\Pi(u) = U(u) - V(u) \tag{2.12}$$

where the PMPE states that the exact solution u minimizes Π, and thus the system is in equilibrium. We apply the stationarity condition on Π, such that $\delta\Pi = 0$. The application of the variation operator $\delta(\bullet)$ can be thought of acting like a time derivative $d(\bullet)/dt$, although it is not a time derivative. Recall the stress-strain curve for linear elasticity in Fig.2.4, where the stored elastic strain energy density $e = \frac{1}{2}\sigma\epsilon$, the total elastic strain energy $U = \int_0^L \int_A (e) dA dx = \int_0^L (\frac{1}{2}\sigma A \epsilon) dx = \frac{1}{2}\int_0^L EA(x)\left(\frac{du}{dx}\right)^2 dx$, and the potential energy of the external loads, $V = \int_0^L u f dx + u(L)F$.

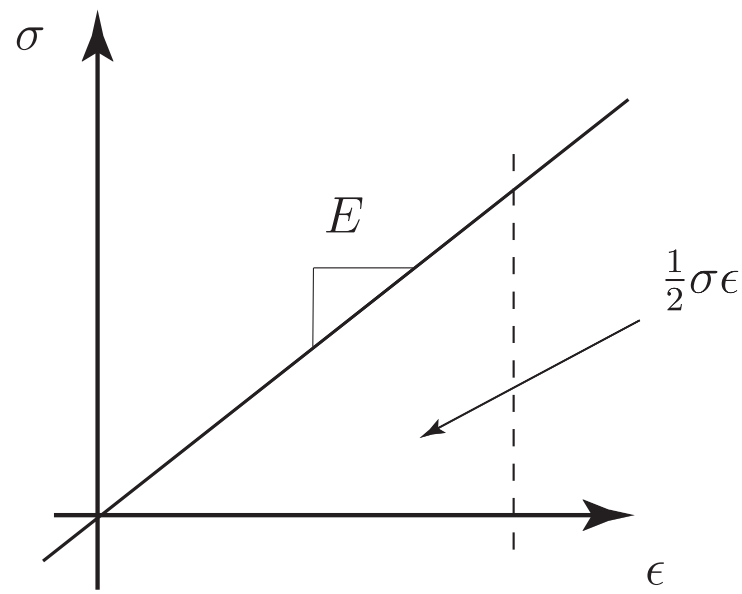

Figure 2.4. Stored strain energy for linear elasticity.

We then **apply the stationarity condition** as $\delta\Pi = \delta U - \delta V = 0$, such that, (fill in blanks yourself)

$$\delta\Pi = \delta U + \delta V = 0 \tag{2.13}$$

$$\delta U = \tag{2.14}$$

$$\delta V = \tag{2.15}$$

and the variational equation for the Weak Form results as before by the Method of Weighted Residuals as,

$$\int_0^L \left(\frac{dw}{dx} EA \frac{du}{dx}\right) dx = \int_0^L w f dx + w(L)F \tag{2.16}$$

2.3 Discretization and Galerkin Form (G)

We now make a subtle step in order to discretize the Weak Form by something called the *Galerkin Form (G)* [Hughes, 1987]. We find the approximate solution $u^h(x) \approx u(x)$, where h is the discretization parameter, or characteristic length of the mesh. We consider our 1D axially loaded bar with length L, and **discretize with straight line elements of length** h (that may not all be equal), where if equal then $h = L/n_{\text{el}}$, and n_{el} is the number of elements (see Fig.2.5).

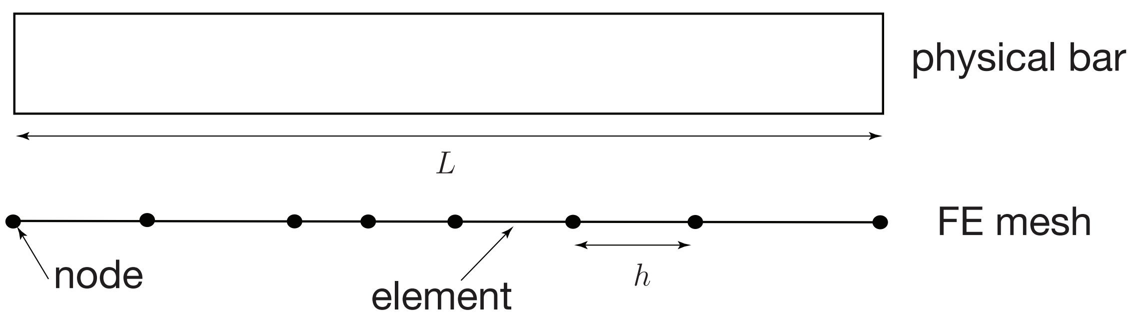

Figure 2.5. Discretized 1D bar.

For 1D, we see that $\Omega^h = (0, L) = \Omega$, but for 2D and 3D (consider meshing a circle with straight edge linear elements), $\Omega^h \subset \Omega$ (i.e., discrete mesh Ω^h is a subset of physical domain Ω). We then **rewrite the Weak form in discrete, Galerkin form** as

$$(G) \begin{cases} \text{Find } u^h(x) \in \mathscr{S}^h = \{u^h : \Omega^h \mapsto \mathbb{R}, u^h \in H^1, u^h(0) = g\}, \text{such that} \\ \int_0^L \left(\frac{dw^h}{dx} EA \frac{du^h}{dx} \right) dx = \int_0^L w^h f dx + w^h(L) F \\ \text{holds } \forall w^h(x) \in \mathscr{V}^h = \{w^h : \Omega^h \mapsto \mathbb{R}, w^h \in H^1, w^h(0) = 0\} \end{cases} \tag{2.17}$$

where $\mathscr{S}^h \subset \mathscr{S}$ is the discrete space of admissible trial functions, $\mathscr{V}^h \subset \mathscr{V}$ is the discrete space of weighting functions, $(G) \approx (W)$, and note that even though u^h and w^h are discrete approximations to u and w, respectively, they must still satisfy restrictions on the spaces (in order to ensure convergence: i.e., $\lim_{h \to 0} u^h = u$). Note that the essential BC is satisfied exactly, $u^h(0) = g$. Next, we treat these discrete line elements as **finite elements** with appropriate interpolation functions, etc.

2.4 Finite Element (FE) Matrix-Vector Form

Starting with the Galerkin Form (G), we now discretize the 1D bar into n_{el} elements with nodal degrees of freedom (dofs). From the **global perspective** (Fig.2.6, the whole mesh), we consider $u^h(x) = \sum_{A=1}^{n_{\text{np}}} N_A(x) d_A$ over $\Omega^h = (0, L)$, n_{np} is the number of global nodal points, and $N_A(x)$ is the shape (interpolation) function at global node A.

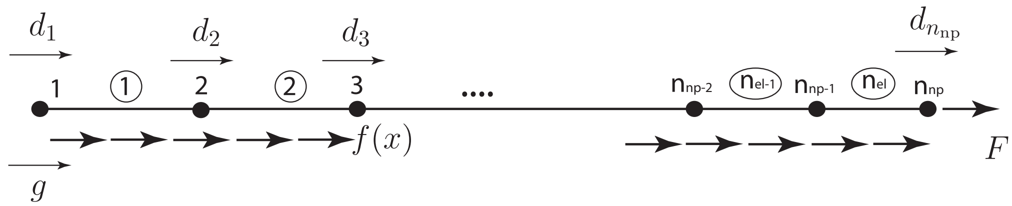

Figure 2.6. Discretized 1D bar into n_{el} finite elements.

From the **element perspective** consider an element e (Fig.2.7). **This is one of the strengths of the FEM**, the fact that element calculations can be generalized for a length h^e, area A^e, and elasticity modulus E^e.

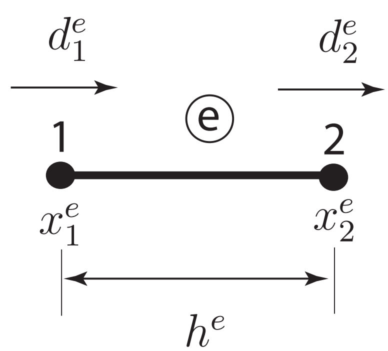

Figure 2.7. Single linear element.

The element length is $h^e = x_2^e - x_1^e$, element domain $\Omega^e = (x_1^e, x_2^e)$, total discrete domain $\Omega^h = \mathbf{A}_{e=1}^{n_{\text{el}}} \Omega^e$, and $\mathbf{A}_{e=1}^{n_{\text{el}}}$ is the **element assembly operator** that must be programmed (more on this later).

Let us consider a 2-noded element with linear shape functions (interpolations, Fig.2.8).

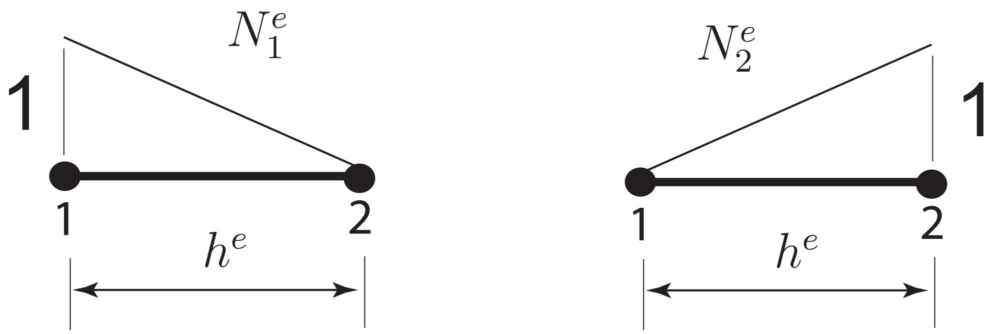

Figure 2.8. Linear shape functions.

The shape function at node 1 of element e is $N_1^e(x) = (x_2^e - x)/h^e$, where the Kronecker-Delta property of shape functions is satisfied as $N_1^e(x_1^e) = 1$, $N_1^e(x_2^e) = 0$. The shape function at node 2 of element e is $N_2^e(x) = (x - x_1^e)/h^e$, where likewise the Kronecker-Delta property of shape functions is satisfied as $N_2^e(x_1^e) = 0$, $N_2^e(x_2^e) = 1$.

Consider the **element interpolation for displacement** as,

$$u^{h^e}(x) = \sum_{a=1}^{n_{\text{en}}} N_a^e(x) d_a^e = N_1^e(x) d_1^e + N_2^e(x) d_2^e \tag{2.18}$$

$$= \begin{bmatrix} N_1^e & N_2^e \end{bmatrix} \begin{bmatrix} d_1^e \\ d_2^e \end{bmatrix} \tag{2.19}$$

$$= \boldsymbol{N}^e(x) \cdot \boldsymbol{d}^e \tag{2.20}$$

where we note that $u^{h^e}(x_1^e) = N_1^e(x_1^e)d_1^e + N_2^e(x_1^e)d_2^e = d_1^e$ and n_{en} is number of element nodes, where $n_{\text{en}} = 2$ for linear 2-node element. $N_a^e(x)$ is the shape function of local element node *a*. Likewise, the **element interpolation for the weighting function** is

$$w^{h^e}(x) = \sum_{a=1}^{n_{\text{en}}} N_a^e(x)c_a^e \quad = \quad N_1^e(x)c_1^e + N_2^e(x)c_2^e \tag{2.21}$$

$$= \begin{bmatrix} N_1^e & N_2^e \end{bmatrix} \begin{bmatrix} c_1^e \\ c_2^e \end{bmatrix} \tag{2.22}$$

$$= \boldsymbol{N}^e(x) \cdot \boldsymbol{c}^e \tag{2.23}$$

where $\boldsymbol{c}^e$ is the vector of nodal weighting function values (which are arbitrary since the weak form must hold "$\forall w(x)$," except at an essential BC). *We choose to use the same shape (interpolation) functions for u^{h^e} and w^{h^e}, which will lead to a symmetric stiffness matrix; when they are the same, it is called **Bubnov-Galerkin**; when they are different, it is called **Petrov-Galerkin**, for assumed enhanced strain methods, for example [Hughes, 1987].*

We rewrite the Galerkin form in terms of finite elements,

$$\mathop{\mathbf{A}}_{e=1}^{n_{\text{el}}} \int_{\Omega^e} \left(\frac{dw^{h^e}}{dx} EA \frac{du^{h^e}}{dx} \right) dx = \mathop{\mathbf{A}}_{e=1}^{n_{\text{el}}} \left[\int_{\Omega^e} w^{h^e} f(x) dx \right] + w^h(L)F \tag{2.24}$$

Taking spatial derivatives, we have

$$\frac{du^{h^e}}{dx} = \frac{d\boldsymbol{N}^e}{dx} \cdot \boldsymbol{d}^e = \boldsymbol{B}^e \cdot \boldsymbol{d}^e \Longrightarrow \boldsymbol{B}^e = \begin{bmatrix} \frac{dN_1^e}{dx} & \frac{dN_2^e}{dx} \end{bmatrix} \tag{2.25}$$

where $\boldsymbol{B}^e$ is called the *element strain-displacement matrix*. Likewise, $\frac{dw^{h^e}}{dx} = \boldsymbol{B}^e \cdot \boldsymbol{c}^e = (\boldsymbol{c}^e)^T \cdot (\boldsymbol{B}^e)^T$, since dw^{h^e}/dx is a scalar. We now substitute these expressions into the Galerkin form as,

$$\mathop{\mathbf{A}}_{e=1}^{n_{\text{el}}} (\boldsymbol{c}^e)^T \cdot \underbrace{\left\{ \int_{\Omega^e} (\boldsymbol{B}^e)^T \cdot \boldsymbol{B}^e EA dx \right\}}_{\boldsymbol{k}^e} \cdot \boldsymbol{d}^e = \mathop{\mathbf{A}}_{e=1}^{n_{\text{el}}} (\boldsymbol{c}^e)^T \cdot \underbrace{\left\{ \int_{\Omega^e} (\boldsymbol{N}^e)^T f(x) dx \right\}}_{\boldsymbol{f}_f^e} + w^h(L)F \tag{2.26}$$

where $\boldsymbol{k}^e$ is the element stiffness matrix, $\boldsymbol{f}_f^e$ is the element distributed load vector, and vector product $(\boldsymbol{B}^e)^T \cdot \boldsymbol{B}^e = \begin{bmatrix} \frac{dN_1^e}{dx} \\ \frac{dN_2^e}{dx} \end{bmatrix} \cdot \begin{bmatrix} \frac{dN_1^e}{dx} & \frac{dN_2^e}{dx} \end{bmatrix}$ is a 2×2 matrix. Note that $w^h(L) = c_{n_{\text{np}}} = c_2^{n_{\text{el}}}$, such that

$$w^h(L)F = \begin{bmatrix} c_1^{n_{\text{el}}} & c_2^{n_{\text{el}}} \end{bmatrix} \cdot \begin{bmatrix} 0 \\ F \end{bmatrix} = (\boldsymbol{c}^{n_{\text{el}}})^T \cdot \boldsymbol{f}_F^{n_{\text{el}}} \tag{2.27}$$

All other $\boldsymbol{f}_F^e = \boldsymbol{0}$ for $e \neq n_{\text{el}}$, so we write $w^h(L)F = \mathbf{A}_{e=1}^{n_{\text{el}}} (\boldsymbol{c}^e)^T \cdot \boldsymbol{f}_F^e$, and

$$\mathop{\mathbf{A}}_{e=1}^{n_{\text{el}}} (\boldsymbol{c}^e)^T \cdot \left\{ \boldsymbol{k}^e \cdot \boldsymbol{d}^e = \boldsymbol{f}_f^e + \boldsymbol{f}_F^e \right\} \tag{2.28}$$

Before we learn how to assemble these individual finite element matrices and vectors into a global matrix form, we will consider a powerful *change of coordinates* for shape functions and numerical integration that makes finite element programs much easier to write and thus more efficient to run.

2.5 Natural coordinates and Isoparametric Formulation

We apply a *change of variables* from the global coordinate x to the natural coordinate ξ that is local to the element (Fig.2.9), where,

$$\xi = \begin{cases} -1 & \text{at local node 1} \\ 0 & \text{at the center} \\ 1 & \text{at local node 2} \end{cases} \tag{2.29}$$

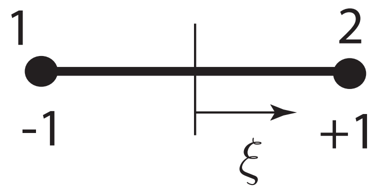

Figure 2.9. Local, or natural coordinate ξ.

The linear shape functions may then be re-written as,

$$N_1(\xi) = \frac{1}{2}(1-\xi)\ , \quad N_2(\xi) = \frac{1}{2}(1+\xi) \tag{2.30}$$

$$N_a(\xi) = \frac{1}{2}(1+\xi_a\xi) \tag{2.31}$$

where ξ_a is the natural coordinate of node a (i.e., for $a=1$, $\xi_1=-1$, and for $a=2$, $\xi_2=1$), and the $N_a(\xi)$ retain the Kronecker-Delta property, such that,

$$N_a(\xi_b) = \begin{cases} 1 & \text{for}\, b=a \\ 0 & \text{for}\, b\neq a \end{cases} \tag{2.32}$$

The element displacement and weighting function can then be written as,

$$u^{h^e}(\xi) = \boldsymbol{N}^e(\xi)\cdot\boldsymbol{d}^e\ , \quad w^{h^e}(\xi) = \boldsymbol{N}^e(\xi)\cdot\boldsymbol{c}^e \tag{2.33}$$

Likewise, the global coordinate x and natural coordinate ξ are *related by the mapping* as,

$$x^{h^e}(\xi) = \sum_{a=1}^{n_{\text{en}}} N_a(\xi)x_a^e \quad = \quad N_1(\xi)x_1^e + N_2(\xi)x_2^e \tag{2.34}$$

$$= \begin{bmatrix} N_1(\xi) & N_2(\xi) \end{bmatrix} \begin{bmatrix} x_1^e \\ x_2^e \end{bmatrix} \tag{2.35}$$

$$= \boldsymbol{N}^e(\xi)\cdot\boldsymbol{x}^e \tag{2.36}$$

Therefore, this formulation is called **isoparametric** because the same shape functions are used to interpolate displacements **and** global coordinates ('iso' means same). *This is how curved element boundary geometries are generated, using higher-order shape functions to interpolate the global coordinates (for 2D and 3D geometries).* We define the Jacobian of element coordinate transformation j^e as,

$$
\begin{aligned}
j^e(\xi) := \frac{dx^{h^e}(\xi)}{d\xi} &= \frac{d\boldsymbol{N}^e(\xi)}{d\xi} \cdot \boldsymbol{x}^e && (2.37) \\
&= \begin{bmatrix} -\frac{1}{2} & \frac{1}{2} \end{bmatrix} \begin{bmatrix} x_1^e \\ x_2^e \end{bmatrix} && (2.38) \\
&= \frac{1}{2}(x_2^e - x_1^e) = \frac{h^e}{2} && (2.39)
\end{aligned}
$$

where the symbol ":=" means a definition. This implies the differential map between coordinates as $dx = j^e d\xi = (h^e/2)d\xi$, where,

$$
\frac{du^{h^e}(\xi)}{dx} = \frac{d\boldsymbol{N}^e(\xi)}{dx} \cdot \boldsymbol{d}^e = \frac{d\boldsymbol{N}^e(\xi)}{d\xi}\frac{d\xi}{dx} \cdot \boldsymbol{d}^e = \frac{1}{j^e}\frac{d\boldsymbol{N}^e(\xi)}{d\xi} \cdot \boldsymbol{d}^e = \boldsymbol{B}^e \cdot \boldsymbol{d}^e \qquad (2.40)
$$

Consider an **example:** a quadratic equation in x with constant coefficients a and b, and global nodal coordinates for a linear 2-node 1D finite element as,

$$
\psi(x) \;=\; a + bx^2\,, \quad \left.\begin{matrix} x_1^e = 4 \\ x_2^e = 6 \end{matrix}\right\} \Longrightarrow h^e = 2\,,\; j^e = 1 \qquad (2.41)
$$

Then, the map from x to ξ occurs as follows,

$$
\begin{aligned}
x^{h^e}(\xi) &= \boldsymbol{N}^e(\xi) \cdot \boldsymbol{x}^e = \frac{1}{2}(1-\xi)4 + \frac{1}{2}(1+\xi)6 = 5 + \xi && (2.42) \\
\hat{\psi}(\xi) &= \psi(x(\xi)) = a + b(5+\xi)^2 && (2.43)
\end{aligned}
$$

Now, let us integrate over the element domain as follows,

$$\int_{x_1^e}^{x_2^e} \psi(x)dx = \int_{-1}^{1} \hat{\psi}(\xi) j^e(\xi) d\xi \tag{2.44}$$

$$\text{recalling } dx = j^e(\xi)d\xi \tag{2.45}$$

$$\int_4^6 (a+bx^2)dx = \int_{-1}^{1} \left[a + b(5+\xi)^2\right](1)d\xi \tag{2.46}$$

For higher-order shape functions (quadratic, cubic, ...), transition elements (when we get to 2D), and for higher spatial dimensions (2D and 3D), isoparametric finite elements simplify considerably the formulation and numerical integration of element matrices and vectors.

Now, recall the stiffness matrix for an element e, with mapping to natural coordinate ξ as,

$$\boldsymbol{k}^e = \int_{x_1^e}^{x_2^e} [\boldsymbol{B}^e(x)]^T EA(x) \boldsymbol{B}^e(x) dx \tag{2.47}$$

$$= \int_{x_1^e}^{x_2^e} EA(x) \begin{bmatrix} \frac{-1}{h^e} \\ \frac{1}{h^e} \end{bmatrix} \begin{bmatrix} \frac{-1}{h^e} & \frac{1}{h^e} \end{bmatrix} dx = \frac{1}{(h^e)^2} \left(\int_{x_1^e}^{x_2^e} EA(x)dx \right) \begin{bmatrix} 1 & -1 \\ -1 & 1 \end{bmatrix}$$

$$= \frac{1}{(h^e)^2} \left(\int_{-1}^{1} \widehat{EA}(\xi) \frac{h^e}{2} d\xi \right) \begin{bmatrix} 1 & -1 \\ -1 & 1 \end{bmatrix} = \frac{1}{2h^e} \left(\int_{-1}^{1} \widehat{EA}(\xi) d\xi \right) \begin{bmatrix} 1 & -1 \\ -1 & 1 \end{bmatrix} \tag{2.48}$$

where $EA(\xi)$ could vary along the element length (e.g., a tapered bar). Likewise, recall the distributed load vector as,

$$\boldsymbol{f}_f^e = \int_{x_1^e}^{x_2^e} [\boldsymbol{N}^e(x)]^T f(x) dx = \int_{-1}^{1} [\boldsymbol{N}^e(\xi)]^T \hat{f}(\xi) \frac{h^e}{2} d\xi \tag{2.49}$$

$$= \frac{h^e}{4} \int_{-1}^{1} \begin{bmatrix} 1-\xi \\ 1+\xi \end{bmatrix} \hat{f}(\xi) d\xi \tag{2.50}$$

2.6 Assembly process for Global Matrix Form

Now, with individual element stiffness matrices and force vectors evaluated, how do we obtain the global matrix system of FE equations to solve for the unknown displacements, to then use to calculate strain and stress? Answer: we form the global matrix FE equations by **assembling** the individual element matrices leading to the following matrix form as,

$$\boldsymbol{K} \cdot \boldsymbol{d} = \boldsymbol{F}_g + \boldsymbol{F}_f + \boldsymbol{F}_F \tag{2.51}$$

where $\boldsymbol{K}$ is the global stiffness matrix, $\boldsymbol{F}_g$ is the global force vector due to applied displacement BCs (for linear problems), $\boldsymbol{F}_f$ is the global distributed force vector, and $\boldsymbol{F}_F$ is the global concentrated force vector. In an FE computer program, an 'algorithm' like the assembly operator $\mathbf{A}_{e=1}^{n_{\text{el}}}$ usually takes the form of an array or matrix. This assembly process will be different depending on the choice of the computer programmer and FE developer. In this case, we will form a **Location Matrix (LM)**. Consider the 2 element example in Fig.2.10, where the LM is,

local node # \ element #	1	2
1	1	2
2	2	3

(entries: global d.o.f.)

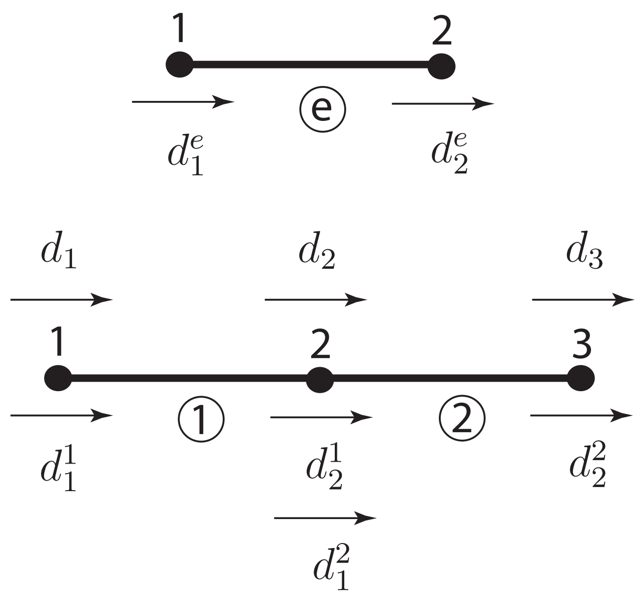

Figure 2.10. Two element mesh example.

2.6.1 Example 1

This example is taken from Pinsky [2001]. We will consider this example for demonstrating the assembly process for the global finite element stiffness matrix and force vectors. Refer to Fig.2.11, where R_1 and R_6 are the reaction forces at the nodes where the displacements are prescribed. These forces can be calculated as a post-processing step after the displacements are solved.

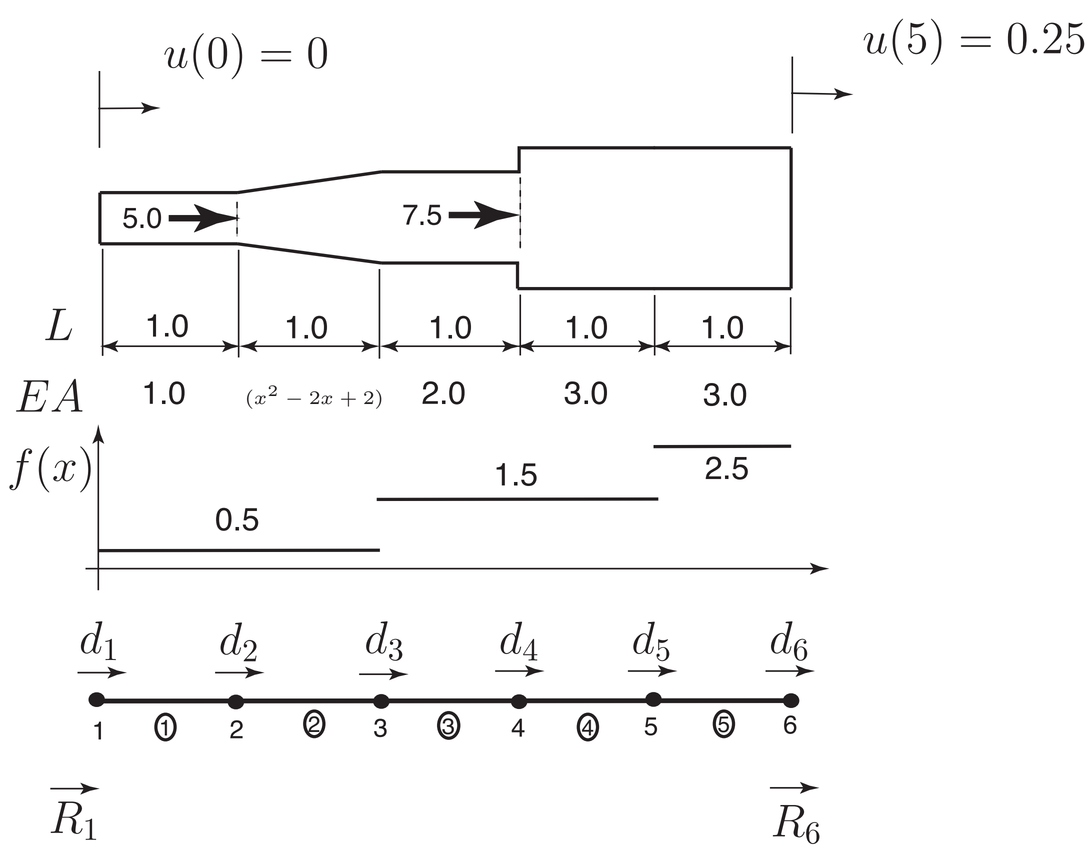

Figure 2.11. Example 1 for assembly procedure.

The bar of length $L = 5$ with variable $EA(x)$ and distributed force $f(x)$ shown in Fig.2.11 is discretized into 5 finite elements ($n_{\text{el}} = 5$), 6 nodes ($n = 6$), and 6 degrees of freedom ($n_{\text{dof}} = 6$) as shown. Essential boundary conditions are $u(0) = 0$ and $u(5) = 0.25$. Concentrated forces of 5.0 and 7.5 are applied at $x = 1.0$ and $x = 3.0$, respectively.

In summary, for the essential B.C.s,

$$\begin{aligned} u^h(0) = 0 &\implies d_1 = 0 \\ u^h(5) = 0.25 &\implies d_6 = 0.25 \\ w^h(0) = 0 &\implies c_1 = 0 \\ w^h(5) = 0 &\implies c_6 = 0 \end{aligned}$$

The concentrated forces can be lumped to one of the element degrees of freedom, or split between two elements. We will split in half the concentrated forces between two elements, but the end result is the same (they are added together at the nodal dofs during the assembly process). The concentrated force vectors are written as,

$$\boldsymbol{f}_F^1 = \begin{bmatrix} R_1 \\ 2.5 \end{bmatrix} \quad \boldsymbol{f}_F^2 = \begin{bmatrix} 2.5 \\ 0 \end{bmatrix} \quad \boldsymbol{f}_F^3 = \begin{bmatrix} 0 \\ 3.75 \end{bmatrix} \quad \boldsymbol{f}_F^4 = \begin{bmatrix} 3.75 \\ 0 \end{bmatrix} \quad \boldsymbol{f}_F^5 = \begin{bmatrix} 0 \\ R_6 \end{bmatrix} \tag{2.52}$$

Recall the equation for the element distributed force vector as,

$$\boldsymbol{f}_f^e = \frac{h^e}{4} \int_{-1}^{1} \begin{bmatrix} 1-\xi \\ 1+\xi \end{bmatrix} \widehat{f}(\xi) d\xi \tag{2.53}$$

So for element 1, $\widehat{f}(\xi) = 0.5$, and then,

$$\boldsymbol{f}_f^1 = \frac{1}{4} \int_{-1}^{1} \begin{bmatrix} 1-\xi \\ 1+\xi \end{bmatrix} 0.5 d\xi = \begin{bmatrix} 0.25 \\ 0.25 \end{bmatrix} \tag{2.54}$$

and so for the other elements, we have,

$$\boldsymbol{f}_f^2 = \begin{bmatrix} 0.25 \\ 0.25 \end{bmatrix} \quad \boldsymbol{f}_f^3 = \begin{bmatrix} 0.75 \\ 0.75 \end{bmatrix} \quad \boldsymbol{f}_f^4 = \begin{bmatrix} 0.75 \\ 0.75 \end{bmatrix} \quad \boldsymbol{f}_f^5 = \begin{bmatrix} 1.25 \\ 1.25 \end{bmatrix} \tag{2.55}$$

For calculating the **element stiffness matrices**, recall the equation for the individual element stiffness matrix for an element e as,

$$\boldsymbol{k}^e = \frac{1}{2h^e}\int_{-1}^{1}\widehat{EA}(\xi)d\xi \begin{bmatrix} 1 & -1 \\ -1 & 1 \end{bmatrix} \tag{2.56}$$

Then for element 1, $h^1 = 1$ and $EA = 1$, we have,

$$\boldsymbol{k}^1 = \begin{bmatrix} 1 & -1 \\ -1 & 1 \end{bmatrix} \tag{2.57}$$

For element 2, $EA(x) = x^2 - 2x + 2$, where recall $x(\xi) = \boldsymbol{N}^e(\xi)\cdot\boldsymbol{x}^e = (3+\xi)/2$, so $\widehat{EA}(\xi) = (1/4)\xi^2 + (1/2)\xi + 5/4$, then after integrating, we have,

$$\boldsymbol{k}^2 = (4/3)\begin{bmatrix} 1 & -1 \\ -1 & 1 \end{bmatrix} \tag{2.58}$$

and so forth for the other elements as,

$$\boldsymbol{k}^3 = 2.0\begin{bmatrix} 1 & -1 \\ -1 & 1 \end{bmatrix} \quad \boldsymbol{k}^4 = 3.0\begin{bmatrix} 1 & -1 \\ -1 & 1 \end{bmatrix} \quad \boldsymbol{k}^5 = 3.0\begin{bmatrix} 1 & -1 \\ -1 & 1 \end{bmatrix} \tag{2.59}$$

Assembly of global stiffness matrix and force vectors using the Location Matrix (LM): How do we obtain the global stiffness matrix and force vector from these individual element ones? Answer: we assemble them. For this example, the Location Matrix (LM) is generated as,

element number

		1	2	3	4	5	
local node number	1	1	2	3	4	5	d.o.f.
	2	2	3	4	5	6	

Then for element 1, the local stiffness matrix values and their corresponding global degrees of freedom are tabulated from the LM as,

		1	2
$\boldsymbol{k}^1$	1	1	-1
	2	-1	1

And its contribution to the global stiffness matrix looks as follows,

		1	2	3	4	5	6
	1	1	-1	0	0	0	0
	2	-1	1	0	0	0	0
$\boldsymbol{K}^1$	3	0	0	0	0	0	0
	4	0	0	0	0	0	0
	5	0	0	0	0	0	0
	6	0	0	0	0	0	0

For element 2, the element local stiffness matrix and its corresponding global dofs are,

		2	3
$\boldsymbol{k}^2$	2	4/3	-4/3
	3	-4/3	4/3

which when placed in the global stiffness matrix, looks like,

$\boldsymbol{K}^2$

	1	2	3	4	5	6
1	0	0	0	0	0	0
2	0	4/3	-4/3	0	0	0
3	0	-4/3	4/3	0	0	0
4	0	0	0	0	0	0
5	0	0	0	0	0	0
6	0	0	0	0	0	0

and so forth, such that,

$$\boldsymbol{K} = \mathop{\mathsf{A}}_{e=1}^{n_{el}} \boldsymbol{k}^e = \sum_{e=1}^{n_{el}} \boldsymbol{K}^e = \begin{bmatrix} 1 & -1 & 0 & 0 & 0 & 0 \\ -1 & 7/3 & -4/3 & 0 & 0 & 0 \\ 0 & -4/3 & 10/3 & -2 & 0 & 0 \\ 0 & 0 & -2 & 5 & -3 & 0 \\ 0 & 0 & 0 & -3 & 6 & -3 \\ 0 & 0 & 0 & 0 & -3 & 3 \end{bmatrix} \tag{2.60}$$

Note that $\boldsymbol{K} = \boldsymbol{K}^T$, i.e., it is symmetric, but it is also singular, meaning currently it is not invertible and therefore there is no unique solution for the displacements. What will we need? Answer: ESSENTIAL B.C.'S!

First, assemble the global force vectors in the same way as the stiffness matrix as,

$$\boldsymbol{F}_f^1 = \begin{bmatrix} 0.25 \\ 0.25 \\ 0 \\ 0 \\ 0 \\ 0 \end{bmatrix} \quad \boldsymbol{F}_f^2 = \begin{bmatrix} 0 \\ 0.25 \\ 0.25 \\ 0 \\ 0 \\ 0 \end{bmatrix} \quad \ldots \boldsymbol{F}_f = \mathop{\mathsf{A}}_{e=1}^{n_{el}} \boldsymbol{f}_f^e = \sum_{e=1}^{n_{el}} \boldsymbol{F}_f^e = \begin{bmatrix} 0.25 \\ 0.5 \\ 1 \\ 1.5 \\ 2 \\ 1.25 \end{bmatrix} \tag{2.61}$$

and the concentrated force vector as,

$$\boldsymbol{F}_F = \begin{bmatrix} R_1 \\ 5 \\ 0 \\ 7.5 \\ 0 \\ R_6 \end{bmatrix} \tag{2.62}$$

Account for essential boundary conditions: The full finite element matrix equations look like (including the pre-multiplication of the nodal weighting function vector $\boldsymbol{c}$) as,

$$\begin{aligned} 0 \;=\; & \begin{bmatrix} c_1 & c_2 & c_3 & c_4 & c_5 & c_6 \end{bmatrix} \times \\ & \left\{ \begin{bmatrix} 1 & -1 & 0 & 0 & 0 & 0 \\ -1 & 7/3 & -4/3 & 0 & 0 & 0 \\ 0 & -4/3 & 10/3 & -2 & 0 & 0 \\ 0 & 0 & -2 & 5 & -3 & 0 \\ 0 & 0 & 0 & -3 & 6 & -3 \\ 0 & 0 & 0 & 0 & -3 & 3 \end{bmatrix} \begin{bmatrix} d_1 \\ d_2 \\ d_3 \\ d_4 \\ d_5 \\ d_6 \end{bmatrix} - \begin{bmatrix} 0.25 \\ 0.5 \\ 1 \\ 1.5 \\ 2 \\ 1.25 \end{bmatrix} - \begin{bmatrix} R_1 \\ 5 \\ 0 \\ 7.5 \\ 0 \\ R_6 \end{bmatrix} \right\} \end{aligned} \tag{2.63}$$

Recall that $c_1 = c_6 = 0$, which in effect cancels the 1st and 6th rows, and that $d_1 = 0$ and

$d_6 = 0.25$. The equations are then reduced to,

$$
\begin{aligned}
0 \;=\; & \begin{bmatrix} c_2 & c_3 & c_4 & c_5 \end{bmatrix} \times \\
& \left\{ \begin{bmatrix} 7/3 & -4/3 & 0 & 0 \\ -4/3 & 10/3 & -2 & 0 \\ 0 & -2 & 5 & -3 \\ 0 & 0 & -3 & 6 \end{bmatrix} \begin{bmatrix} d_2 \\ d_3 \\ d_4 \\ d_5 \end{bmatrix} + 0.0 \begin{bmatrix} -1 \\ 0 \\ 0 \\ 0 \end{bmatrix} + 0.25 \begin{bmatrix} 0 \\ 0 \\ 0 \\ -3 \end{bmatrix} - \begin{bmatrix} 0.5 \\ 1 \\ 1.5 \\ 2 \end{bmatrix} - \begin{bmatrix} 5 \\ 0 \\ 7.5 \\ 0 \end{bmatrix} \right\}
\end{aligned}
\tag{2.64}
$$

Written in symbolic form, the reduced matrix equations look like,

$$
\mathbf{0} = \boldsymbol{c}^T \cdot (\boldsymbol{K} \cdot \boldsymbol{d} - \boldsymbol{F}_g - \boldsymbol{F}_f - \boldsymbol{F}_F) \tag{2.65}
$$

Arbitrary weighting function vector $\boldsymbol{c}$: Recall the Galerkin form, which states that: "Find u^h ... **for all** $w^h \in \mathcal{V}^h$ " Then the weighting function nodal values in the vector $\boldsymbol{c}$ must be arbitrary (except at essential BCs where they are 0), such that to satisfy the residual equality in Eq.(2.65), we must satisfy the Finite Element Matrix equations as,

$$
\boldsymbol{K} \cdot \boldsymbol{d} = \boldsymbol{F}_g + \boldsymbol{F}_f + \boldsymbol{F}_F \tag{2.66}
$$

To summarize, the **General Approach to Assembly of Global FE Equations:**

1. discretize and assign node and element numbers
2. assign degrees of freedom (dofs) to each node
3. create LM and assemble
4. for dof with fixed displacement ($u = 0$), cancel those rows and columns of the global

stiffness matrix and rows of the forcing vectors

5. for dof with prescribed displacement ($u = g$), cancel those rows of the global stiffness matrix and forcing vectors, and multiply the corresponding columns of the stiffness matrix to calculate the force vector $\boldsymbol{F}_g$ associated with the prescribed displacements

6. now you have $\boldsymbol{K}$ and $\boldsymbol{F}$, so solve $\boldsymbol{K} \cdot \boldsymbol{d} = \boldsymbol{F}$ for the displacements $\boldsymbol{d}$

7. do any post-processing to calculate stresses within the elements and/or forces at the nodes (we will discuss via the examples)

2.6.2 Example 2

This example is taken from Pinsky [2001]. The Young's modulus and cross-sectional area are constant: $E = 8$, $A = 1$. Consider the example in Fig.2.12.

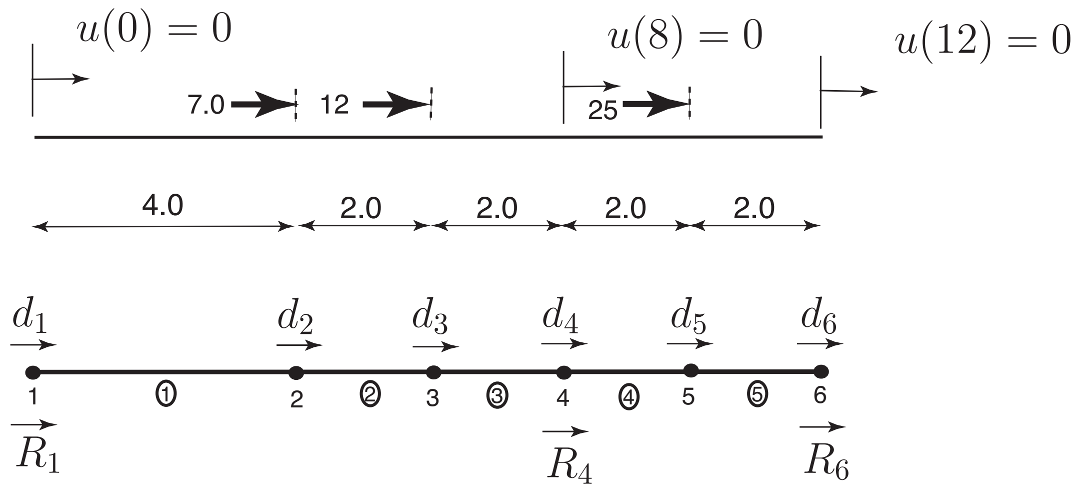

Figure 2.12. Example 2 for assembly procedure.

For the essential B.C.s,

$$
\begin{aligned}
u^h(0) = 0 &\implies d_1 = 0 \\
u^h(8) = 0 &\implies d_4 = 0 \\
u^h(12) = 0 &\implies d_6 = 0 \\
w^h(0) = 0 &\implies c_1 = 0 \\
w^h(8) = 0 &\implies c_4 = 0 \\
w^h(12) = 0 &\implies c_6 = 0
\end{aligned}
$$

For the concentrated forces,

$$
\begin{aligned}
(F_2)_F &= 7 \\
(F_3)_F &= 12 \\
(F_5)_F &= 25
\end{aligned}
$$

Recall the element stiffness matrix, which for constant EA is,

$$\boldsymbol{k}^e = \frac{1}{2h^e}\left(\int_{-1}^{1} \widehat{EA}(\xi)d\xi\right)\begin{bmatrix} 1 & -1 \\ -1 & 1 \end{bmatrix} = \frac{EA}{h^e}\begin{bmatrix} 1 & -1 \\ -1 & 1 \end{bmatrix} \tag{2.67}$$

where EA/h^e is the axial stiff of element e with constant EA. There is no distributed axial force along the bar, so $\boldsymbol{f}_f^e = \mathbf{0}$ for all elements.

Generate the LM as,

	element number	1	2	3	4	5	
local node number	1	1	2	3	4	5	d.o.f.
	2	2	3	4	5	6	

For element 1, the local stiffness matrix is

$\boldsymbol{k}^1$		1	2
	1	2	-2
	2	-2	2

When placed in the global matrix, it becomes

$\boldsymbol{K}^1$		1	2	3	4	5	6
	1	2	-2	0	0	0	0
	2	-2	2	0	0	0	0
	3	0	0	0	0	0	0
	4	0	0	0	0	0	0
	5	0	0	0	0	0	0
	6	0	0	0	0	0	0

For element 2 (and all other elements), the local stiffness matrix is,

$\boldsymbol{k}^2$		2	3
	2	4	-4
	3	-4	4

And when placed in the global matrix, it becomes,

$\boldsymbol{K}^2$		1	2	3	4	5	6
	1	0	0	0	0	0	0
	2	0	4	-4	0	0	0
	3	0	-4	4	0	0	0
	4	0	0	0	0	0	0
	5	0	0	0	0	0	0
	6	0	0	0	0	0	0

And so forth, such that

$$\boldsymbol{K} = \mathop{\mathbf{A}}_{e=1}^{n_{el}} \boldsymbol{k}^e = \sum_{e=1}^{n_{el}} \boldsymbol{K}^e = \begin{bmatrix} 2 & -2 & 0 & 0 & 0 & 0 \\ -2 & 6 & -4 & 0 & 0 & 0 \\ 0 & -4 & 8 & -4 & 0 & 0 \\ 0 & 0 & -4 & 8 & -4 & 0 \\ 0 & 0 & 0 & -4 & 8 & -4 \\ 0 & 0 & 0 & 0 & -4 & 4 \end{bmatrix} \tag{2.68}$$

Assemble the global concentrated force vector in the same way as the stiffness matrix, or just place the concentrated forces at the corresponding dofs (but make sure they do not add up to more than what is applied), such that,

$$\boldsymbol{F}_F = \begin{bmatrix} R_1 \\ 7 \\ 12 \\ R_4 \\ 25 \\ R_6 \end{bmatrix} \tag{2.69}$$

Now, strike out rows and columns of $\boldsymbol{K}$ associated with the fixed dofs, and rows of $\boldsymbol{F}$ with fixed dof, such that,

$$\boldsymbol{K} = \begin{bmatrix} 6 & -4 & 0 \\ -4 & 8 & 0 \\ 0 & 0 & 8 \end{bmatrix} \quad ; \quad \boldsymbol{F}_F = \begin{bmatrix} 7 \\ 12 \\ 25 \end{bmatrix} \tag{2.70}$$

and solve for $\boldsymbol{d} = \begin{bmatrix} d_2 & d_3 & d_5 \end{bmatrix}^T = \begin{bmatrix} 3.25 & 3.125 & 3.125 \end{bmatrix}^T$. We post-process to calculate the element axial stress σ^e as,

$$\sigma^e = E\epsilon^e = E\boldsymbol{B}^e \cdot \boldsymbol{d}^e = E \begin{bmatrix} \frac{-1}{h^e} & \frac{1}{h^e} \end{bmatrix} \cdot \begin{bmatrix} d_1^e \\ d_2^e \end{bmatrix} \tag{2.71}$$

and for each element,

$$\sigma^1 = E\begin{bmatrix} \frac{-1}{4} & \frac{1}{4} \end{bmatrix} \cdot \begin{bmatrix} 0 \\ d_2 \end{bmatrix} = 2d_2 = 6.5 \tag{2.72}$$

$$\sigma^2 = E\begin{bmatrix} \frac{-1}{2} & \frac{1}{2} \end{bmatrix} \cdot \begin{bmatrix} d_2 \\ d_3 \end{bmatrix} = 4(d_3 - d_2) = -0.5 \tag{2.73}$$

$$\sigma^3 = -4d_3 = -12.5 \tag{2.74}$$

$$\sigma^4 = 4d_5 = 12.5 \tag{2.75}$$

$$\sigma^5 = -4d_5 = -12.5 \tag{2.76}$$

What do you notice about the stresses within the elements? Also, you can calculate the internal element axial force $N^e = \sigma^e A^e$.

We can plot the displacement and stress solution along the bar as (plot by hand to visualize),

$$\boldsymbol{d} = \begin{bmatrix} 0 & 3.25 & 3.125 & 0 & 3.125 & 0 \end{bmatrix}^T \tag{2.77}$$

$$\sigma^1 = 6.5\ ,\ \sigma^2 = -0.5\ ,\ \sigma^3 = -12.5\ ,\ \sigma^4 = 12.5\ ,\ \sigma^5 = -12.5 \tag{2.78}$$

Note that the internal axial element forces N^e do not equal the applied nodal forces at the respective nodes. Let us try to understand why. We revisit the Galerkin form (recall $E = 8$ and $A = 1$, and body force $f = 0$), where,

$$\int_0^{12} w^h_{,x} E A u^h_{,x} dx = w^h(4)7 + w^h(6)12 + w^h(10)25 \tag{2.79}$$

or since $\sigma^h = E\epsilon^h = Eu^h_{,x} = 8u^h_{,x}$, we have,

$$\int_0^{12} w^h_{,x} \sigma^h dx = 7c_2 + 12c_3 + 25c_5 \tag{2.80}$$

Should this equation hold? It better! We see that,

$$\int_0^{12} w^h_{,x}\sigma^h dx = \begin{bmatrix} c_1 & c_2 \end{bmatrix} \int_0^4 \begin{bmatrix} \frac{-1}{4} \\ \frac{1}{4} \end{bmatrix} 6.5dx \tag{2.81}$$

$$+ \begin{bmatrix} c_2 & c_3 \end{bmatrix} \int_4^6 \begin{bmatrix} \frac{-1}{2} \\ \frac{1}{2} \end{bmatrix} (-0.5)dx + \begin{bmatrix} c_3 & c_4 \end{bmatrix} \int_6^8 \begin{bmatrix} \frac{-1}{2} \\ \frac{1}{2} \end{bmatrix} (-12.5)dx$$

$$+ \begin{bmatrix} c_4 & c_5 \end{bmatrix} \int_8^{10} \begin{bmatrix} \frac{-1}{2} \\ \frac{1}{2} \end{bmatrix} 12.5dx + \begin{bmatrix} c_5 & c_6 \end{bmatrix} \int_{10}^{12} \begin{bmatrix} \frac{-1}{2} \\ \frac{1}{2} \end{bmatrix} (-12.5)dx$$

$$= (6.5 - (-0.5))c_2 + (-0.5 + 12.5)c_3 + (12.5 - (-12.5))c_5 = 7c_2 + 12c_3 + 25c_5$$

OK, in an integral average sense, the nodally applied forces balance in the Galerkin form! Recall that the Galerkin form is the discrete version of the Weak form.

2.6.3 Example 3

This example is taken from Pinsky [2001]. This example is the same as Example 2, except we have prescribed displacements as shown in Fig.2.13.

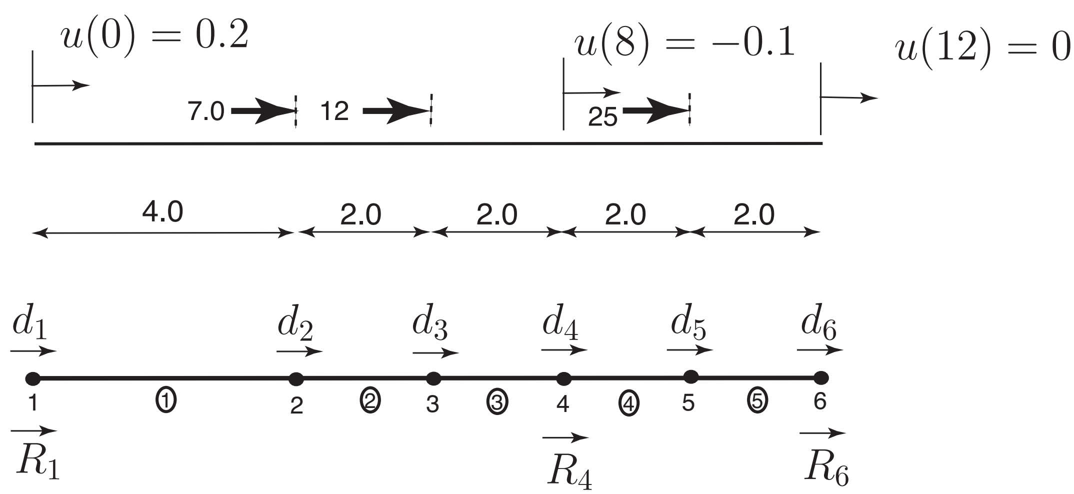

Figure 2.13. Example 3 for assembly procedure.

Recall the global stiffness matrix and force vector before applying essential BCs,

$$\boldsymbol{K} = \begin{bmatrix} 2 & -2 & 0 & 0 & 0 & 0 \\ -2 & 6 & -4 & 0 & 0 & 0 \\ 0 & -4 & 8 & -4 & 0 & 0 \\ 0 & 0 & -4 & 8 & -4 & 0 \\ 0 & 0 & 0 & -4 & 8 & -4 \\ 0 & 0 & 0 & 0 & -4 & 4 \end{bmatrix} \quad ; \quad \boldsymbol{F}_F = \begin{bmatrix} R_1 \\ 7 \\ 12 \\ R_4 \\ 25 \\ R_6 \end{bmatrix} \tag{2.82}$$

Then, cancel rows and columns associated with fixed displacements ($d_6 = 0$) as,

$$\boldsymbol{K} = \begin{bmatrix} 2 & -2 & 0 & 0 & 0 \\ -2 & 6 & -4 & 0 & 0 \\ 0 & -4 & 8 & -4 & 0 \\ 0 & 0 & -4 & 8 & -4 \\ 0 & 0 & 0 & -4 & 8 \end{bmatrix} \quad ; \quad \boldsymbol{F}_F = \begin{bmatrix} R_1 \\ 7 \\ 12 \\ R_4 \\ 25 \end{bmatrix} \tag{2.83}$$

and cancel rows associated with prescribed displacements such that,

$$\boldsymbol{K} = \begin{bmatrix} -2 & 6 & -4 & 0 & 0 \\ 0 & -4 & 8 & -4 & 0 \\ 0 & 0 & 0 & -4 & 8 \end{bmatrix} \quad ; \quad \boldsymbol{F}_F = \begin{bmatrix} 7 \\ 12 \\ 25 \end{bmatrix} \tag{2.84}$$

and multiply corresponding columns of $\boldsymbol{K}$ by prescribed displacements to calculate $\boldsymbol{F}_g$ as,

$$-\boldsymbol{F}_g = 0.2 \begin{bmatrix} -2 \\ 0 \\ 0 \end{bmatrix} + (-0.1) \begin{bmatrix} 0 \\ -4 \\ -4 \end{bmatrix} = \begin{bmatrix} -0.4 \\ 0.4 \\ 0.4 \end{bmatrix} \tag{2.85}$$

The total force vector is then,

$$\boldsymbol{F} = \boldsymbol{F}_F + \boldsymbol{F}_g = \begin{bmatrix} 7.4 \\ 11.6 \\ 24.6 \end{bmatrix} \tag{2.86}$$

The stiffness matrix is the same as the previous example, so the displacements can be calculated as,

$$\boldsymbol{d} = \begin{bmatrix} d_2 & d_3 & d_5 \end{bmatrix}^T = \begin{bmatrix} 3.3 & 3.1 & 3.075 \end{bmatrix}^T \tag{2.87}$$

In order to calculate the reaction forces, once we have the displacements, we calculate as follows,

$$\boldsymbol{d} = \begin{bmatrix} 0.2 & 3.3 & 3.1 & -0.1 & 3.075 & 0 \end{bmatrix}^T \tag{2.88}$$

$$\begin{bmatrix} R_1 \\ R_4 \\ R_6 \end{bmatrix} = \begin{bmatrix} 2 & -2 & 0 & 0 & 0 & 0 \\ 0 & 0 & -4 & 8 & -4 & 0 \\ 0 & 0 & 0 & 0 & -4 & 4 \end{bmatrix} \cdot \begin{bmatrix} d_1 \\ d_2 \\ d_3 \\ d_4 \\ d_5 \\ d_6 \end{bmatrix} = \begin{bmatrix} -6.2 \\ -25.5 \\ -12.3 \end{bmatrix} \tag{2.89}$$

2.7 Numerical integration - Gaussian Quadrature

It is not possible always to evaluate in closed-form the integral for an element stiffness matrix or forcing vector. Thus, we resort to numerical integration (even if the integral can be evaluated analytically for special cases: i.e., element shape, etc.); see Sect.3.8 of Hughes [1987]. Consider our example in 1D as,

$$\int_{\Omega^e} \psi(x)dx = \int_{-1}^{1} \hat{\psi}(\xi) j^e(\xi) d\xi \tag{2.90}$$

First, let us introduce an **integration rule** as follows,

$$\int_{-1}^{1} g(\xi)d\xi = \left(\sum_{l=1}^{n_{int}} g(\tilde{\xi}_l) W_l \right) + R \approx \sum_{l=1}^{n_{int}} g(\tilde{\xi}_l) W_l \tag{2.91}$$

where n_{int} is the number of integration points, $\tilde{\xi}_l$ is the natural coordinate of integration point l, W_l is the 'weight' of the lth integration point, and R the remainder.

Examples of rules:

1. **trapezoidal rule:**

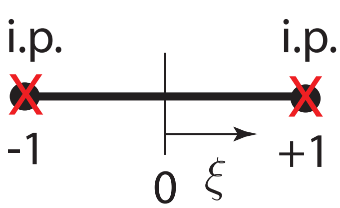

- $n_{int} = 2$
- $\tilde{\xi}_1 = -1$, $\tilde{\xi}_2 = 1$
- $W_l = 1$ for $l = 1, 2$
- $R = (-2/3) g_{,\xi\xi}(\tilde{\xi})$, $\tilde{\xi} \in [-1, 1]$

This rule is 2nd order accurate since it can exactly integrate constants and linear polynomials, but is approximate for higher order polynomials or non-polynomial functions.

2. **Simpson's rule:**

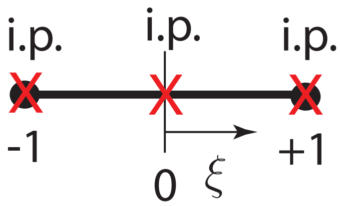

- $n_{int} = 3$
- $\tilde{\xi}_1 = -1$, $\tilde{\xi}_2 = 0$, $\tilde{\xi}_3 = 1$
- $W_1 = W_3 = 1/3$, $W_2 = 4/3$
- $R = (-1/90)g_{,\xi\xi\xi\xi}(\tilde{\xi})$, $\tilde{\xi} \in [-1, 1]$

This rule is 4th order accurate because it can integrate polynomials up to 3rd order (cubic) exactly.

BUT there is an integration rule just as accurate that uses fewer i.p.'s, and thus is more efficient computationally; it is called **Gaussian quadrature**.

Gaussian quadrature is exact only for polynomials, and approximate otherwise, but we use it regardless because it is efficient computationally (stability considerations are beyond the scope of this discussion; let us assume for the problems we are considering that Gaussian quadrature remains stable, i.e., there are no oscillations of strain and stress spatially along the Gauss points of an element).

1. **1pt (2nd order accurate):**

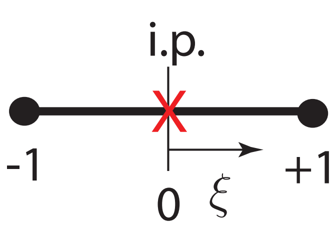

- $n_{int} = 1$
- $\tilde{\xi}_1 = 0$
- $W_1 = 2$
- $R = (1/3)g_{,\xi\xi}(\tilde{\xi})$, $\tilde{\xi} \in [-1, 1]$

2. **2pt (4th order accurate):**

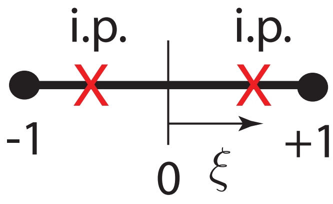

- $n_{int} = 2$
- $\tilde{\xi}_1 = -1/\sqrt{3}$, $\tilde{\xi}_2 = 1/\sqrt{3}$
- $W_1 = W_2 = 1$
- $R = (1/135)g_{,\xi\xi\xi\xi}(\tilde{\xi})$, $\tilde{\xi} \in [-1, 1]$

3. **3pt (6th order accurate):**

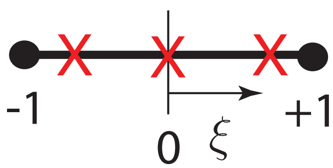

- $n_{int} = 3$
- $\tilde{\xi}_1 = -\sqrt{3/5}$, $\tilde{\xi}_2 = 0$, $\tilde{\xi}_3 = \sqrt{3/5}$
- $W_1 = W_3 = 5/9$, $W_2 = 8/9$
- $R = (1/15750)g_{,\xi\xi\xi\xi\xi\xi}(\tilde{\xi})$, $\tilde{\xi} \in [-1, 1]$

Recall our example $\hat{\psi}(\xi) = a + b(5 + \xi)^2$, where the analytical solution is,

$$\int_{-1}^{1} \left[a + b(5 + \xi)^2\right] d\xi = 2a + (50 + \frac{2}{3})b \tag{2.92}$$

Let us try 1pt and 2pt Gaussian quadrature rules as follows,

1. **1pt:**

$$\int_{-1}^{1} g(\xi) d\xi \approx 2g(0) = 2(a + 25b) \tag{2.93}$$

This is an approximate integration.

2. **2pt:**

$$\int_{-1}^{1} g(\xi) d\xi \approx g\left(\frac{-1}{\sqrt{3}}\right) + g\left(\frac{1}{\sqrt{3}}\right) = 2a + (50 + \frac{2}{3})b \tag{2.94}$$

This is exact integration!

2.8 Convergence of FEM

We only expect a convergent FE solution for **well-posed** partial differential equations (PDEs). A PDE is well-posed if it has the following properties:

1. **existence**: there exists *at least* one solution $u(x)$ satisfying the differential equation and BCs.

2. **uniqueness**: there is *at most* one solution $u(x)$ satisfying the differential equation and BCs.

3. **stability**: the unique solution $u(x)$ depends in a stable manner on the data of problem (i.e., spatial domain, BCs, material properties, ..., any input). If there is a small change in the data, there should be a small change in the solution $u(x)$.

Convergence is of particular concern for *computational failure mechanics simulations*, where, for example, classical strain softening plasticity leads to an **ill-posed** PDE regardless of whether the FEM is convergent for strain hardening plasticity and elasticity.

For example, consider a plane strain compression test on dense sand [Vardoulakis et al., 1978, Vardoulakis and Goldschieder, 1981] in Fig.2.14.

There is mesh-dependence associated with a classical, strain softening local plasticity model. We observe a finer shear band width as the mesh is refined (function of element size) in Fig.2.15.

We can replicate this result in Abaqus. We observe a softening curve approaching the force axis upon further refinement in Fig.2.16.

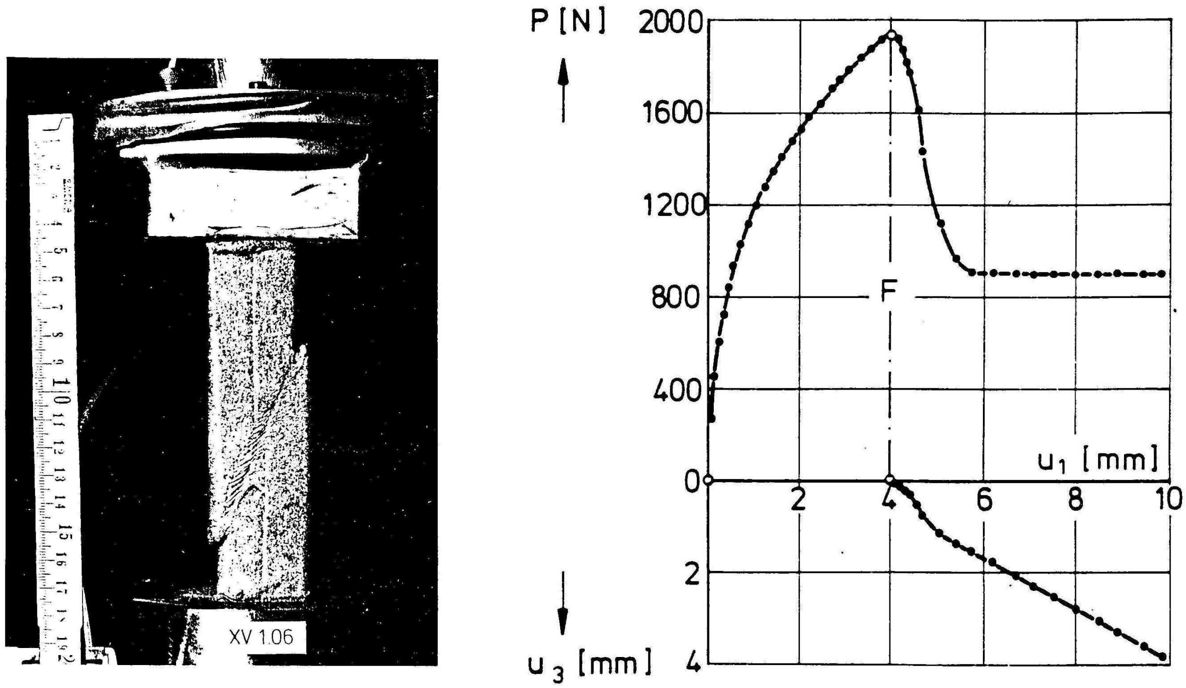

Figure 2.14. Shear banding in dense sand, and post-peak softening [Vardoulakis et al., 1978, Vardoulakis and Goldschieder, 1981].

To obtain convergence, we expect that as the mesh is refined $h \to 0$, the discrete FE solution approaches the exact solution of the PDE, such that,

$$\lim_{h\to 0} u^h(x) = u(x) \tag{2.95}$$

For convergence, we require two things: (I) **compatibility** of u^h, and (II) **completeness** of u^h. For the purpose of discussion, consider (S), (W), and (G) of the Bernoulli-Euler beam without derivation (see Chapter 3 and Pinsky [2001]). We assume a thin, long structure experiencing transverse deflection (transverse shear deformation is negligible) as shown in Fig.2.17, where $v(x)$ is the transverse deflection, $EI(x)$ is the flexural rigidity, $f(x)$ is the transverse distributed force, F is the transverse point load, and M_L is the moment at $x = L$.

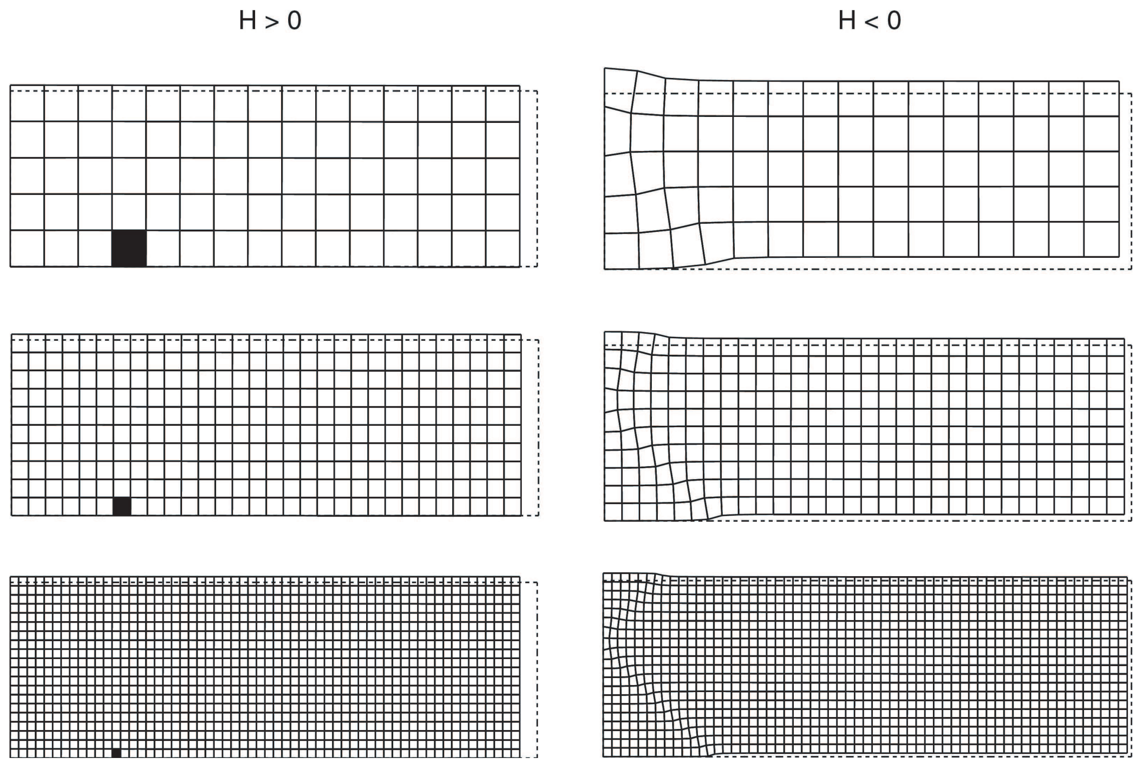

Figure 2.15. Plane strain compression with one element in each mesh (colored black) with lower yield stress, and deformed meshes for hardening $H > 0$ and softening $H < 0$.

We write the Strong form (S) for the Bernoulli-Euler beam as,

$$(S)\begin{cases} \text{Find } v(x) : \bar{\Omega} \mapsto \mathbb{R}, \quad \bar{\Omega} = [0, L], \quad \text{such that} \\ \frac{d^2}{dx^2}\left(EI(x)\frac{d^2 v}{dx^2}\right) = f(x) & x \in \Omega \\ v = 0 & x = 0 \\ v_{,x} = 0 & x = 0 \\ EIv_{,xx} = M_L & x = L \\ -(EIv_{,xx})_{,x} = F & x = L \end{cases} \tag{2.96}$$

where v is the transverse displacement, $v_{,x}$ is the 'rotation' (assuming small transverse deflections), $EIv_{,xx}$ is the internal bending moment, and $-(EIv_{,xx})_{,x}$ is the internal shear force.

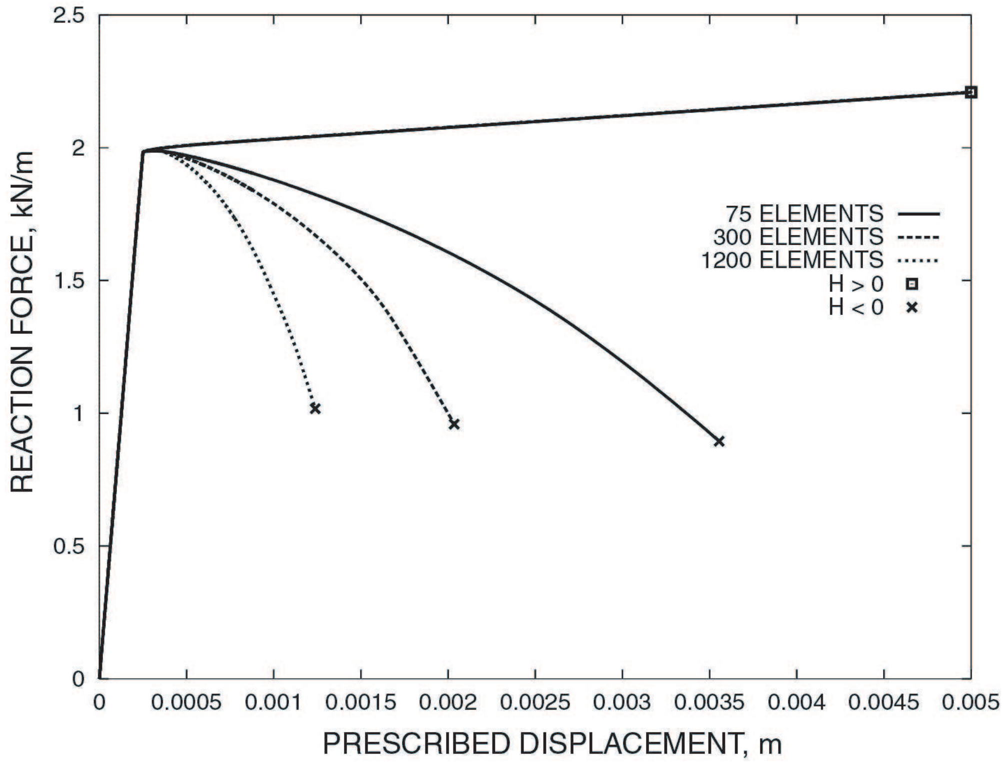

Figure 2.16. Force versus displacement plot for plane strain compression, showing less dissipation for finer shear band mesh.

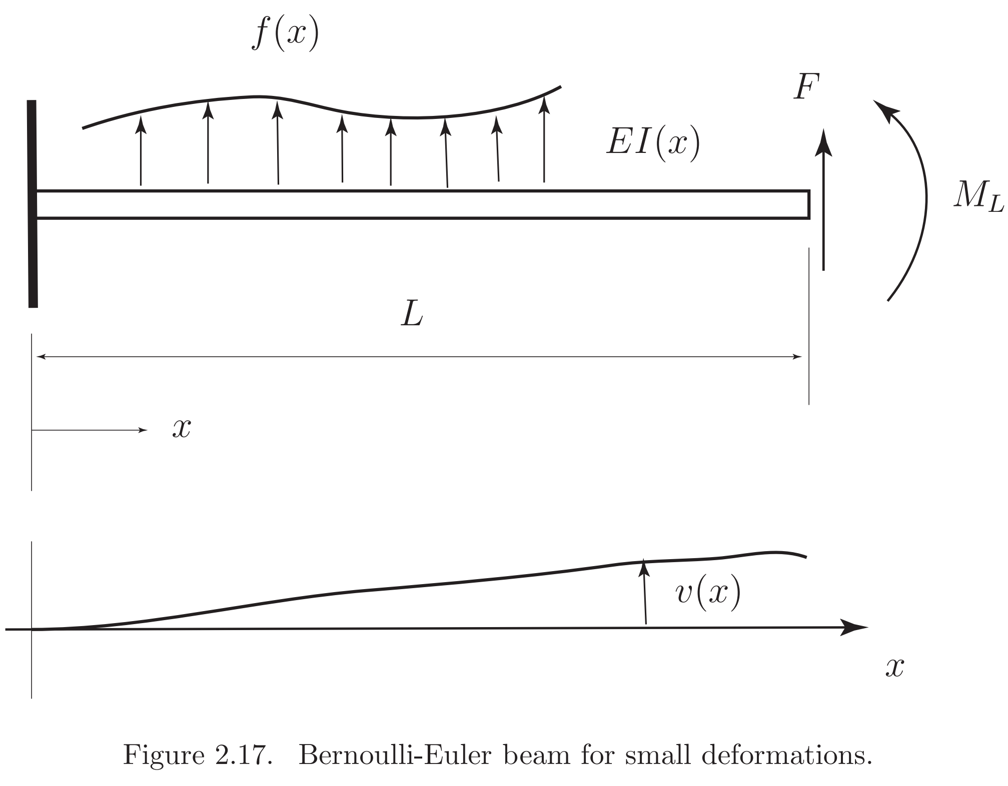

Figure 2.17. Bernoulli-Euler beam for small deformations.

2.8.1 Compatibility

There is a general rule for BCs for a linear differential equation of order $2m$ such that,

$$\text{essential}\begin{cases} 0 \\ 1 \\ \vdots \\ m-1 \end{cases} \qquad \text{natural}\begin{cases} m \\ m+1 \\ \vdots \\ 2m-1 \end{cases}$$

where m will be the order of the variational equation. Let us consider our two examples, a (1) bar, and (2) beam:

(1) bar: $2m = 2 \Longrightarrow m = 1$

$$\begin{array}{rll} \text{essential} & 0 & u \\ \text{natural} & 1 & EAu_{,x} \end{array}$$

(2) beam: $2m = 4 \Longrightarrow m = 2$

$$\text{essential}\begin{cases} 0 & v \\ 1 & v_{,x} \end{cases} \qquad \text{natural}\begin{cases} 2 & EIv_{,xx} \\ 3 & -(EIv_{,xx})_{,x} \end{cases}$$

The Weak form (integration by parts twice) for the B-E beam may be written as,

$$(W)\begin{cases} \text{Find } v(x) \in \mathscr{S} = \{v : \Omega \mapsto \mathbb{R}, v \in H^2, v(0) = 0, v_{,x}(0) = 0\}, \text{such that} \\ \int_0^L w_{,xx} EIv_{,xx} dx = \int_0^L wf dx + w(L)F + w_{,x}(L)M_L \\ \text{holds } \forall w(x) \in \mathscr{V} = \{w : \Omega \mapsto \mathbb{R}, w \in H^2, w(0) = 0, w_{,x}(0) = 0\} \end{cases} \tag{2.97}$$

where v and w are in H^2 (2nd Sobolev space) so that the variational equation is defined (i.e., the internal strain energy is finite), such that,

$$H^2(\Omega) = \left(v : \Omega \mapsto \mathbb{R}, \int_\Omega \left[v^2 + (v_{,x})^2 + (v_{,xx})^2 \right] dx < \infty \right) \tag{2.98}$$

This means that v is continuous, $v_{,x}$ is continuous, and $v_{,xx}$ may be discontinuous; i.e., we can define the square of a Heaviside function but NOT the square of a Dirac-Delta function, such that,

$$\int_\Omega [H(x-a)]^2 g(x)dx = \int_a^L g(x)dx \tag{2.99}$$

$$\int_\Omega [\delta(x-a)]^2 g(x)dx = \text{no definition} \tag{2.100}$$

Thought exercise: consider if v is continuous, $v_{,x}$ is discontinuous, and thus $v_{,xx}$ is a Delta function. What would happen with the variational equation? Is it defined? Let us draw a figure.

Recall the bar problem for which $u \in H^1(\Omega)$ and,

$$H^1(\Omega) = \left(u : \Omega \mapsto \mathbb{R}, \int_\Omega \left[u^2 + (u_{,x})^2 \right] dx < \infty \right) \tag{2.101}$$

Thus, u must be continuous, or $\mathscr{S} \subset C^0(\Omega)$, where $C^0(\Omega)$ is the space of continuous functions.

The Galerkin form for the B-E beam is written as follows,

$$(G) \begin{cases} \text{Find } v^h(x) \in \mathscr{S}^h = \{v^h : \Omega^h \mapsto \mathbb{R}, v^h \in H^2, v^h(0) = 0, v^h_{,x}(0) = 0\}, \text{such that} \\ \int_0^L w^h_{,xx} EI v^h_{,xx} dx = \int_0^L w^h f dx + w^h(L)F + w^h_{,x}(L) M_L \\ \text{holds } \forall w^h(x) \in \mathscr{V}^h = \{w^h : \Omega^h \mapsto \mathbb{R}, w^h \in H^2, w^h(0) = 0, w^h_{,x}(0) = 0\} \end{cases} \tag{2.102}$$

Thus, this requires $v^h \in \mathscr{S}^h \subset C^1(\Omega^h)$, or that v^h and $v^h_{,x}$ must be **continuous at the**

nodes, or that there are **2 dofs per node:** (i) transverse displacement v^h, and (ii) rotation $v^h_{,x}$. Thus, **Compatibility** states: $u^h(x) \in C^{m-1}(\Omega^h)$, or that

$$\text{bar } u^h \in C^0(\Omega^h) \quad ; \quad \text{beam } v^h \in C^1(\Omega^h)$$

2.8.2 Completeness

Completeness states that for the mth derivative in the variational equation, the FE approximation u^h must represent up to an mth-order polynomial. For example:

- **bar:** $m = 1 \Longrightarrow$ 1st order polynomial

$$\begin{aligned} u^h(x) &= a_0 + a_1 x + \text{h.o.t.s} \\ & a_0 = \text{rigid body motion} \\ & a_1 = \text{constant axial strain} \end{aligned} \tag{2.103}$$

- **beam:** $m = 2 \Longrightarrow$ 2nd order polynomial

$$\begin{aligned} v^h(x) &= a_0 + a_1 x + a_2 x^2 + \text{h.o.t.s} \\ & a_0 = \text{rigid body translation} \\ & a_1 = \text{rigid body rotation} \\ & a_2 = \text{constant curvature} \end{aligned} \tag{2.104}$$

For **isoparametric elements**, completeness is satisfied automatically to 1st order such that,

1. $\sum_{a=1}^{n_{\text{en}}} N_a(\xi) = 1$

2. $x^{h^e}(\xi) = \boldsymbol{N}^e(\xi) \cdot \boldsymbol{x}^e$

We consider as an example the 1D linear bar element as,

1. $\sum_{a=1}^{n_{en}} N_a(\xi) = N_1 + N_2 = \frac{1}{2}(1-\xi) + \frac{1}{2}(1+\xi) = 1$

2. $x^{h^e}(\xi) = \boldsymbol{N}^e(\xi) \cdot \boldsymbol{x}^e = \sum_{a=1}^{n_{en}} N_a(\xi) x_a^e$

Let $d_a^e = u^{h^e}(x_a^e) = a_0 + a_1 x_a^e$, where then

$$u^{h^e}(\xi) = \boldsymbol{N}^e \cdot \boldsymbol{d}^e = \sum_{a=1}^{2} N_a(\xi) d_a^e = \sum_{a=1}^{2} N_a(\xi)(a_0 + a_1 x_a^e) \tag{2.105}$$

$$= \left(\sum_{a=1}^{n_{en}} N_a\right) a_0 + \left(\sum_{a=1}^{n_{en}} N_a x_a^e\right) a_1 \tag{2.106}$$

$$= a_0 + a_1 x \tag{2.107}$$

Thus, it is complete to first order.

Generally speaking, the **rate of convergence** increases as $h \to 0$ depending on the order of polynomial shape function used (2-node linear versus 3-node quadratic 1D element); for **linear analysis**, it is often preferred to use quadratic elements because the rate of convergence is a factor of 2 more accurate than a linear element. For nonlinear analysis, other factors may dominate (such as convergence of the iterative nonlinear solver, rather than convergence of the mesh size).

2.9 Elastodynamics

Refer to Chapters 7 and 9 of Hughes [1987].

include more details here: D'Alembert's principle, and Hamilton's principle

We now include inertia terms, where loading is no longer quasi-static, thus acceleration and wave propagation become important. Reconsider the bar element, now with inertia (Newton's second law of motion):

$$\sum_{\rightarrow +} F_x = m\ddot{u} \; , \quad m = \int_\Omega \rho A dx \tag{2.108}$$

where ρ (kg/m^3) is the mass density. Also consider Rayleigh damping in two forms:

include equations from Rayleigh's Theory of Sound, and scans of pages showing linear form?

1. **mass proportional** (like moving in a viscous fluid):

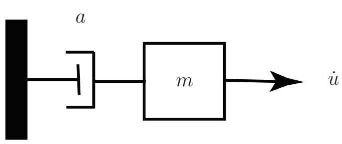

$$\Longrightarrow \; \rho A(a\dot{u}) \tag{2.109}$$

2. **stiffness proportional** ("viscoelasticity"; Kelvin-Voigt element):

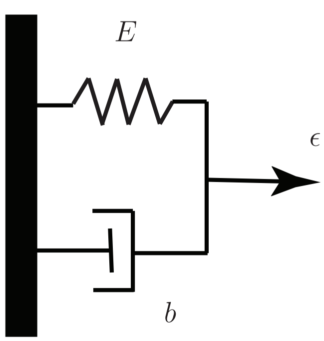

$$\sigma = E(\epsilon + b\dot{\epsilon}) \tag{2.110}$$

The stress is dependent on the axial "strain-rate" of the bar, or how quickly it deforms.

Given the differential form, BCs, and ICs, we may state the Strong Form as,

$$
(S)\left\{\begin{array}{rcll}
\multicolumn{4}{l}{\text{Find } u(x,t):\bar{\Omega}\times[0,T]\mapsto\mathbb{R},\quad \bar{\Omega}=[0,L],\quad \text{such that}} \\
\rho A\left(\frac{\partial^2 u}{\partial t^2}+a\frac{\partial u}{\partial t}\right) & & & \\
-\frac{\partial}{\partial x}\left[EA\left(\frac{\partial u}{\partial x}+b\frac{\partial^2 u}{\partial x\partial t}\right)\right] & = & f(x,t) & x\in\Omega, t\in(0,T) \\
u(0,t) & = & g(t) & x=0, t\in(0,T) \\
\sigma(t)A & = & F(t) & x=L, t\in(0,T) \\
u(x,0) & = & u_0(x) & x\in\Omega, t=0 \\
\dot{u}(x,0) & = & \dot{u}_0(x) & x\in\Omega, t=0
\end{array}\right. \tag{2.111}
$$

where $u(x,t) : \bar{\Omega} \times [0,T] \mapsto \mathbb{R}$ reads "with x in $\bar{\Omega}$, and t in $[0,T]$, u maps to the real number line $\mathbb{R}$," distributed axial force $f(x,t)$ is a body force that can be a function of time t, concentrated force $F(t)$ is a natural, or Neumann, BC, prescribed displacement $g(t)$ is an essential, or Dirichlet, BC, $u_0(x)$ and $\dot{u}_0(x)$ are the initial displacement and velocity, respectively, which can vary with x over the length of the bar.

Going through the derivation of the Weak form and Galerkin form as before, and recognizing that the time derivatives of the finite element displacement $u^{h^e}(\xi,t)$ are applied to the nodal dofs as,

$$
\begin{aligned}
\dot{u}^{h^e}(\xi,t) &= \sum_{a=1}^{n_{en}} N_a(\xi)\dot{d}_a^e(t)\ , \quad \ddot{u}^{h^e}(\xi,t) = \sum_{a=1}^{n_{en}} N_a(\xi)\ddot{d}_a^e(t) \\
\dot{u}_{,x}^{h^e}(\xi,t) &= \sum_{a=1}^{n_{en}} N_{a,x}(\xi)\dot{d}_a^e(t)
\end{aligned} \tag{2.112}
$$

we have the FE matrix form before assembly as,

$$
\mathop{\mathbf{A}}_{e=1}^{n_{\text{el}}} (\boldsymbol{c}^e)^T \cdot \left\{ \boldsymbol{m}^e \cdot \ddot{\boldsymbol{d}}^e + \boldsymbol{c}^e_{\text{damp}} \cdot \dot{\boldsymbol{d}}^e + \boldsymbol{k}^e \cdot \boldsymbol{d}^e = \boldsymbol{f}^e_f + \boldsymbol{f}^e_F \right\} \tag{2.113}
$$

where the element mass and damping matrices are,

$$\boldsymbol{m}^e = \int_{\Omega^e} \rho A (\boldsymbol{N}^e)^T \cdot \boldsymbol{N}^e dx = \int_{-1}^{1} \rho A (\boldsymbol{N}^e)^T \cdot \boldsymbol{N}^e j^e d\xi \ , \quad \boldsymbol{c}^e_{\text{damp}} = a\boldsymbol{m}^e + b\boldsymbol{k}^e \tag{2.114}$$

After element assembly, we have

$$\boldsymbol{M} \cdot \ddot{\boldsymbol{d}} + \boldsymbol{C} \cdot \dot{\boldsymbol{d}} + \boldsymbol{K} \cdot \boldsymbol{d} = \boldsymbol{F}_f + \boldsymbol{F}_F + \boldsymbol{F}_g \tag{2.115}$$

Before we integrate these FE equations discretely in time using Newmark's method, let is consider a **modal analysis** using the FE equations. We consider the geometry and properties for 2 equal-length linear elements in Fig.2.18.

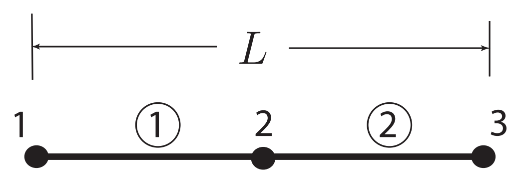

Figure 2.18. Two-element mesh for modal analysis example.

The length $L = 15$ and properties $EA = 60$, $\rho A = 1$, $a = b = 0 \Longrightarrow \boldsymbol{c}^e_{\text{damp}} = \boldsymbol{0}$ (no damping), and BC $u(0, t) = 0$. The stiffness matrices are,

$$\boldsymbol{k}^1 = \boldsymbol{k}^2 = \begin{bmatrix} 8 & -8 \\ -8 & 8 \end{bmatrix} \tag{2.116}$$

and the mass matrices are,

$$\boldsymbol{m}^e = \int_{-1}^{1} \rho A (\boldsymbol{N}^e)^T \cdot \boldsymbol{N}^e j^e d\xi \ , \quad \boldsymbol{N}^e(\xi) = \begin{bmatrix} N_1(\xi) & N_2(\xi) \end{bmatrix} \tag{2.117}$$

$$\boldsymbol{m}^1 = \boldsymbol{m}^2 = \frac{5}{4} \begin{bmatrix} 2 & 1 \\ 1 & 2 \end{bmatrix} \tag{2.118}$$

During assembly, we account for the essential BC, $d_1 = c_1 = 0$, such that,

$$\boldsymbol{M} = \frac{5}{4}\begin{bmatrix} 2 & 1 & 0 \\ 1 & 4 & 1 \\ 0 & 1 & 2 \end{bmatrix}, \quad \boldsymbol{K} = \begin{bmatrix} 8 & -8 & 0 \\ -8 & 16 & -8 \\ 0 & -8 & 8 \end{bmatrix} \tag{2.119}$$

But $\boldsymbol{d}(t)$ is still time dependent. Thus, we formulate an **eigenvalue problem** using the FE matrix equations. For example, assume that,

$$\boldsymbol{d}(t) = \cos(\omega t)\boldsymbol{\phi} \Longrightarrow \ddot{\boldsymbol{d}}(t) = -\omega^2 \cos(\omega t)\boldsymbol{\phi} \tag{2.120}$$

where ω is the circular frequency (rad/s), and $\boldsymbol{\phi}$ the mode shape (m). We have an eigenvalue problem written as,

$$\boldsymbol{M} \cdot \ddot{\boldsymbol{d}} + \boldsymbol{K} \cdot \boldsymbol{d} = \boldsymbol{0} \Longrightarrow (\boldsymbol{K} - \lambda \boldsymbol{M}) \cdot \boldsymbol{\phi} = \boldsymbol{0} \tag{2.121}$$

where eigenvalue $\lambda = \omega^2$. We can solve in Mathematica or Python or other program that has an eigensolver. The solution (only 2 modes because only 2 dofs) is as follows:

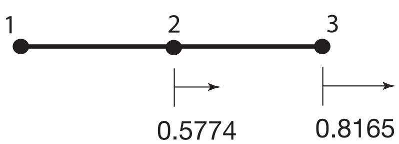

$$\lambda_1 = 0.692$$

$$\boldsymbol{\phi}_1 = \begin{bmatrix} 0.5774 & 0.8165 \end{bmatrix}^T$$

$$\text{analytical} : \lambda_1 = \omega_1^2 = \left(\frac{\pi}{2}\right)^2 \frac{EA}{\rho L^2} = 0.658$$

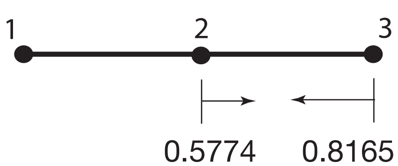

$$\lambda_2 = 8.45$$

$$\boldsymbol{\phi}_2 = \begin{bmatrix} 0.5774 & -0.8165 \end{bmatrix}^T$$

$$\text{analytical} : \lambda_2 = \left(\frac{3\pi}{2}\right)^2 \frac{EA}{\rho L^2} = 5.922$$

We note that the 2-element mesh is quite stiff, meaning the eigenvalues λ are higher than the analytical solution (i.e., the circular frequencies ω predicted by the modal FEA are higher than the analytical solution). The first mode is reasonably close (0.866 vs 0.658), whereas the second mode of the FE solution is much stiffer (10.563 vs 5.922).

To **integrate in time the finite element equations**, recall first the FE equations as,

$$\boldsymbol{M} \cdot \ddot{\boldsymbol{d}}(t) + \boldsymbol{C} \cdot \dot{\boldsymbol{d}}(t) + \boldsymbol{K} \cdot \boldsymbol{d}(t) = \boldsymbol{F}(t) \tag{2.122}$$

$$\boldsymbol{F}(t) = \boldsymbol{F}_f(t) + \boldsymbol{F}_F(t) + \boldsymbol{F}_g(t) \tag{2.123}$$

We can solve using a **finite differencing in time** to obtain an approximate solution over time, such as Newmark's method [Hughes, 1987]. First, we introduce some notation and terminology as follows,

$$\text{time increment } \Delta t = t_{n+1} - t_n$$

$$t_{n+1} = \text{current time at step } n+1$$

$$t_n = \text{past (known) time at step } n$$

We solve for

$$\begin{aligned} \text{displacement at time } t_{n+1}, \quad \boldsymbol{d}_{n+1} &= \boldsymbol{d}(t_{n+1}) \\ \text{velocity at time } t_{n+1}, \quad \boldsymbol{v}_{n+1} &= \dot{\boldsymbol{d}}(t_{n+1}) \\ \text{acceleration at time } t_{n+1}, \quad \boldsymbol{a}_{n+1} &= \ddot{\boldsymbol{d}}(t_{n+1}) \end{aligned}$$

given

$$\begin{aligned} \text{displacement at time } t_n, \quad \boldsymbol{d}_n &= \boldsymbol{d}(t_n) \\ \text{velocity at time } t_n, \quad \boldsymbol{v}_n &= \dot{\boldsymbol{d}}(t_n) \\ \text{acceleration at time } t_n, \quad \boldsymbol{a}_n &= \ddot{\boldsymbol{d}}(t_n) \end{aligned}$$

The procedure is carried out as follows. We are given $\boldsymbol{d}_n$, $\boldsymbol{v}_n$, and $\boldsymbol{a}_n$ from the previous time step, and we need to solve for $\boldsymbol{d}_{n+1}$, $\boldsymbol{v}_{n+1}$, and $\boldsymbol{a}_{n+1}$ at the current time step, whereby,

$$\boldsymbol{M} \cdot \boldsymbol{a}_{n+1} + \boldsymbol{C} \cdot \boldsymbol{v}_{n+1} + \boldsymbol{K}\boldsymbol{d}_{n+1} = \boldsymbol{F}_{n+1} \tag{2.124}$$

$$\boldsymbol{d}_{n+1} = \boldsymbol{d}_n + \Delta t \boldsymbol{v}_n + \frac{\Delta t^2}{2}\left[(1-2\beta)\boldsymbol{a}_n + 2\beta \boldsymbol{a}_{n+1}\right] \tag{2.125}$$

$$\boldsymbol{v}_{n+1} = \boldsymbol{v}_n + \Delta t\left[(1-\gamma)\boldsymbol{a}_n + \gamma \boldsymbol{a}_{n+1}\right] \tag{2.126}$$

where γ, β are **integration parameters**. We can substitute to solve for $\boldsymbol{a}_{n+1}$, and then $\boldsymbol{d}_{n+1}$ and $\boldsymbol{v}_{n+1}$. First, we introduce "predictors" from known values as,

$$\tilde{\boldsymbol{d}}_{n+1} = \boldsymbol{d}_n + \Delta t \boldsymbol{v}_n + \frac{\Delta t^2}{2}(1-2\beta)\boldsymbol{a}_n \tag{2.127}$$

$$\tilde{\boldsymbol{v}}_{n+1} = \boldsymbol{v}_n + \Delta t(1-\gamma)\boldsymbol{a}_n \tag{2.128}$$

such that

$$\boldsymbol{d}_{n+1} = \tilde{\boldsymbol{d}}_{n+1} + \beta \Delta t^2 \boldsymbol{a}_{n+1} \tag{2.129}$$

$$\boldsymbol{v}_{n+1} = \tilde{\boldsymbol{v}}_{n+1} + \gamma \Delta t \boldsymbol{a}_{n+1} \tag{2.130}$$

To initialize time-stepping, we must solve for the initial acceleration $\boldsymbol{a}_0$ from the FE equation as,

$$\boldsymbol{M} \cdot \boldsymbol{a}_0 = \boldsymbol{F}_0 - \boldsymbol{C} \cdot \boldsymbol{v}_0 - \boldsymbol{K}\boldsymbol{d}_0 \tag{2.131}$$

Then we solve for $\boldsymbol{a}_{n+1}$ as,

$$\left(\boldsymbol{M} + \gamma \Delta t \boldsymbol{C} + \beta \Delta t^2 \boldsymbol{K}\right)\boldsymbol{a}_{n+1} = \boldsymbol{F}_{n+1} - \boldsymbol{C}\tilde{\boldsymbol{v}}_{n+1} - \boldsymbol{K}\tilde{\boldsymbol{d}}_{n+1} \tag{2.132}$$

and we can update $\boldsymbol{d}_{n+1}$ and $\boldsymbol{v}_{n+1}$ from the above equations.

For linear problems, and symmetric matrices, the numerical stability regimes for choices of integration parameters are (see pg.493 of Hughes [1987]):

unconditional, $2\beta \geq \gamma \geq 1/2$; or

conditional, $\gamma \geq 1/2$, $\beta < \gamma/2$;

and $\omega^h \Delta t \leq \Omega_{\text{crit}}$ (undamped frequency ω^h, critical sampling frequency Ω_{crit}), where,

$$\Omega_{\text{crit}} = \frac{\zeta(\gamma - 1/2) + \left[\frac{\gamma}{2} - \beta + \zeta^2(\gamma - 1/2)^2\right]^{1/2}}{(\gamma/2 - \beta)} \tag{2.133}$$

and $\zeta = (a/\omega + b\omega)/2$ is the damping coefficient. This analysis assumes that the FE system could be reduced to a single dof problem using modal decomposition (which will hold for linear problems and Rayleigh damping), such that if $\gamma = 1/2$, damping has no effect on stability, and if $\gamma > 1/2$, damping increases the critical time step. Thus, it is a conservative estimate (if ζ is unknown) to assume the undamped ($\zeta = 0$) critical sampling frequency as,

$$\Omega_{\text{crit}} = \frac{1}{\sqrt{\gamma/2 - \beta}} \Longrightarrow \Delta t \leq \frac{\Omega_{\text{crit}}}{\omega^h_{\max}} \tag{2.134}$$

We will consider two choices of parameters leading to two classic time integrators for elastodynamics:

1. **trapezoidal rule:** implicit (requires solution of $\boldsymbol{Ax} = \boldsymbol{b}$), $\beta = 1/4$, $\gamma = 1/2$, unconditionally stable, order of accuracy = 2 (error $\mathcal{O}(\Delta t^2)$)

2. **central difference:** explicit (no solution of $\boldsymbol{Ax} = \boldsymbol{b}$, assuming $\boldsymbol{M}$ and $\boldsymbol{C}$ are diagonalizable, or lumped), $\beta = 0$, $\gamma = 1/2$, $\Omega_{\text{crit}} = 2$, order of accuracy = 2

For conditionally stable schemes, such as central difference, $\omega^h_{\max}$ will depend on the element type. Consider the 2-node linear element, such that $\omega^h_{\max} = \sqrt{\lambda^h_{\max}} = 2\sqrt{3}c/h$, where h is taken to be the smallest element length. Recall the bar wave velocity $c = \sqrt{E/\rho}$, then $\Delta t \leq \frac{\Omega_{\text{crit}}}{\omega^h_{\max}} = \frac{h}{c\sqrt{3}}$ for 1D wave propagation using linear finite elements.

This page intentionally left blank.

Chapter 3

2D Linear Frame Analysis with FEM

For the 2D linear frame FEM, we assume linearity in the form of small strain, linear isotropic elasticity. These notes are drawn from Pinsky [2001]. Topics covered in remaining sections include the following:

(1) differential equation and Strong (S) form for Bernoulli-Euler beam;

(2) Weak form (W) for Bernoulli-Euler beam;

(3) Galerkin form (G) for Bernoulli-Euler beam;

(4) Finite Element (FE) matrix form for Bernoulli-Euler beam;

(5) Example of FE assembly for beam element;

(6) 2D frame FE;

(7) 2D frame analysis examples.

3.1 Differential equation and Strong (S) form for Bernoulli-Euler beam

Bernoulli-Euler beam theory assumes a thin, long structure experiences transverse deflection (transverse shear deformation is negligible), such as that shown in Fig.3.1, where,

$$
\begin{aligned}
v(x) &= \text{transverse deflection}(m) \\
EI(x) &= \text{flexural rigidity}(Nm^2) \\
f(x) &= \text{transverse distributed load}(N/m) \\
F_L &= \text{transverse point load}(N) \\
M_L &= \text{moment at } x = L(Nm)
\end{aligned}
$$

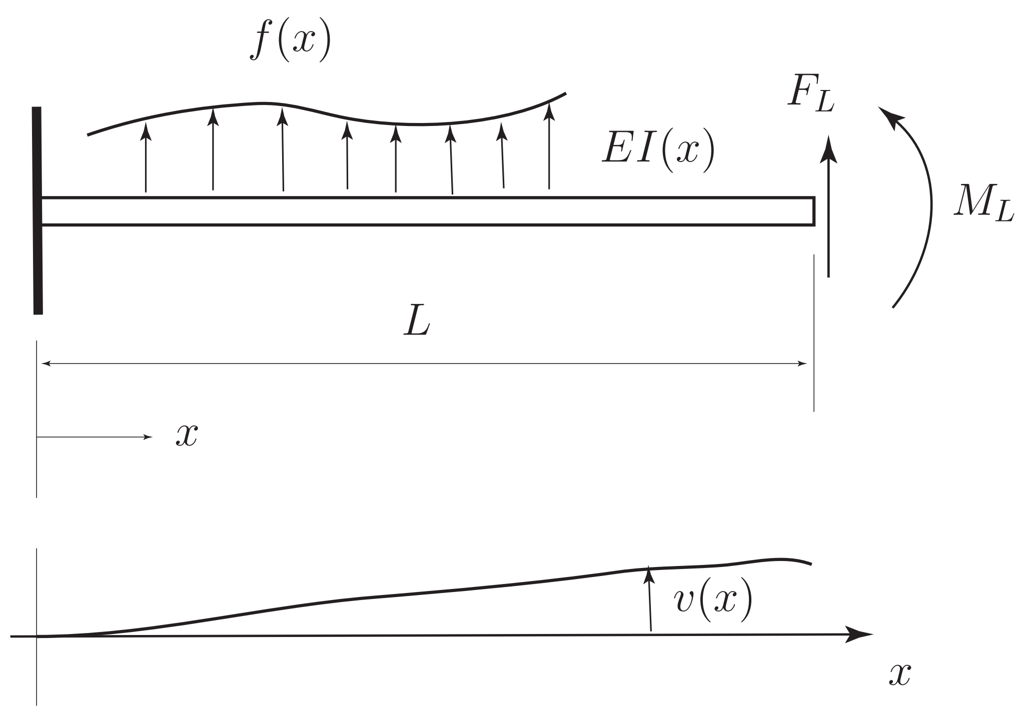

Figure 3.1. Transversely loaded beam with BCs.

The differential beam "element" (NOT a finite element) is shown in Fig.3.2 with the following shear force equilibrium as,

$$-V + f dx + V + \frac{dV}{dx}dx = 0 \tag{3.1}$$

$$\implies -\frac{dV}{dx} = f \tag{3.2}$$

and moment about 0 (ignore dx^2 terms) as,

$$-M + f dx(\frac{dx}{2}) + (V + \frac{dV}{dx}dx)dx + M + \frac{dM}{dx}dx = 0 \tag{3.3}$$

$$\implies -\frac{dM}{dx} = V \tag{3.4}$$

such that **static equilibrium** is written as,

$$\frac{d^2M}{dx^2} = f \tag{3.5}$$

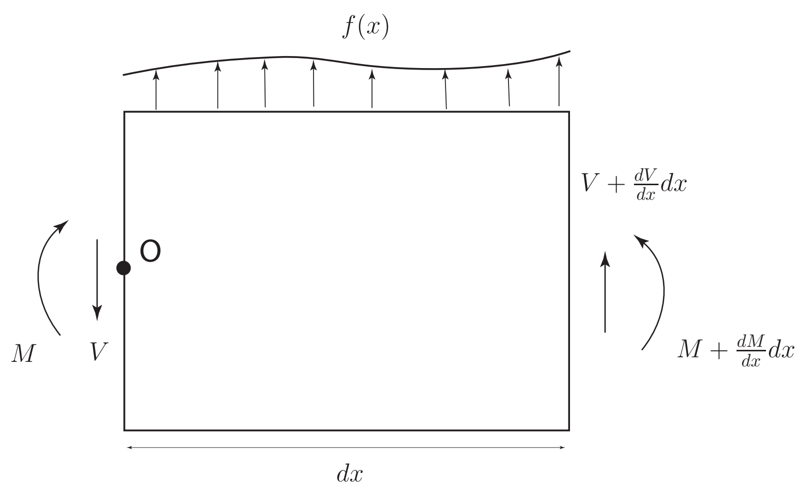

Figure 3.2. Differential beam "element" (not a finite element).

We use Hooke's law to calculate the internal moment through the linear elastic constitutive equation, where curvature $\kappa \approx \frac{d^2v}{dx^2}$ for small transverse deflections, such that,

$$M(x) = EI(x)\frac{d^2v}{dx^2} \tag{3.6}$$

and

$$\frac{d^2}{dx^2}\left(EI(x)\frac{d^2v}{dx^2}\right) = f \tag{3.7}$$

Then, the **Strong Form** for the Bernoulli-Euler beam can be stated as,

$$(S)\begin{cases} \text{Find } v(x) : \bar{\Omega} \mapsto \mathbb{R}, \quad \bar{\Omega} = [0, L], \quad \text{such that} \\ \frac{d^2}{dx^2}\left(EI(x)\frac{d^2v}{dx^2}\right) = f(x) & x \in \Omega \\ v = 0 & x = 0 \\ v_{,x} = 0 & x = 0 \\ EIv_{,xx} = M_L & x = L \\ -(EIv_{,xx})_{,x} = F_L & x = L \end{cases} \tag{3.8}$$

where v is the transverse displacement, $v_{,x}$ is the rotation (assuming small transverse deflections), $EIv_{,xx}$ is the internal bending moment, and $-(EIv_{,xx})_{,x}$ is the internal shear force.

3.2 Weak (W) form for Bernoulli-Euler beam

We apply the apply **method of weighted residuals** with weighted residual statement as,

$$\int_0^L w\left[(EIv_{,xx})_{,xx} - f\right] dx = 0 \tag{3.9}$$

and trial solution space as,

$$v \in \mathscr{S} \subset C^1(\Omega) = \{v : \Omega \to \mathbb{R} | v(0) = 0, v_{,x}(0) = 0\} \tag{3.10}$$

and weighting function space as,

$$w \in \mathscr{V} \subset C^1(\Omega) = \{w : \Omega \to \mathbb{R} | w(0) = 0, w_{,x}(0) = 0\}. \tag{3.11}$$

We apply integration by parts twice (use chain rule and divergence theorem) to balance derivatives on w and u in the variational equation for the weak form as,

$$\begin{aligned} \left[w(EIv_{,xx})_{,x}\right]_{,x} &= w_{,x}(EIv_{,xx})_{,x} + w(EIv_{,xx})_{,xx} && (3.12) \\ \Longrightarrow w(EIv_{,xx})_{,xx} &= \left[w(EIv_{,xx})_{,x}\right]_{,x} - w_{,x}(EIv_{,xx})_{,x} && (3.13) \\ (w_{,x}EIv_{,xx})_{,x} &= w_{,xx}EIv_{,xx} + w_{,x}(EIv_{,xx})_{,x} && (3.14) \\ \Longrightarrow w_{,x}(EIv_{,xx})_{,x} &= (w_{,x}EIv_{,xx})_{,x} - w_{,xx}EIv_{,xx} && (3.15) \end{aligned}$$

where,

$$\begin{aligned} 0 &= \int_0^L w\left[(EIv_{,xx})_{,xx} - f\right] dx && (3.16) \\ &= \int_0^L \Big[\left[w(EIv_{,xx})_{,x}\right]_{,x} - w_{,x}(EIv_{,xx})_{,x}\Big] dx - \int_0^L wf dx && (3.17) \\ &= w(EIv_{,xx})_{,x}|_0^L - \int_0^L \left[(w_{,x}EIv_{,xx})_{,x} - w_{,xx}EIv_{,xx}\right] dx - \int_0^L wf dx && (3.18) \\ &= w(EIv_{,xx})_{,x}|_0^L - w_{,x}EIv_{,xx}|_0^L + \int_0^L w_{,xx}EIv_{,xx}dx - \int_0^L wf dx && (3.19) \end{aligned}$$

and

$$\int_0^L w_{,xx}EIv_{,xx}dx = \int_0^L wf dx + w(L)F_L + w_{,x}(L)M_L \qquad (3.20)$$

We may then state the **weak form** as,

$$(W) \begin{cases} \text{Find } v(x) \in \mathscr{S} \subset C^1(\Omega), \text{ such that} \\ \int_0^L w_{,xx}EIv_{,xx}dx = \int_0^L wf dx + w(L)F_L + w_{,x}(L)M_L \\ \text{holds } \forall w(x) \in \mathscr{V} \subset C^1(\Omega) \end{cases} \qquad (3.21)$$

where $\forall$ reads "for all;" $\mathscr{S}$ is the space of admissible trial functions, and $v \in H^2$; $\mathscr{V}$ is the space of weighting functions, and $w \in H^2$; C^1 is the space of functions with continuous first derivatives; H^2 is the second Sobolev space, such that the H^2 norm is finite: i.e.,

$\|v\|_2 = \left(\int_0^L (v^2 + v_{,x}^2 + v_{,xx}^2) dx\right)^{1/2} < \infty$; $\|u\|_2$ is called the H^2 norm; and $v \in H^2$ essentially states that second spatial derivatives $v_{,xx}$ CANNOT be Dirac Delta functions, but can be Heaviside functions (discontinuous), **which means that we must include dofs for v and $v_{,x}$ at the nodes of a Bernoulli-Euler beam finite element to ensure that they are continuous along the beam; we see this in the statement of the Galerkin form**.

3.3 Discretization and Galerkin Form (G) for Bernoulli-Euler beam

We state the Galerkin form as,

$$(G) \begin{cases} \text{Find } v^h(x) \in \mathscr{S}^h \subset C^1(\Omega^h), \text{ such that} \\ \int_0^L w_{,xx}^h EI v_{,xx}^h dx = \int_0^L w^h f dx + w^h(L) F_L + w_{,x}^h(L) M_L \\ \text{holds } \forall w^h(x) \in \mathscr{V}^h \subset C^1(\Omega^h) \end{cases} \tag{3.22}$$

where $\mathscr{S}^h \subset \mathscr{S}$ is the discrete space of admissible trial functions; $\mathscr{V}^h \subset \mathscr{V}$ is the discrete space of weighting functions; to ensure $\mathscr{S}^h \subset \mathscr{S}$ and $\mathscr{V}^h \subset \mathscr{V}$, two dofs are introduced at the finite element nodes: (1) transverse displacement v^h, and (2) rotation $v_{,x}^h$ (for small transverse deflections).

3.4 Finite Element (FE) Matrix Form for Bernoulli-Euler beam

From the **element perspective**, consider an element e, with length h^e, moment of inertia I^e, and elasticity modulus E^e as in Fig.3.3, where element length $h^e = x_2^e - x_1^e$, element domain

$\Omega^e = (x_1^e, x_2^e)$, discrete domain $\Omega^h = \mathbf{A}_{e=1}^{n_{\text{el}}} \Omega^e$, $\mathbf{A}_{e=1}^{n_{\text{el}}}$ is the element assembly operator; and the element is NOT isoparametric such that $x^{h^e}(\xi) = \boldsymbol{N}^e(\xi) \cdot \boldsymbol{x}^e$, and $v^{h^e}(\xi) = \boldsymbol{H}^e(\xi) \cdot \boldsymbol{d}^e$.

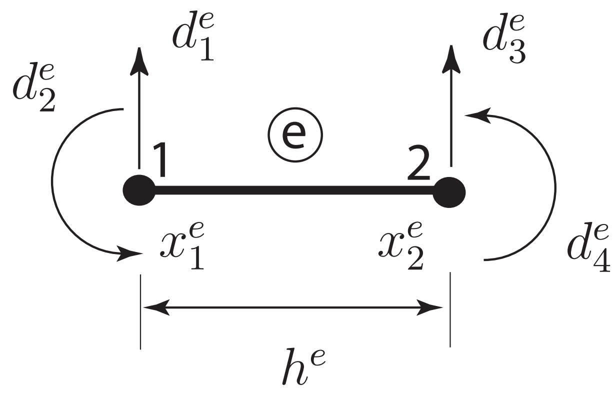

Figure 3.3. Beam finite element.

The **element dofs** are,

$$\boldsymbol{d}^e = \begin{Bmatrix} d_1^e \\ d_2^e \\ d_3^e \\ d_4^e \end{Bmatrix} = \begin{Bmatrix} v^{h^e}(\xi = -1) \\ v^{h^e}_{,x}(-1) \\ v^{h^e}(1) \\ v^{h^e}_{,x}(1) \end{Bmatrix} \tag{3.23}$$

We introduce the **Hermite cubic shape functions** as,

$$v^{h^e}(\xi) = \begin{bmatrix} H_1^e & j^e H_2^e & H_3^e & j^e H_4^e \end{bmatrix} \begin{bmatrix} d_1^e \\ d_2^e \\ d_3^e \\ d_4^e \end{bmatrix} = \boldsymbol{H}^e(\xi) \cdot \boldsymbol{d}^e \tag{3.24}$$

where we used $j^e = dx^{h^e}/d\xi = h^e/2$, and $\frac{dv^{h^e}}{d\xi} = \frac{dv^{h^e}}{dx}\frac{dx}{d\xi}$; likewise $w^{h^e}(\xi) = \boldsymbol{H}^e \cdot \boldsymbol{c}^e = (\boldsymbol{c}^e)^T \cdot (\boldsymbol{H}^e)^T$.

For **completeness**, it is possible to show completeness to 2nd order for $v^{h^e}(\xi)$, such that $v^{h^e}(\xi) = a_0 + a_1 x + a_2 x^2$; use Eq.(3.23) when substituting for d_a^e at the nodes; use $x^{h^e}(\xi) = \boldsymbol{N}^e(\xi) \cdot \boldsymbol{x}^e$ for the spatial coordinate interpolation. The **'strain-displacement matrix'** $\boldsymbol{B}^e$

is,

$$v^{h^e}_{,xx}(\xi) = \frac{d^2 \boldsymbol{H}^e(\xi)}{dx^2} \cdot \boldsymbol{d}^e = \frac{1}{(j^e)^2} \frac{d^2 \boldsymbol{H}^e(\xi)}{d\xi^2} \cdot \boldsymbol{d}^e = \boldsymbol{B}^e(\xi) \cdot \boldsymbol{d}^e \tag{3.25}$$

where likewise $w^{h^e}_{,xx}(\xi) = \boldsymbol{B}^e \cdot \boldsymbol{c}^e = (\boldsymbol{c}^e)^T \cdot (\boldsymbol{B}^e)^T$; note that $M^{h^e}(\xi) = \widehat{EI(\xi)} \boldsymbol{B}^e(\xi) \cdot \boldsymbol{d}^e$, and

$$\boldsymbol{B}^e(\xi) = \frac{1}{(j^e)^2} \left[\begin{array}{cccc} \frac{d^2 H_1^e}{d\xi^2} & j^e \frac{d^2 H_2^e}{d\xi^2} & \frac{d^2 H_3^e}{d\xi^2} & j^e \frac{d^2 H_4^e}{d\xi^2} \end{array} \right] \tag{3.26}$$

The Hermite cubic shape functions are shown in Fig.3.4.

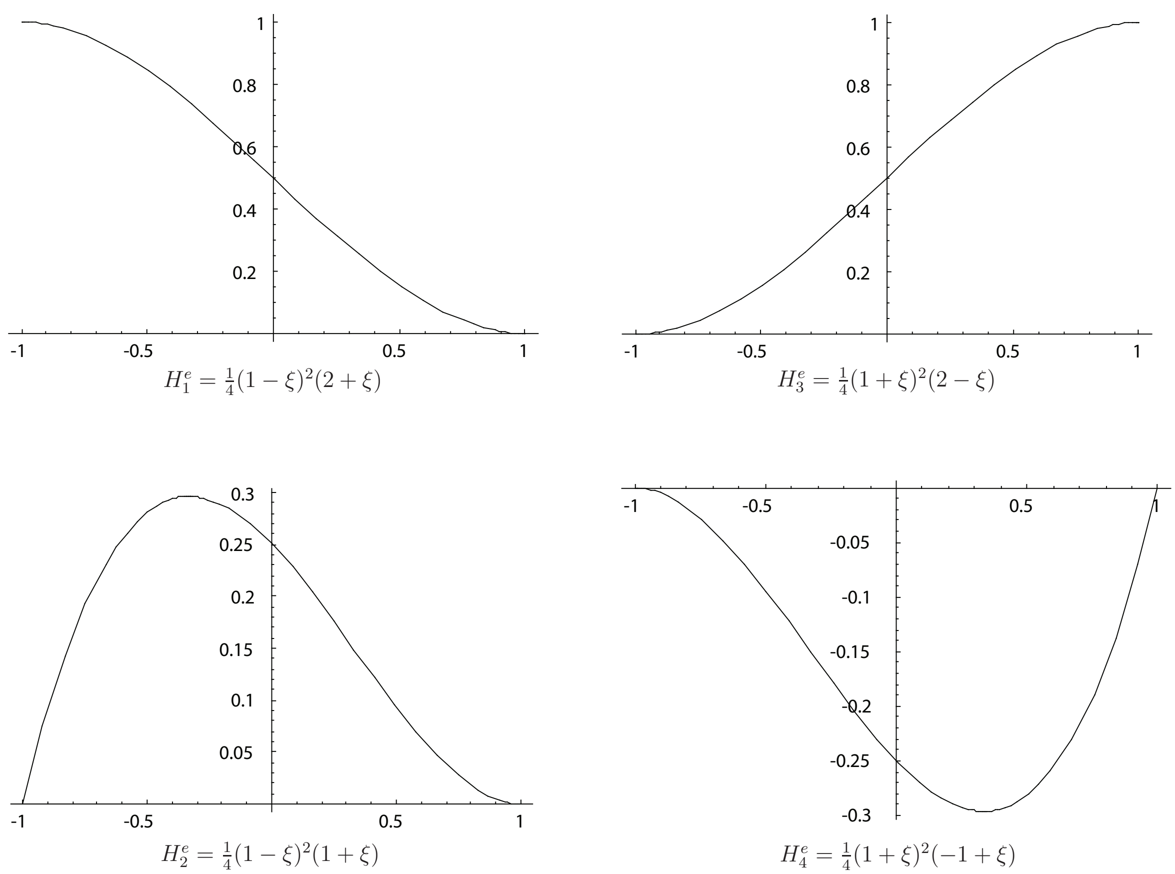

Figure 3.4. Hermite cubic shape functions.

The finite element (FE) form is then written as,

$$\mathop{\mathbf{A}}_{e=1}^{n_{\rm el}} (\boldsymbol{c}^e)^T \cdot \underbrace{\left\{ \int_{-1}^{1} (\boldsymbol{B}^e)^T \cdot \boldsymbol{B}^e \widehat{EI(\xi)} j^e d\xi \right\}}_{\boldsymbol{k}^e} \cdot \boldsymbol{d}^e =$$
$$\mathop{\mathbf{A}}_{e=1}^{n_{\rm el}} (\boldsymbol{c}^e)^T \cdot \underbrace{\left\{ \int_{-1}^{1} (\boldsymbol{H}^e)^T \widehat{f(\xi)} j^e d\xi \right\}}_{\boldsymbol{f}_f^e} + w^h(L) F_L + w^h_{,x}(L) M_L \tag{3.27}$$

where $\boldsymbol{k}^e$ is the element stiffness matrix, and $\boldsymbol{f}^e_f$ is the element distributed shear force vector. If EI and f are constant (not functions of coordinate x), then,

$$\boldsymbol{k}^e = \frac{EI}{(h^e)^3} \begin{bmatrix} 12 & 6h^e & -12 & 6h^e \\ 6h^e & 4(h^e)^2 & -6h^e & 2(h^e)^2 \\ -12 & -6h^e & 12 & -6h^e \\ 6h^e & 2(h^e)^2 & -6h^e & 4(h^e)^2 \end{bmatrix} , \quad \boldsymbol{f}^e_f = \frac{f h^e}{2} \begin{bmatrix} 1 \\ h^e/6 \\ 1 \\ -h^e/6 \end{bmatrix} \tag{3.28}$$

Note the contribution of the natural BCs as,

$$w^h(L) F_L + w^h_{,x}(L) M_L = \mathop{\mathbf{A}}_{e=1}^{n_{\rm el}} (\boldsymbol{c}^e)^T \cdot \boldsymbol{f}^e_F \tag{3.29}$$

where

$$\boldsymbol{f}^{n_{\rm el}}_F = \begin{bmatrix} 0 \\ 0 \\ F_L \\ M_L \end{bmatrix} , \quad \boldsymbol{f}^e_F = \boldsymbol{0} \text{ for } e \neq n_{\rm el} \tag{3.30}$$

and then,

$$\mathop{\mathbf{A}}_{e=1}^{n_{\rm el}} (\boldsymbol{c}^e)^T \cdot \left\{ \boldsymbol{k}^e \cdot \boldsymbol{d}^e = \boldsymbol{f}^e_f + \boldsymbol{f}^e_F \right\} \tag{3.31}$$

The assembly process is the same ... except **for frame analysis we include axial stiffness,**

and the possible rotation of the element in space. But first, let us consider a beam example.

3.5 FE assembly Example for Bernoulli-Euler beam

In Fig.3.5 is an example used to demonstrate the assembly process for a beam FE mesh. The location matrix is as follows,

		element number 1	2	3	
local nodal dof	1	0	1	0	d.o.f.
	2	0	2	3	
	3	1	0	0	
	4	2	3	0	

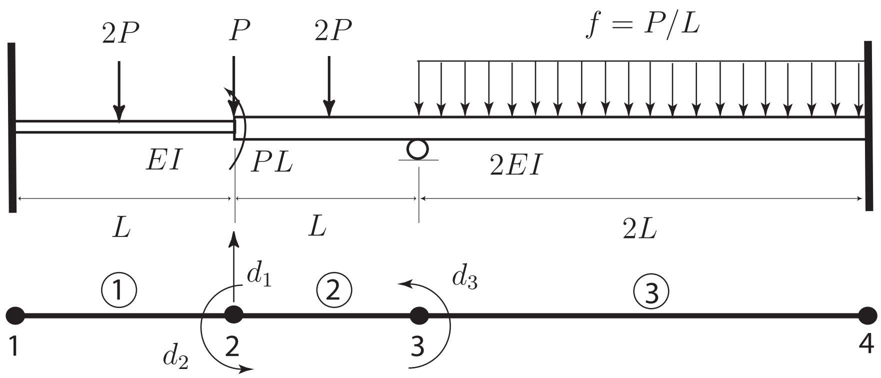

Figure 3.5. Beam finite element assembly example.

The element stiffness matrices are,

$$\boldsymbol{k}^1 = \frac{EI}{L^3}\begin{bmatrix} 12 & 6L & -12 & 6L \\ 6L & 4L^2 & -6L & 2L^2 \\ -12 & -6L & 12 & -6L \\ 6L & 2L^2 & -6L & 4L^2 \end{bmatrix}, \quad \boldsymbol{K}^1 = \frac{EI}{L^3}\begin{bmatrix} 12 & -6L & 0 \\ -6L & 4L^2 & 0 \\ 0 & 0 & 0 \end{bmatrix} \tag{3.32}$$

and

$$\boldsymbol{k}^2 = \frac{EI}{L^3}\begin{bmatrix} 24 & 12L & -24 & 12L \\ 12L & 8L^2 & -12L & 4L^2 \\ -24 & -12L & 24 & -12L \\ 12L & 4L^2 & -12L & 8L^2 \end{bmatrix}, \quad \boldsymbol{K}^2 = \frac{EI}{L^3}\begin{bmatrix} 24 & 12L & 12L \\ 12L & 8L^2 & 4L^2 \\ 12L & 4L^2 & 8L^2 \end{bmatrix} \tag{3.33}$$

and

$$\boldsymbol{k}^3 = \frac{EI}{L^3}\begin{bmatrix} 12 & 6L & -12 & 6L \\ 6L & 4L^2 & -6L & 2L^2 \\ -12 & -6L & 12 & -6L \\ 6L & 2L^2 & -6L & 4L^2 \end{bmatrix}, \quad \boldsymbol{K}^3 = \frac{EI}{L^3}\begin{bmatrix} 0 & 0 & 0 \\ 0 & 0 & 0 \\ 0 & 0 & 4L^2 \end{bmatrix} \tag{3.34}$$

and

$$\boldsymbol{K} = \sum_{e=1}^{n_{\text{el}}} \boldsymbol{K}^e = \frac{EI}{L^3}\begin{bmatrix} 36 & 6L & 12L \\ 6L & 12L^2 & 4L^2 \\ 12L & 4L^2 & 12L^2 \end{bmatrix} \tag{3.35}$$

To handle the transverse point load within element 2, consider figure 3.6 which displays a point load P applied mid-way along a beam element.

The forcing vector may then be written as,

$$\boldsymbol{f}_f^e = \int_{\Omega^e} \boldsymbol{H}^{eT} f(x)dx = \int_{\Omega^e} \boldsymbol{H}^{eT} P\delta(x-a)dx = P\boldsymbol{H}^{eT}|_{x=a} \tag{3.36}$$

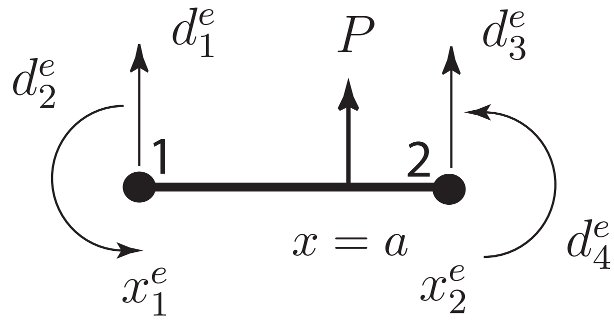

Figure 3.6. Point load in mid-element section.

Thus, at the element center, with length L and load $-2P$, we have,

$$\boldsymbol{f}_f^e = -2P\boldsymbol{H}^{eT}|_{\xi=0}\ ; \quad \boldsymbol{f}_f^2 = \boldsymbol{f}_f^1 = -2P \begin{bmatrix} \frac{1}{2} \\ \frac{L}{2}\frac{1}{4} \\ \frac{1}{2} \\ \frac{L}{2}(-\frac{1}{4}) \end{bmatrix} = \begin{bmatrix} -P \\ -\frac{PL}{4} \\ -P \\ \frac{PL}{4} \end{bmatrix} \tag{3.37}$$

$$\boldsymbol{F}_f^1 = \begin{bmatrix} -P \\ \frac{PL}{4} \\ 0 \end{bmatrix}\ ; \quad \boldsymbol{F}_f^2 = \begin{bmatrix} -P \\ -\frac{PL}{4} \\ \frac{PL}{4} \end{bmatrix} \tag{3.38}$$

The nodal force vector accounting for distributed constant load f is written as,

$$\boldsymbol{f}_f^e = fh^e \begin{bmatrix} \frac{1}{2} \\ \frac{h^e}{12} \\ \frac{1}{2} \\ -\frac{h^e}{12} \end{bmatrix}\ ; \quad \boldsymbol{f}_f^3 = (-P/L)2L \begin{bmatrix} \frac{1}{2} \\ \frac{2L}{12} \\ \frac{1}{2} \\ -\frac{2L}{12} \end{bmatrix} = \begin{bmatrix} -P \\ -\frac{PL}{3} \\ -P \\ \frac{PL}{3} \end{bmatrix} \tag{3.39}$$

$$\boldsymbol{F}_f^3 = \begin{bmatrix} 0 \\ 0 \\ -\frac{PL}{3} \end{bmatrix} \tag{3.40}$$

where the total distributed nodal load vector, and concentrated load vector are,

$$\boldsymbol{F}_f = \sum_{e=1}^{n_{\text{el}}} \boldsymbol{F}_f^e = \begin{bmatrix} -2P \\ 0 \\ -\frac{PL}{12} \end{bmatrix} \; ; \quad \boldsymbol{F}_F = \begin{bmatrix} -P \\ PL \\ 0 \end{bmatrix} \tag{3.41}$$

We then solve for unknown dofs $\boldsymbol{d}$ as,

$$\boldsymbol{K} \cdot \boldsymbol{d} = \boldsymbol{F}_f + \boldsymbol{F}_F \; ; \quad \boldsymbol{d} = \frac{PL^2}{3024EI} \begin{bmatrix} -398L \\ 366 \\ 253 \end{bmatrix} \tag{3.42}$$

We can go back and solve for reaction forces and moments like we did for the axially-loaded bar problem (for reaction forces), as well as calculate moment and shear within a finite element.

3.6 2D FE Frame Analysis

Consider a **2D frame element** in Fig.3.7.

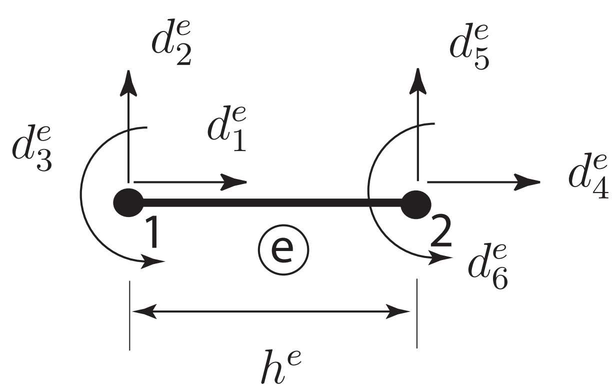

Figure 3.7. 2D frame element.

If E^e, A^e, and I^e are constant, then,

$$\boldsymbol{k}^e_{\text{axial}} = \frac{E^e A^e}{h^e}\begin{bmatrix} 1 & -1 \\ -1 & 1 \end{bmatrix} \tag{3.43}$$

$$\boldsymbol{k}^e_{\text{flexural}} = \frac{E^e I^e}{(h^e)^3}\begin{bmatrix} 12 & 6h^e & -12 & 6h^e \\ 6h^e & 4(h^e)^2 & -6h^e & 2(h^e)^2 \\ -12 & -6h^e & 12 & -6h^e \\ 6h^e & 2(h^e)2 & -6h^e & 4(h^e)^2 \end{bmatrix} \tag{3.44}$$

We can combine (superimpose; assumes GEOMETRIC LINEARITY! i.e., no coupling between axial and transverse displacements) the axial and flexure element stiffness matrices to obtain the **frame stiffness matrix** as,

$$\begin{aligned} \boldsymbol{k}^e_{\text{frame}} &= \boldsymbol{k}^e_{\text{axial}} + \boldsymbol{k}^e_{\text{flexural}} \\ &= \frac{E^e I^e}{(h^e)^3}\begin{bmatrix} \frac{A^e(h^e)^2}{I^e} & 0 & 0 & -\frac{A^e(h^e)^2}{I^e} & 0 & 0 \\ 0 & 12 & 6h^e & 0 & -12 & 6h^e \\ 0 & 6h^e & 4(h^e)^2 & 0 & -6h^e & 2(h^e)^2 \\ -\frac{A^e(h^e)^2}{I^e} & 0 & 0 & \frac{A^e(h^e)^2}{I^e} & 0 & 0 \\ 0 & -12 & -6h^e & 0 & 12 & -6h^e \\ 0 & 6h^e & 2(h^e)^2 & 0 & -6h^e & 4(h^e)^2 \end{bmatrix} \end{aligned} \tag{3.45}$$

The distributed force vector, if distributed transverse f_t and axial f_a loads are constant, may be written as,

$$\boldsymbol{f}_f^e = \frac{h^e}{2}\begin{bmatrix} f_a \\ f_t \\ f_t h^e/6 \\ f_a \\ f_t \\ -f_t h^e/6 \end{bmatrix}$$

But frame elements are usually not horizontal. They can be at various angles. Thus, consider the **relation between global and local 2D frame element degrees of freedom (dof)** in Fig.3.8 where,

$$\cos\alpha^e = \frac{X_2^e - X_1^e}{h^e} \; ; \quad \sin\alpha^e = \frac{Y_2^e - Y_1^e}{h^e} \tag{3.46}$$

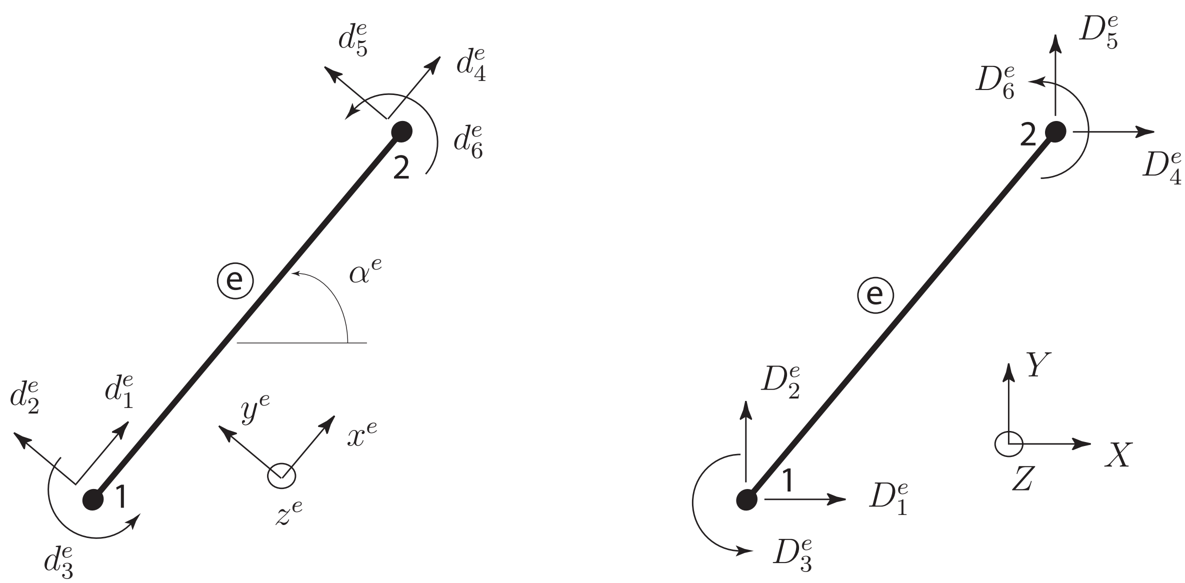

Figure 3.8. Local to global 2D frame element degrees of freedom (dof).

Thus, we **transform the dofs** through a rotation matrix $\boldsymbol{\Lambda}^e$ as,

$$\boldsymbol{d}^e = \boldsymbol{\Lambda}^e \cdot \boldsymbol{D}^e \tag{3.47}$$

$$\begin{bmatrix} d_1^e \\ d_2^e \\ d_3^e \\ d_4^e \\ d_5^e \\ d_6^e \end{bmatrix} = \begin{bmatrix} \cos\alpha^e & \sin\alpha^e & 0 & 0 & 0 & 0 \\ -\sin\alpha^e & \cos\alpha^e & 0 & 0 & 0 & 0 \\ 0 & 0 & 1 & 0 & 0 & 0 \\ 0 & 0 & 0 & \cos\alpha^e & \sin\alpha^e & 0 \\ 0 & 0 & 0 & -\sin\alpha^e & \cos\alpha^e & 0 \\ 0 & 0 & 0 & 0 & 0 & 1 \end{bmatrix} \begin{bmatrix} D_1^e \\ D_2^e \\ D_3^e \\ D_4^e \\ D_5^e \\ D_6^e \end{bmatrix} \tag{3.48}$$

Note that the nodal weighting function values similarly transform as $\boldsymbol{c}^e = \boldsymbol{\Lambda}^e \cdot \boldsymbol{C}^e$. Recall the FE form before assembly as,

$$\mathop{\mathbf{A}}_{e=1}^{n_{\rm el}} (\boldsymbol{c}^e)^T \cdot \left\{ \boldsymbol{k}^e \cdot \boldsymbol{d}^e = \boldsymbol{f}_f^e + \boldsymbol{f}_F^e \right\} \tag{3.49}$$

and **introduce transformations** as,

$$\mathop{\mathbf{A}}_{e=1}^{n_{\rm el}} (\boldsymbol{C}^e)^T \cdot \left\{ (\boldsymbol{\Lambda}^e)^T \cdot \boldsymbol{k}^e \cdot \boldsymbol{\Lambda}^e \cdot \boldsymbol{D}^e = (\boldsymbol{\Lambda}^e)^T \cdot \boldsymbol{f}_f^e + (\boldsymbol{\Lambda}^e)^T \cdot \boldsymbol{f}_F^e \right\} \tag{3.50}$$

Let us consider an example.

3.6.1 2D FE Frame Analysis: Example 1

Consider the 2D frame meshed with two frame elements in Fig.3.9, with Location Matrix (LM) as,

local nodal dof \ element number	1	2
1	0	1
2	0	2
3	0	3
4	1	0
5	2	0
6	3	4

(entries: d.o.f.)

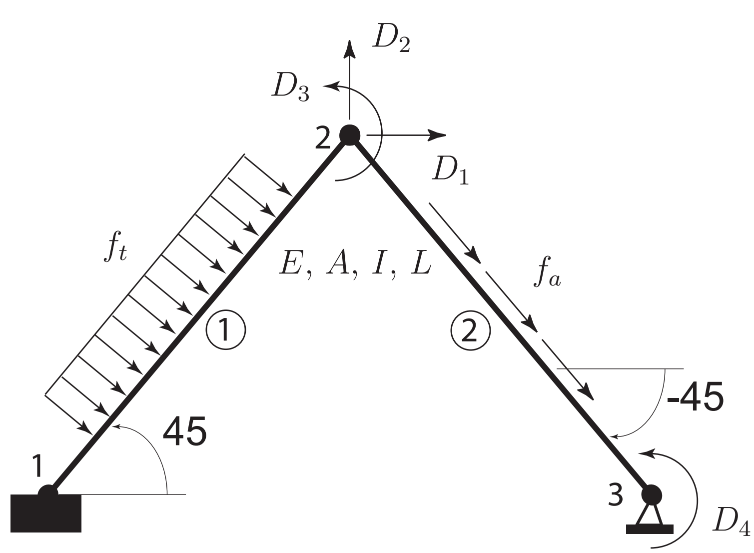

Figure 3.9. 2D frame mesh for Example 1.

The **element stiffness matrices** are the same in local coordinates as,

$$\boldsymbol{k}^1 = \boldsymbol{k}^2 = \frac{EI}{L^3}\begin{bmatrix} \frac{AL^2}{I} & 0 & 0 & -\frac{AL^2}{I} & 0 & 0 \\ 0 & 12 & 6L & 0 & -12 & 6L \\ 0 & 6L & 4L^2 & 0 & -6L & 2L^2 \\ -\frac{AL^2}{I} & 0 & 0 & \frac{AL^2}{I} & 0 & 0 \\ 0 & -12 & -6L & 0 & 12 & -6L \\ 0 & 6L & 2L^2 & 0 & -6L & 4L^2 \end{bmatrix} \tag{3.51}$$

$$\boldsymbol{K}^e = (\boldsymbol{\Lambda}^e)^T \cdot \boldsymbol{k}^e \cdot \boldsymbol{\Lambda}^e \tag{3.52}$$

with **rotation matrices**,

$$\boldsymbol{\Lambda}^1 = \begin{bmatrix} \frac{\sqrt{2}}{2} & \frac{\sqrt{2}}{2} & 0 & 0 & 0 & 0 \\ -\frac{\sqrt{2}}{2} & \frac{\sqrt{2}}{2} & 0 & 0 & 0 & 0 \\ 0 & 0 & 1 & 0 & 0 & 0 \\ 0 & 0 & 0 & \frac{\sqrt{2}}{2} & \frac{\sqrt{2}}{2} & 0 \\ 0 & 0 & 0 & -\frac{\sqrt{2}}{2} & \frac{\sqrt{2}}{2} & 0 \\ 0 & 0 & 0 & 0 & 0 & 1 \end{bmatrix}, \ \boldsymbol{\Lambda}^2 = \begin{bmatrix} \frac{\sqrt{2}}{2} & -\frac{\sqrt{2}}{2} & 0 & 0 & 0 & 0 \\ \frac{\sqrt{2}}{2} & \frac{\sqrt{2}}{2} & 0 & 0 & 0 & 0 \\ 0 & 0 & 1 & 0 & 0 & 0 \\ 0 & 0 & 0 & \frac{\sqrt{2}}{2} & -\frac{\sqrt{2}}{2} & 0 \\ 0 & 0 & 0 & \frac{\sqrt{2}}{2} & \frac{\sqrt{2}}{2} & 0 \\ 0 & 0 & 0 & 0 & 0 & 1 \end{bmatrix} \tag{3.53}$$

The **forcing vectors** for distributed loading (there are no concentrated forces or moments, such that $\boldsymbol{F}_F = \boldsymbol{0}$) are as follows,

$$\boldsymbol{f}_f^1 = \frac{L}{2}\begin{bmatrix} 0 \\ -f_t \\ -\frac{f_t L}{6} \\ 0 \\ -f_t \\ \frac{f_t L}{6} \end{bmatrix} \ ; \quad \boldsymbol{f}_f^2 = \frac{L}{2}\begin{bmatrix} f_a \\ 0 \\ 0 \\ f_a \\ 0 \\ 0 \end{bmatrix} \tag{3.54}$$

$$\boldsymbol{F}_f^e = (\boldsymbol{\Lambda}^e)^T \cdot \boldsymbol{f}_f^e \tag{3.55}$$

For the **element assembly** for element 1, we cancel rows and columns 1-3; for element 2, we cancel rows and columns 4,5 (where $\boldsymbol{K}$ is symmetric), such that,

$$\boldsymbol{K} = \begin{bmatrix} K^1_{44}+K^2_{11} & K^1_{45}+K^2_{12} & K^1_{46}+K^2_{13} & K^2_{16} \\ \cdot & K^1_{55}+K^2_{22} & K^1_{56}+K^2_{23} & K^2_{26} \\ \cdot & \cdot & K^1_{66}+K^2_{33} & K^2_{36} \\ \cdot & \cdot & \cdot & K^2_{66} \end{bmatrix} \quad ; \quad \boldsymbol{F} = \begin{bmatrix} F^1_{f4}+F^2_{f1} \\ F^1_{f5}+F^2_{f2} \\ F^1_{f6}+F^2_{f3} \\ F^2_{f6} \end{bmatrix} \tag{3.56}$$

and then solve for the unknown dofs from the linear system of equations as,

$$\boldsymbol{K} \cdot \boldsymbol{D} = \boldsymbol{F} \tag{3.57}$$

3.6.2 2D FE Frame Analysis: Example 2

Consider the 2D frame meshed without and with flexural release (a hinge) in Fig.3.10, with Location Matrices (LM) as follows,

element number

local nodal dof	1	2	3
1	0	1	4
2	0	2	5
3	0	3	6
4	1	4	0
5	2	5	0
6	3	6	0

element number

d.o.f.	1	2	3	4
1	0	1	4	8
2	0	2	5	9
3	0	3	7	10
4	1	4	8	0
5	2	5	9	0
6	3	6	10	0

Note that to introduce a hinge, all we have to do is change the Location Matrix (LM) to include separate, global, rotational degrees of freedom D_6 and D_7 on each side of the joint.

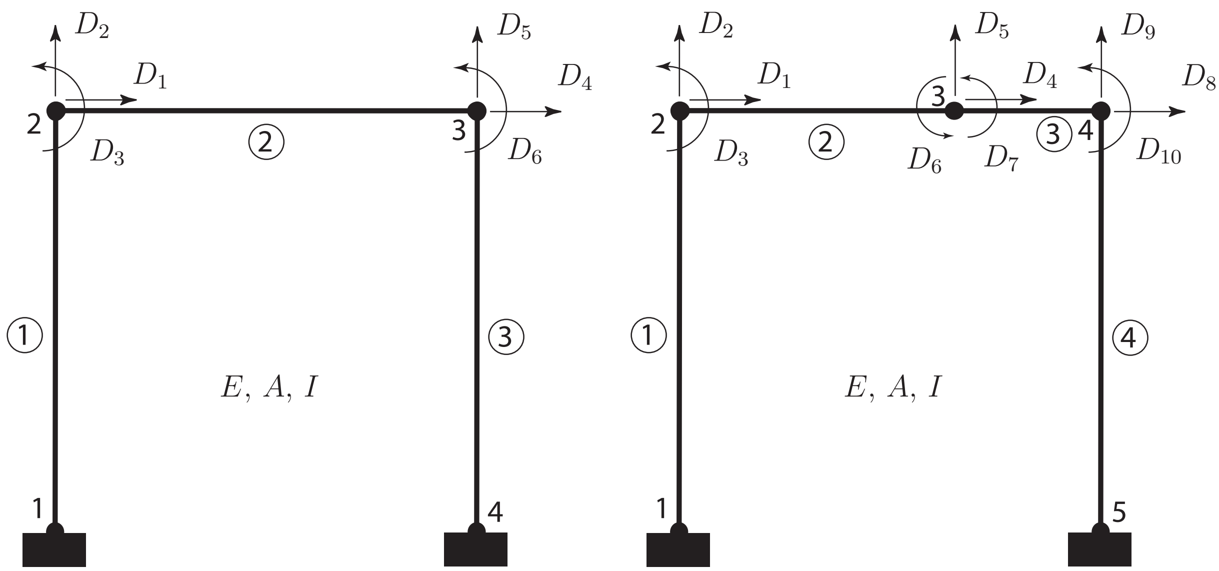

Figure 3.10. 2D frame mesh for example 2 showing without and with flexure release.

Chapter 4

2D Linear Heat Conduction

For the 2D linear heat conduction FEM, we assume linearity in the form of a rigid material and Fourier's law. These notes are drawn from Hughes [1987]. Topics covered in the remaining sections include the following:

(1) linearity in the form of Fourier's law;

(2) differential form and boundary conditions (BCs) for Strong Form (S) of 2D heat conduction;

(3) review of tensor notation in index form;

(4) variational, Weak Form (W);

(5) discrete, Galerkin Form (G);

(6) Finite Element (FE), Matrix form;

(7) bilinear, quadrilateral shape functions in natural coordinates (ξ, η);

(8) triangular element shape functions (time permitting);

(9) element assembly to obtain Global Matrix form;

(10) convergence: (i) compatibility, and (ii) completeness;

(11) numerical integration using 2D Gaussian quadrature;

(12) taking advantage of symmetry for boundary value problems (BVPs);

(13) transient heat conduction, numerical time integration (parabolic matrix ODE);

(14) analogy to saturated ground water flow in rigid soil or rock;

(15) higher order 2D elements, and construction of transition elements.

4.1 Differential equation and Strong (S) form for Static, steady-state heat conduction

Assume steady-state conditions, such that the total heat change is zero. In 2D (assuming region is 1m thick into page), the heat flux vector is $\boldsymbol{q} = [\, q_x \; q_y \,]^T$ (W/m^2), heat source is $f(x, y)$ (W/m^3), and prescribed temperature g_θ (°C) on Γ_θ, and prescribed heat flux q on Γ_q (in-flow positive), where total domain with boundaries $\bar{\Omega} = \Omega \cup \Gamma_\theta \cup \Gamma_q$. Refer to Fig.4.1 for applied BCs and deriving the differential equation for balance of energy.

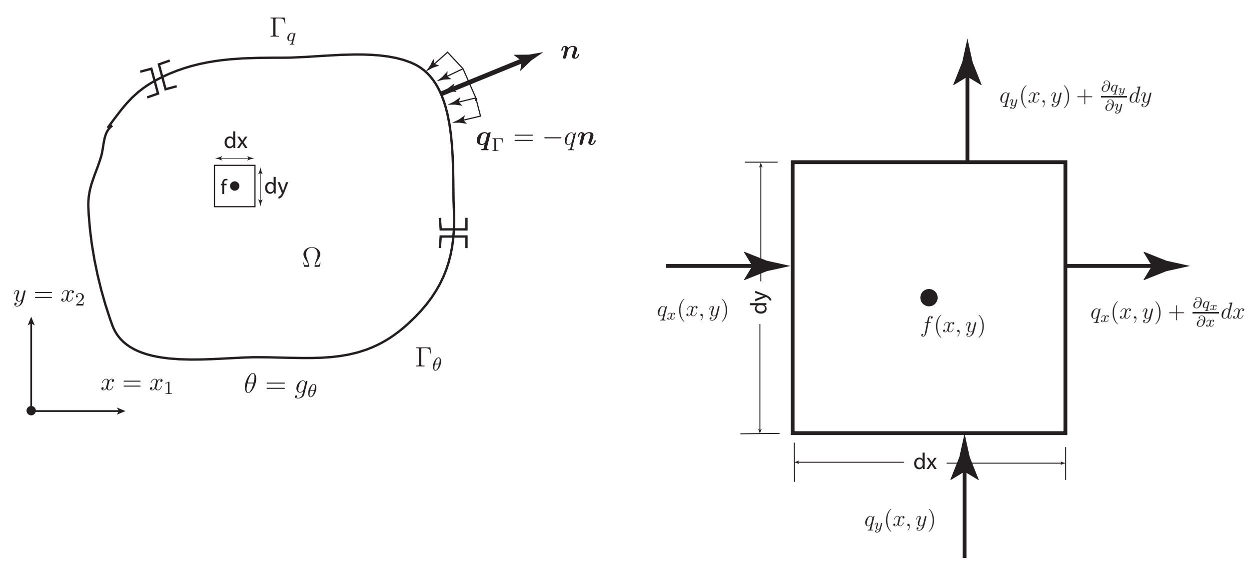

Figure 4.1. Body Ω and differential element dx, dy for applying balance of energy (first law of thermodynamics).

We sum the heat fluxes to obtain the **balance of energy** as,

$$(dy)(1)(q_x) - (dy)\left(q_x + \frac{\partial q_x}{\partial x}dx\right) + (dx)(1)(q_y) - (dx)(1)\left(q_y + \frac{\partial q_y}{\partial y}dy\right) + f(dx)(dy)(1) = 0 \tag{4.1}$$

To derive the **heat equation**, we introduce Fourier's law as our constitutive equation,

$$\begin{bmatrix} q_x \\ q_y \end{bmatrix} = -\begin{bmatrix} \kappa_{xx} & \kappa_{xy} \\ \kappa_{yx} & \kappa_{yy} \end{bmatrix} \begin{bmatrix} \frac{\partial \theta}{\partial x} \\ \frac{\partial \theta}{\partial y} \end{bmatrix} \tag{4.2}$$

$$\boldsymbol{q} = -\boldsymbol{\kappa} \cdot \frac{\partial \theta}{\partial \boldsymbol{x}} \tag{4.3}$$

where the units for heat flux $\boldsymbol{q}$ are $\mathrm{W/m^2}$, and for thermal conductivity $\boldsymbol{\kappa}$ are W/(m °C). Consider a brief review of **tensor notation** in index form as,

- coordinate vector $\boldsymbol{x} = [\, x \; y \,]^T = [\, x_1 \; x_2 \,]^T$
- heat flux vector $\boldsymbol{q} = [\, q_x \; q_y \,]^T = [\, q_1 \; q_2 \,]^T$
- sum over repeated indices: $\boldsymbol{q} = q_i \boldsymbol{e}_i = q_1 \boldsymbol{e}_1 + q_2 \boldsymbol{e}_2$
- thermal conductivity matrix: $\boldsymbol{\kappa} = \begin{bmatrix} \kappa_{11} & \kappa_{12} \\ \kappa_{21} & \kappa_{22} \end{bmatrix} = \kappa_{ij} \boldsymbol{e}_i \otimes \boldsymbol{e}_j$
- vector or dyadic product $\otimes$
- isotropic thermal conductivity: $\boldsymbol{\kappa} = \kappa \begin{bmatrix} 1 & 0 \\ 0 & 1 \end{bmatrix}$, or $\kappa_{ij} = \kappa \delta_{ij}$
- Fourier's law in index notation: $q_i = -\kappa_{ij} \frac{\partial \theta}{\partial x_j}$
- heat equation (balance of energy, first law of thermodynamics): $\frac{\partial q_i}{\partial x_i} = f$, or $q_{i,i} = f$

We may then state the Strong form (S) as,

$$
(S)\begin{cases}
\text{Find } \theta(x,y) : \bar{\Omega} \mapsto \mathbb{R}, & \text{such that} \\
\qquad q_{i,i} = f & \in \Omega \\
\qquad \theta = g_\theta & \text{on}\, \Gamma_\theta \\
\qquad -q_i n_i = q & \text{on}\, \Gamma_q
\end{cases}
\tag{4.4}
$$

where $\theta(x,y) : \bar{\Omega} \mapsto \mathbb{R}$ reads "with (x,y) in $\bar{\Omega}$ and θ maps to the real number line $\mathbb{R}$," the heat source is $f(x,y)$, the heat flux q is a positive in-flux natural, Neumann BC, and prescribed temperature g_θ is an essential, or Dirichlet, BC.

4.2 Weak form (W) by Method of Weighted Residuals

For the Method of Weighted Residuals as applied to the balance of energy, we introduce a weighting function $w(x,y)$, which if a variational principle can be established (which it can for heat conduction), then it is thought of as a variation of temperature $w = \delta\theta$. Put the balance equation in residual form, multiply by w, and integrate over Ω as,

$$
\int_\Omega w(q_{i,i} - f)da = 0 \tag{4.5}
$$

where $da = dxdy = dx_1dx_2$. Apply the chain rule as,

$$
\frac{\partial}{\partial x_i}(wq_i) = \frac{\partial w}{\partial x_i}q_i + w\frac{\partial q_i}{\partial x_i} \tag{4.6}
$$

where then,

$$
\int_\Omega wq_{i,i}da = \int_\Omega \left[(wq_i)_{,i} - w_{,i}q_i\right] da \tag{4.7}
$$

Recall the divergence theorem,

$$\int_{\Omega}(wq_i)_{,i}da = \int_{\Gamma}(wq_i)n_i ds \tag{4.8}$$

and $w = 0$ on Γ_θ, and $-q_i n_i = q$ on Γ_q, such that

$$\begin{aligned}\int_{\Gamma}(wq_i)n_i ds &= \int_{\Gamma_\theta} wq_i n_i ds + \int_{\Gamma_q} wq_i n_i ds \\ &= -\int_{\Gamma_q} wq ds\end{aligned}$$

We substitute to get,

$$-\int_{\Omega} w_{,i}q_i da - \int_{\Omega} wf da - \int_{\Gamma_q} wq ds = 0 \tag{4.9}$$

Then, using Fourier's law ($q_i = -\kappa_{ij}\theta_{,j}$), we state the Weak form (W) as,

$$(W)\begin{cases}\text{Find } \theta(x,y) \in \mathscr{S} = \{\theta : \Omega \mapsto \mathbb{R}, \theta \in H^1, \theta = g_\theta \text{ on } \Gamma_\theta\}, \text{such that} \\ \int_{\Omega} w_{,i}\kappa_{ij}\theta_{,j} da = \int_{\Omega} wf da + \int_{\Gamma_q} wq ds \\ \text{holds } \forall w(x,y) \in \mathscr{V} = \{w : \Omega \mapsto \mathbb{R}, w \in H^1, w = 0 \text{ on } \Gamma_\theta\}\end{cases} \tag{4.10}$$

where $\forall$ reads "for all," $\mathscr{S}$ is the space of admissible trial functions, $\mathscr{V}$ is the space of weighting functions, H^1 is the first Sobolev space, such that the H^1 norm is finite: i.e., $\|\theta\|_1 = \left(\int_{\Omega}(\theta^2 + (\theta_{,i})^2)\,dx\right)^{1/2} < \infty$, where $\|\theta\|_1$ is called the natural norm, and $\theta \in H^1$ essentially says that first spatial derivatives $\theta_{,i}$ CANNOT be Dirac-Delta functions, but can be Heaviside functions (discontinuous) which leads to a "C^0 theory" for linear heat conduction (as we had for the 1D axially-loaded bar problem).

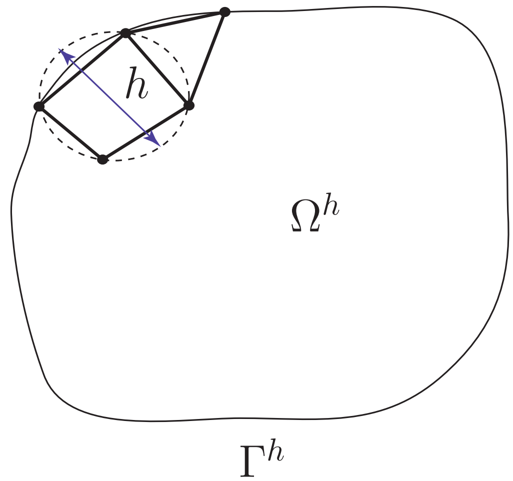

Figure 4.2. Discrete body $\Omega^h \subset \Omega$, $\bar{\Omega}^h = \Omega^h \cup \Gamma^h$.

4.3 Discrete, Galerkin form (G)

Referring to Fig.4.2, we may rewrite the Weak form in discrete, Galerkin form as,

$$(G)\begin{cases} \text{Find } \theta^h(x,y) \in \mathscr{S}^h = \{\theta^h : \Omega^h \mapsto \mathbb{R}, \theta^h \in H^1, \theta^h = g_\theta \text{ on } \Gamma^h_\theta\}, \text{such that} \\ \int_{\Omega^h} w^h_{,i}\kappa_{ij}\theta^h_{,j}da = \int_{\Omega^h} w^h f da + \int_{\Gamma^h_q} w^h q ds \\ \text{holds } \forall w^h(x,y) \in \mathscr{V}^h = \{w^h : \Omega^h \mapsto \mathbb{R}, w^h \in H^1, w^h = 0 \text{ on } \Gamma^h_\theta\} \end{cases} \quad (4.11)$$

where $\mathscr{S}^h \subset \mathscr{S}$ is the discrete subspace of admissible trial functions, $\mathscr{V}^h \subset \mathscr{V}$ is the discrete subspace of weighting functions, and $(G) \approx (W)$, where note that even though θ^h and w^h are discrete approximations to θ and w, respectively, they must still satisfy restrictions on the spaces (in order to ensure convergence, i.e., $\lim_{h\to 0}\theta^h = \theta$).

4.4 Finite Element (FE), Matrix form

Discretize the 2D body into finite elements (quadrilaterals or triangles), such as in Fig.4.3.

Now, consider a bilinear quadrilateral in Fig.4.4.

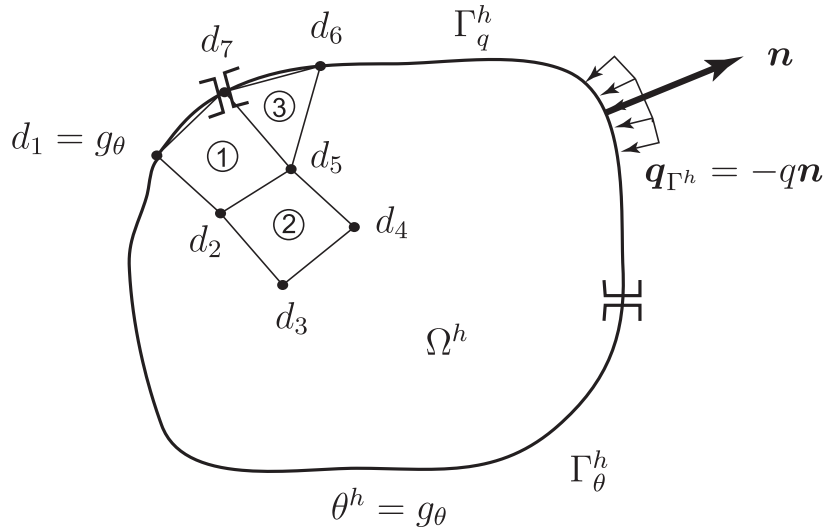

Figure 4.3. **Global perspective** on FE mesh with $\theta^h(x, y) = \sum_{A=1}^{n_{\mathrm{np}}} N_A(x, y)d_A$, n_{np} is the number of nodal points, and $N_A(x, y)$ is the shape function at global node A.

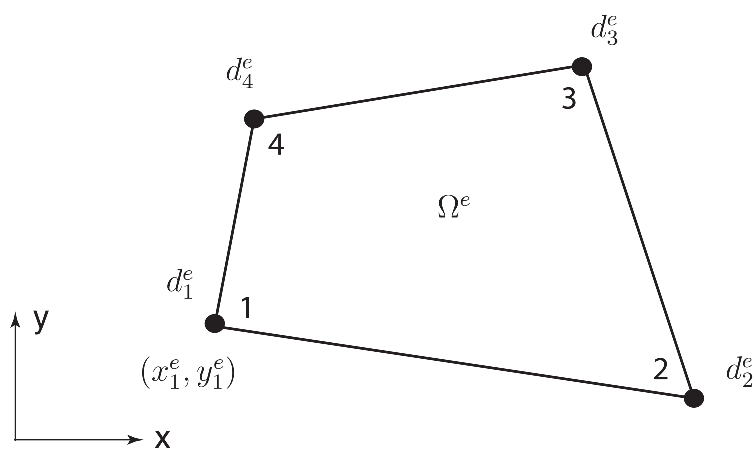

Figure 4.4. **Element perspective** on FE mesh with local element nodal dof $d_a^e = \theta^{h^e}(x_a^e, y_a^e)$, element domain Ω^e, discrete domain $\Omega^h = \mathbf{A}_{e=1}^{n_{\mathrm{el}}} \Omega^e$, and $\mathbf{A}_{e=1}^{n_{\mathrm{el}}}$ is the element assembly operator.

The next step is to discretize the Galerkin integral equation into finite elements as,

$$\mathop{\mathbf{A}}_{e=1}^{n_{\mathrm{el}}} \left[\int_{\Omega^e} w_{,i}^{h^e} \kappa_{ij} \theta_{,j}^{h^e} da = \int_{\Omega^e} w^{h^e} f da + \int_{\Gamma_q^e} w^{h^e} q ds \right] \tag{4.12}$$

and write the interpolations and their derivatives as,

$$\theta^{h^e}(\boldsymbol{x}) = \sum_{a=1}^{n_{\text{en}}} N_a(\boldsymbol{x}) d_a^e = \underbrace{\boldsymbol{N}^e}_{1\times n_{\text{en}}} \cdot \underbrace{\boldsymbol{d}^e}_{n_{\text{en}}\times 1} \tag{4.13}$$

$$w^{h^e}(\boldsymbol{x}) = \sum_{a=1}^{n_{\text{en}}} N_a(\boldsymbol{x}) c_a^e = \boldsymbol{N}^e \cdot \boldsymbol{c}^e \tag{4.14}$$

$$\left[\theta^{h^e}_{,i}(\boldsymbol{x})\right] = \sum_{a=1}^{n_{\text{en}}} \left[\frac{\partial N_a(\boldsymbol{x})}{\partial x_i}\right] d_a^e = \underbrace{\boldsymbol{B}^e}_{n_{\text{sd}}\times n_{\text{en}}} \cdot \underbrace{\boldsymbol{d}^e}_{n_{\text{en}}\times 1} \tag{4.15}$$

$$\left[w^{h^e}_{,i}(\boldsymbol{x})\right] = \sum_{a=1}^{n_{\text{en}}} \left[\frac{\partial N_a(\boldsymbol{x})}{\partial x_i}\right] c_a^e = \boldsymbol{B}^e \cdot \boldsymbol{c}^e \tag{4.16}$$

where n_{en} is the number of element nodes, and $n_{\text{sd}} = 2$ is the number of spatial dimensions.

Let $\boldsymbol{\kappa} = \boldsymbol{D}$ be the matrix form of the thermal conductivity tensor, and then,

$$\mathop{\mathsf{A}}_{e=1}^{n_{\text{el}}} (\boldsymbol{c}^e)^T \cdot \left[\underbrace{\left(\int_{\Omega^e} (\boldsymbol{B}^e)^T \cdot \boldsymbol{D} \cdot \boldsymbol{B}^e da \right)}_{\boldsymbol{k}^e} \cdot \boldsymbol{d}^e = \underbrace{\int_{\Omega^e} (\boldsymbol{N}^e)^T f da}_{\boldsymbol{f}^e_f} + \underbrace{\int_{\Gamma^e_q} (\boldsymbol{N}^e)^T q ds}_{\boldsymbol{f}^e_q} \right] \tag{4.17}$$

and

$$\mathop{\mathsf{A}}_{e=1}^{n_{\text{el}}} (\boldsymbol{c}^e)^T \cdot \left[\boldsymbol{k}^e \cdot \boldsymbol{d}^e = \boldsymbol{f}^e_f + \boldsymbol{f}^e_q \right] \tag{4.18}$$

Before assembling, let's introduce the bilinear, quadrilateral element in natural coordinates.

4.5 Bilinear quadrilateral element

For the bilinear quadrilateral element, (pg.164 F&B, pg.112 Hughes), in natural coordinates, refer to Fig.4.5.

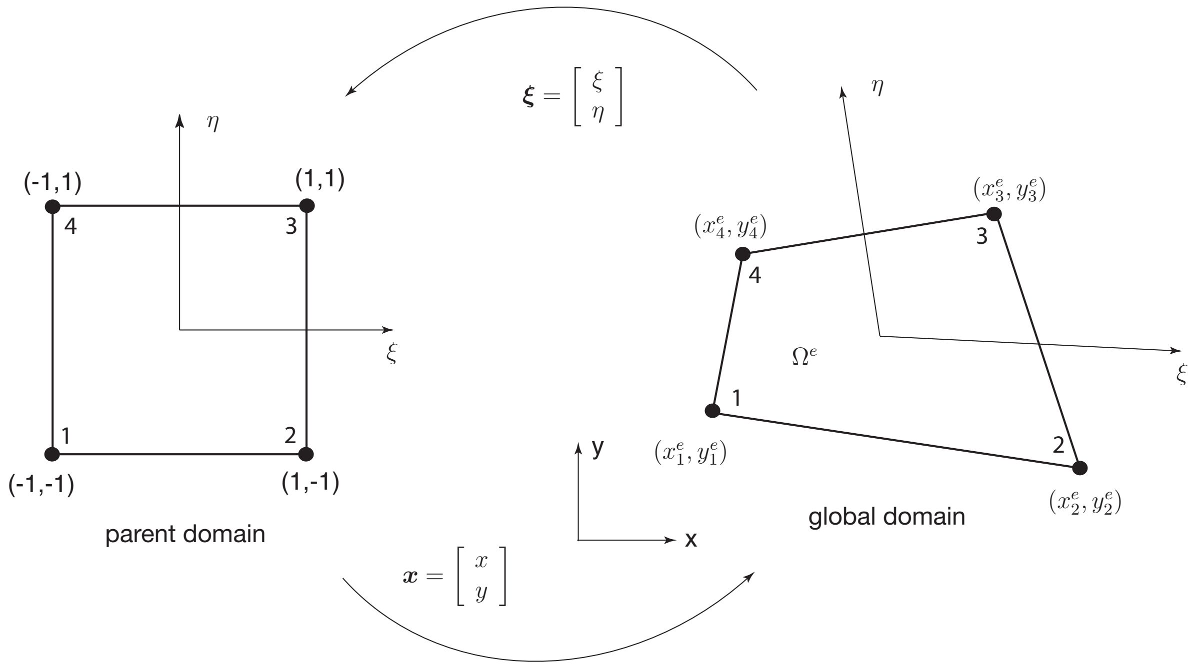

Figure 4.5. In natural coordinates, note the isoparametric mapping, $\boldsymbol{x}^{h^e}(\boldsymbol{\xi}) = \sum_{a=1}^{4} N_a(\boldsymbol{\xi})\boldsymbol{x}_a^e$, and bilinear shape functions, $N_a(\xi,\eta) = \frac{1}{4}(1+\xi_a\xi)(1+\eta_a\eta)$.

We then interpolate in terms of $\boldsymbol{\xi}$ as,

$$\theta^{h^e}(\boldsymbol{\xi}) = \sum_{a=1}^{4} N_a(\boldsymbol{\xi}) d_a^e \tag{4.19}$$

$$w^{h^e}(\boldsymbol{\xi}) = \sum_{a=1}^{4} N_a(\boldsymbol{\xi}) c_a^e \tag{4.20}$$

The bilinear shape functions $N_a(\xi,\eta) = \frac{1}{4}(1+\xi_a\xi)(1+\eta_a\eta)$ may be visualized in Fig.4.6.

To take spatial derivatives in 2D, we need the Jacobian matrix of coordinate transformation

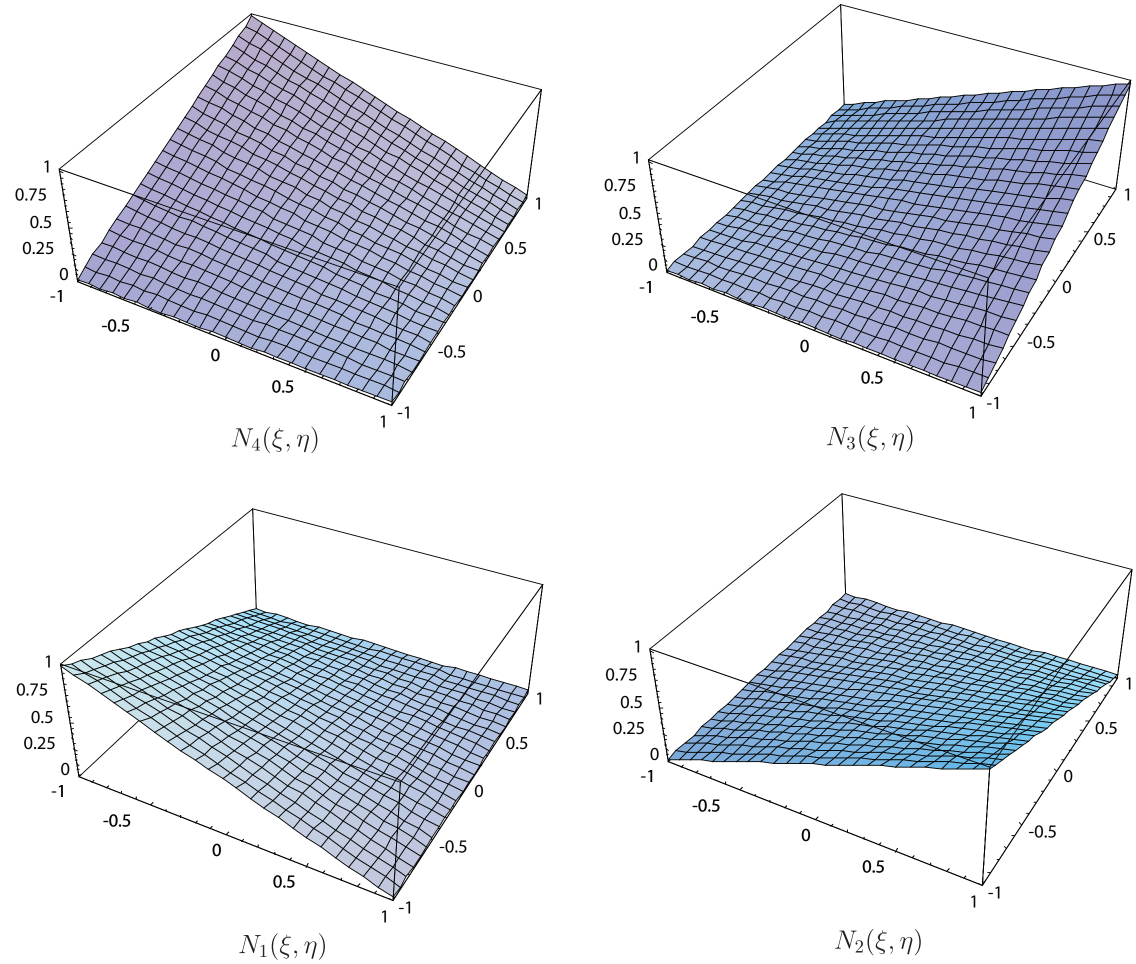

Figure 4.6. bilinear shape functions $N_a(\xi, \eta) = \frac{1}{4}(1 + \xi_a \xi)(1 + \eta_a \eta)$.

$\boldsymbol{J}^e$ as,

$$d\boldsymbol{x} = \frac{\partial \boldsymbol{x}}{\partial \boldsymbol{\xi}} \cdot d\boldsymbol{\xi} = \boldsymbol{J}^e \cdot d\boldsymbol{\xi} \tag{4.21}$$

$$\begin{bmatrix} dx \\ dy \end{bmatrix} = \begin{bmatrix} \frac{\partial x}{\partial \xi} & \frac{\partial x}{\partial \eta} \\ \frac{\partial y}{\partial \xi} & \frac{\partial y}{\partial \eta} \end{bmatrix} \begin{bmatrix} \partial \xi \\ \partial \eta \end{bmatrix} \tag{4.22}$$

$$da = dxdy = j^e d\xi d\eta \tag{4.23}$$

$$j^e = \det \boldsymbol{J}^e \tag{4.24}$$

The 'strain-displacement' matrix (to calculate temperature gradient from temperature) is then $\boldsymbol{B}^e = [\,\boldsymbol{B}_1\,\boldsymbol{B}_2\,\boldsymbol{B}_3\,\boldsymbol{B}_4\,]$ where,

$$\boldsymbol{B}_a = \begin{bmatrix} \frac{\partial N_a}{\partial x} \\ \frac{\partial N_a}{\partial y} \end{bmatrix}, \quad \boldsymbol{B}_a^T = \begin{bmatrix} \frac{\partial N_a}{\partial x} & \frac{\partial N_a}{\partial y} \end{bmatrix} = \frac{\partial N_a}{\partial \boldsymbol{x}}$$

$$\boldsymbol{B}_a^T = \frac{\partial N_a}{\partial \boldsymbol{x}} = \frac{\partial N_a}{\partial \boldsymbol{\xi}} \cdot \frac{\partial \boldsymbol{\xi}}{\partial \boldsymbol{x}} = \begin{bmatrix} \frac{\partial N_a}{\partial \xi} & \frac{\partial N_a}{\partial \eta} \end{bmatrix} \begin{bmatrix} \frac{\partial \xi}{\partial x} & \frac{\partial \xi}{\partial y} \\ \frac{\partial \eta}{\partial x} & \frac{\partial \eta}{\partial y} \end{bmatrix} = \frac{\partial N_a}{\partial \boldsymbol{\xi}} \cdot (\boldsymbol{J}^e)^{-1}$$

$$\boldsymbol{B}_a = (\boldsymbol{J}^e)^{-T} \cdot \left(\frac{\partial N_a}{\partial \boldsymbol{\xi}}\right)^T$$

$$(\boldsymbol{J}^e)^{-1} = \frac{1}{j^e} \begin{bmatrix} y_{,\eta} & -x_{,\eta} \\ -y_{,\xi} & x_{,\xi} \end{bmatrix}$$

Let's consider an example shown in Fig.4.7.

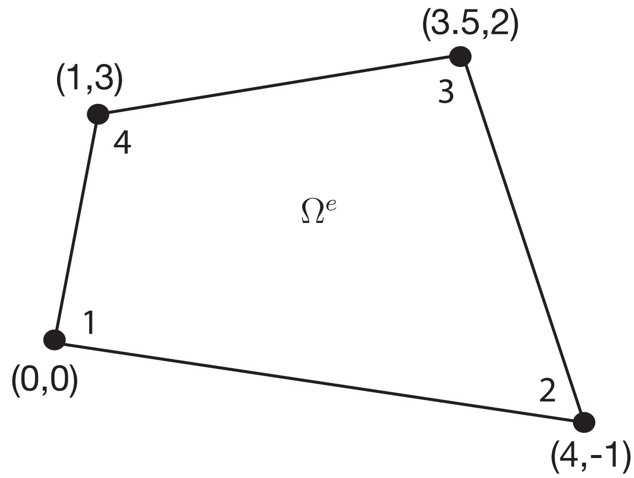

Figure 4.7. Example for calculating j^e.

We have $\frac{\partial N_a}{\partial \xi} = \frac{1}{4}\xi_a(1+\eta_a\eta)$, $\frac{\partial N_a}{\partial \eta} = \frac{1}{4}\eta_a(1+\xi_a\xi)$,

$x^{h^e}_{,\xi} = \sum_{a=1}^{4} \frac{\partial N_a}{\partial \xi} x_a^e = 1.625 - 0.375\eta$,

$x^{h^e}_{,\eta} = \sum_{a=1}^{4} \frac{\partial N_a}{\partial \eta} x_a^e = 0.125 - 0.375\xi$,

$y^{h^e}_{,\xi} = \sum_{a=1}^{4} \frac{\partial N_a}{\partial \xi} y_a^e = -0.5$,

$y^{h^e}_{,\eta} = \sum_{a=1}^{4} \frac{\partial N_a}{\partial \eta} y_a^e = 1.5$,

and $j^e = x_{,\xi}y_{,\eta} - x_{,\eta}y_{,\xi} = 2.5 - 0.1875\xi - 0.5625\eta$.

Recall that $(\boldsymbol{J}^e)^{-1} = \frac{1}{j^e}\begin{bmatrix} y_{,\eta} & -x_{,\eta} \\ -y_{,\xi} & x_{,\xi} \end{bmatrix}$, and $\boldsymbol{B}_a = (\boldsymbol{J}^e)^{-T} \cdot \left(\frac{\partial N_a}{\partial \boldsymbol{\xi}}\right)^T$. Thus, the integrand of the conductivity matrix is not a polynomial (it is a rational function). We will use Gauss quadrature to approximate finite element integration (this is what finite element programs like `ABAQUS` do).

Thus, we can evaluate the thermal conductivity matrix and heat source vector in the parent domain using Gaussian quadrature (introduce later) as,

$$\boldsymbol{k}^e = \int_{-1}^{1}\int_{-1}^{1} [\boldsymbol{B}^e(\boldsymbol{\xi})]^T \cdot \boldsymbol{D} \cdot \boldsymbol{B}^e(\boldsymbol{\xi}) j^e d\xi d\eta \tag{4.25}$$

$$\boldsymbol{f}_f^e = \int_{-1}^{1}\int_{-1}^{1} [\boldsymbol{N}^e(\boldsymbol{\xi})]^T \hat{f}(\boldsymbol{\xi}) j^e d\xi d\eta \tag{4.26}$$

But what about the heat flux vector at the element boundary Γ^e (if the element is on the boundary Γ_q^h)?

$$\boldsymbol{f}_q^e = \int_{\Gamma_q^e} (\boldsymbol{N}^e)^T q ds \tag{4.27}$$

Let's look at the surface of integration in Fig.4.8.

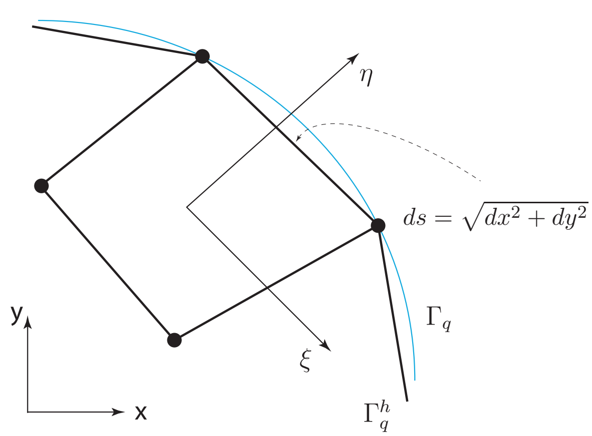

Figure 4.8. Integration over boundary Γ^e of element e. $dx = x_{,\xi}d\xi + x_{,\eta}d\eta$ and $dy = y_{,\xi}d\xi + y_{,\eta}d\eta$. Along ds, $\eta = 1 \Longrightarrow d\eta = 0$, and note that $ds = \sqrt{x_{,\xi}^2 + y_{,\xi}^2}d\xi$.

4.6 Triangular element

For the triangular element formulation, see attached handwritten notes.

4.7 Element assembly process

Consider the Element assembly process for the example on pg.71 of Hughes 1987. We use the IEN and ID "arrays" to obtain the Location Matrix (LM). For the **element nodes array**, IEN$(a, e) = A$, where a is the local element node number, e the element number, and A the global node number. The **ID array** relates global node numbers A to global equation numbers (dofs). The **location matrix (LM)** can then be determined from the IEN and ID as LM(a, e) =ID(IEN(a, e)) to return the global dof given local element node number a and element number e. Refer to Fig.4.9.

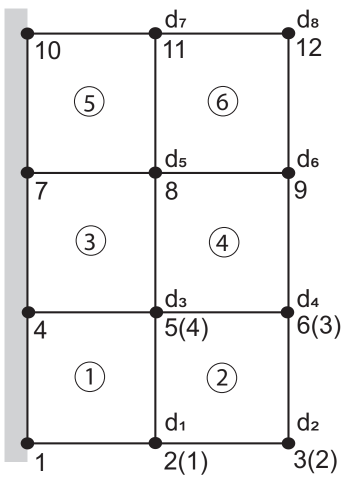

- **ID array**:

global node number

1	2	3	4	5	6	7	8	9	10	11	12	
0	1	2	0	3	4	0	5	6	0	7	8	d.o.f.

- **IEN array**:

	e: 1	2	3	4	5	6
a 1	1	2	4	5	7	8
2	2	3	5	6	8	9
3	5	6	8	9	11	12
4	4	5	7	8	10	11

Figure 4.9. Location matrix example.

Then the LM(a, e) =ID(IEN(a, e)), which is populated with global d.o.f. as,

	e: 1	2	3	4	5	6
a 1	0	1	0	3	0	5
2	1	2	3	4	5	6
3	3	4	5	6	7	8
4	0	3	0	5	0	7

Let's look at element 1, where recall the element conductivity matrix as,

$$\boldsymbol{k}^e = \begin{bmatrix} k_{11}^e & k_{12}^e & k_{13}^e & k_{14}^e \\ k_{12}^e & k_{22}^e & k_{23}^e & k_{24}^e \\ k_{13}^e & k_{23}^e & k_{33}^e & k_{34}^e \\ k_{14}^e & k_{24}^e & k_{34}^e & k_{44}^e \end{bmatrix} \tag{4.28}$$

Now, recall the element assembly operation:

$$\mathop{\mathbf{A}}_{e=1}^{n_{\text{el}}} (\boldsymbol{c}^e)^T \cdot \left[\boldsymbol{k}^e \cdot \boldsymbol{d}^e = \boldsymbol{f}_f^e + \boldsymbol{f}_q^e\right] \tag{4.29}$$

$$\boldsymbol{K} \cdot \boldsymbol{d} = \boldsymbol{F} = \boldsymbol{F}_q + \boldsymbol{F}_f + \boldsymbol{F}_g \tag{4.30}$$

After placing individual conductivity and flux contributions into the global matrix/vector form, we can sum up the element contributions as,

$$\boldsymbol{K} = \sum_{e=1}^{n_{\text{el}}} \boldsymbol{K}^e \ , \quad \boldsymbol{F}_q = \sum_{e=1}^{n_{\text{el}}} \boldsymbol{F}_q^e \ , \quad \boldsymbol{F}_f = \sum_{e=1}^{n_{\text{el}}} \boldsymbol{F}_f^e \ , \quad \boldsymbol{F}_g = \sum_{e=1}^{n_{\text{el}}} \boldsymbol{F}_g^e \tag{4.31}$$

and then solve for $\boldsymbol{d}$ such that for element 1:

$$\boldsymbol{K}^1 = \begin{bmatrix} k_{22}^1 & \cdot & k_{23}^1 & \dots \\ \cdot & \cdot & \cdot & \dots \\ k_{23}^1 & \cdot & k_{33}^1 & \dots \\ \vdots & \vdots & \vdots & \vdots \dots \end{bmatrix} \ , \quad \boldsymbol{F}_g^1 = \begin{bmatrix} k_{12}^1 g_{\theta(1)} + k_{24}^1 g_{\theta(4)} \\ \cdot \\ k_{13}^1 g_{\theta(1)} + k_{34}^1 g_{\theta(4)} \\ \vdots \end{bmatrix} \tag{4.32}$$

and so on for other elements and for $\boldsymbol{F}_q$ and $\boldsymbol{F}_f$.

4.8 Convergence

Recall that for **convergence**, we need **compatibility** and **completeness**. These lead to 3 conditions that we will satisfy for linear heat conduction finite elements:

(i) **compatibility**:

(1) θ^{h^e} smooth on Ω^e,

(2) θ^{h^e} continuous across element boundaries Γ^e;

(ii) **completeness**:

(3) represent constant temperature θ^{h^e} and constant temperature flux $\theta^{h^e}_{,i}$.

For **(1) smoothness**, use the bilinear quadrilateral element in Fig.4.10 as an example. We require the interior angles to be $< 180°$, or that $j^e = \det \boldsymbol{J}^e > 0$; this checks for input error in local element node numbering, and whether an element is extremely distorted for large deformation analysis (small strain analysis doesn't care if the element is highly distorted or not because the element Jacobian and coordinates are not updated).

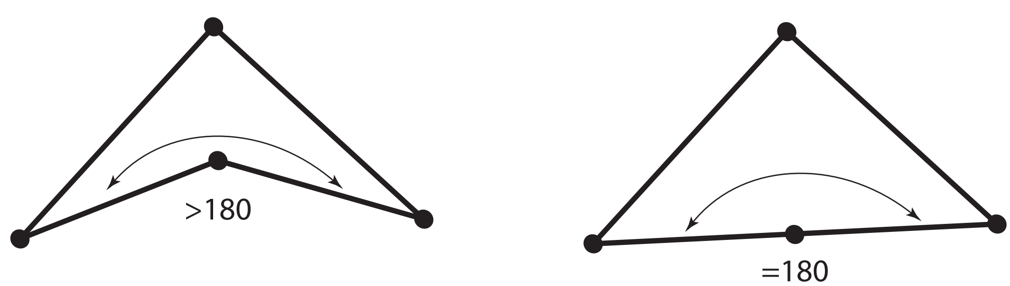

Figure 4.10. Problems with bilinear quadrilaterals.

For **(2) continuity** across Γ^e, it is automatically satisfied by the shape functions $N_a(\boldsymbol{\xi})$, as shown in Fig.4.11.

For **(3) completeness**, we need to represent constant temperature θ^{h^e} and constant temperature flux $\theta^{h^e}_{,i}$, needing at a minimum a linear polynomial for θ^{h^e}; with first order completeness

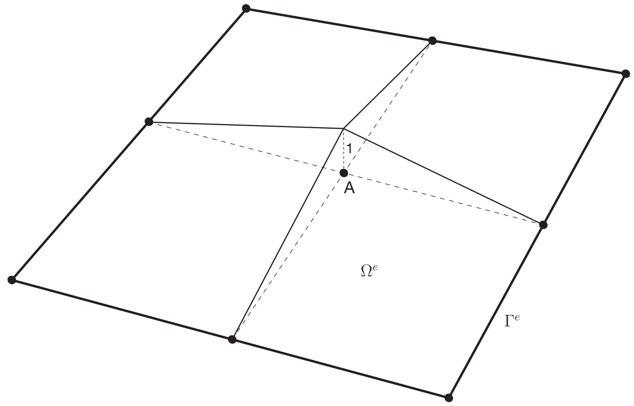

Figure 4.11. Continuity of four bilinear quadrilaterals.

required. The interpolations are,

$$\theta^{h^e}(\boldsymbol{\xi}) = \sum_{a=1}^{n_{\text{en}}} N_a(\boldsymbol{\xi}) d_a^e \tag{4.33}$$

$$\boldsymbol{x}^{h^e}(\boldsymbol{\xi}) = \sum_{a=1}^{n_{\text{en}}} N_a(\boldsymbol{\xi}) \boldsymbol{x}_a^e \tag{4.34}$$

and then let $d_a^e = c_0 + c_1 x_a^e + c_2 y_a^e$, and substitute into θ^{h^e} where,

$$\theta^{h^e}(\boldsymbol{\xi}) = \left(\sum_{a=1}^{n_{\text{en}}} N_a\right) c_0 + \left(\sum_{a=1}^{n_{\text{en}}} N_a x_a^e\right) c_1 + \left(\sum_{a=1}^{n_{\text{en}}} N_a y_a^e\right) c_2 \tag{4.35}$$

$$= c_0 + c_1 x + c_2 y \tag{4.36}$$

Thus, the bilinear quadrilateral element is complete to first order by virtue of the isoparametric formulation.

4.9 Gaussian quadrature

The Gaussian quadrature for a square parent domain (quadrilateral element) is presented on pg.178 F&B, pg.143 Hughes. Gaussian quadrature in higher dimensions (2D and 3D) essentially involves applying the Gaussian quadrature rule in 1D to each direction in 2D (i.e., the ξ and η directions) such as,

$$\int_{-1}^{1}\int_{-1}^{1} g(\xi,\eta)d\xi d\eta \approx \int_{-1}^{1}\left(\sum_m g(\tilde{\xi}_m,\eta)W_m\right)d\eta$$
$$\approx \sum_m\sum_n g(\tilde{\xi}_m,\tilde{\eta}_n)W_mW_n = \sum_{l=1}^{n_{\text{int}}} g(\tilde{\xi}_l,\tilde{\eta}_l)W_l \tag{4.37}$$

Figure 4.12 shows **1pt (2nd order accurate), 4pt (4th order accurate), 9pt (6th order accurate)** rules.

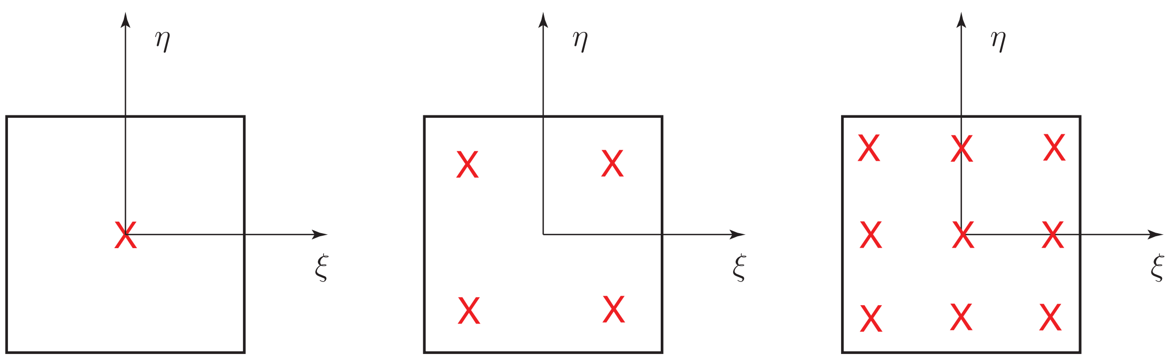

- $n_{\text{int}} = 1$
- $\tilde{\xi}_1 = \tilde{\eta}_1 = 0$
- $W_1 = 2*2 = 4$

- $n_{\text{int}} = 4$
- $\tilde{\xi}_1 = -1/\sqrt{3}$, $\tilde{\eta}_1 = -1/\sqrt{3}$, ...
- $W_1 = W_2 = W_3 = W_4 = 1$

- $n_{\text{int}} = 9$
- $\tilde{\xi}_1 = -\sqrt{3/5}$, $\tilde{\eta}_1 = -\sqrt{3/5}$, ...
- $W_1 = (5/9)(5/9)$, ...

Figure 4.12. Gaussian quadrature rules for 1×1, 2×2, and 3×3 integration points.

4.10 Symmetry in Boundary Value Problems (BVPs)

Consider the examples in Fig.4.13. Can we take advantage of symmetry or not for problems when using FEA?

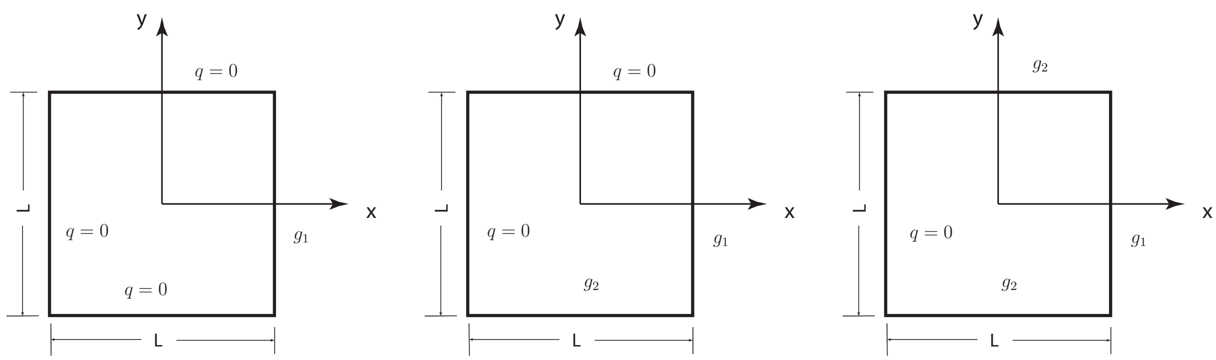

Figure 4.13. Examples for symmetry BCs.

4.11 Transient Heat Conduction

We introduce the specific heat c (J/(kg °C)), and temperature rate $\frac{\partial \theta}{\partial t}$, with I.C. on θ. The Strong Form is re-stated as,

$$(S)\left\{\begin{array}{rcll} \text{Find } \theta(x,y):\bar{\Omega}\times[0,T]\mapsto\mathbb{R}, & & \text{such that} & \\ \rho c\theta_{,t}+q_{i,i} & = & f & \in\Omega\times]0,T[\\ \theta & = & g_\theta & \text{on}\,\Gamma_\theta\times]0,T[\\ -q_i n_i & = & q & \text{on}\,\Gamma_q\times]0,T[\\ \theta(\boldsymbol{x},0) & = & \theta_0(\boldsymbol{x}) & \boldsymbol{x}\in\Omega \end{array}\right. \tag{4.38}$$

Assume Fourier's law for heat flux, $q_i = -\kappa_{ij}\theta_{,j}$, and interpolate as before:

$$\theta^{h^e}(\boldsymbol{\xi},t) = \sum_{a=1}^{n_{\text{en}}} N_a(\boldsymbol{\xi})d_a^e(t) = \boldsymbol{N}^e\cdot\boldsymbol{d}^e \tag{4.39}$$

$$\dot{\theta}^{h^e} = \boldsymbol{N}^e\cdot\dot{\boldsymbol{d}}^e \tag{4.40}$$

After deriving the Weak form, and stating the Galerkin form (both not shown), we have,

$$\mathop{\mathbf{A}}_{e=1}^{n_{\text{el}}}(\boldsymbol{c}^e)^T\cdot\left[\boldsymbol{m}^e\cdot\dot{\boldsymbol{d}}^e+\boldsymbol{k}^e\cdot\boldsymbol{d}^e=\boldsymbol{f}_f^e+\boldsymbol{f}_q^e\right] \tag{4.41}$$

$$\boldsymbol{m}^e = \int_{\Omega^e}\rho c[\boldsymbol{N}^e]^T\cdot\boldsymbol{N}^e da \tag{4.42}$$

$$= \int_{-1}^{1}\int_{-1}^{1}\rho c[\boldsymbol{N}^e(\boldsymbol{\xi})]^T\cdot\boldsymbol{N}^e(\boldsymbol{\xi})j^e d\xi d\eta \tag{4.43}$$

After element assembly, we have,

$$\boldsymbol{M}\cdot\dot{\boldsymbol{d}}+\boldsymbol{K}\cdot\boldsymbol{d}=\boldsymbol{F} \tag{4.44}$$

which is a parabolic matrix ODE. We use the generalized trapezoidal rule to integrate in time.

Evaluate the FE balance of energy equation at time t_{n+1}, and introduce difference formulas for $\boldsymbol{d}_{n+1}$ and $\boldsymbol{v}_{n+1}$, where α is the time integration parameter,

$$\boldsymbol{M} \cdot \boldsymbol{v}_{n+1} + \boldsymbol{K} \cdot \boldsymbol{d}_{n+1} = \boldsymbol{F}_{n+1} \tag{4.45}$$

$$\boldsymbol{d}_{n+1} = \boldsymbol{d}_n + \Delta t \boldsymbol{v}_{n+\alpha} \tag{4.46}$$

$$\boldsymbol{v}_{n+\alpha} = (1-\alpha)\boldsymbol{v}_n + \alpha \boldsymbol{v}_{n+1} \tag{4.47}$$

Common examples for choice of α are,

α	method	type
0	forward Euler	explicit (if $\boldsymbol{M}$ diagonal)
1/2	trapezoidal rule	implicit
1	backward Euler	implicit

The Implementation steps in a code are as follows:

- **initialize:** given initial temperature $\boldsymbol{d}_0$, solve for $\boldsymbol{v}_0$

$$\boldsymbol{M} \cdot \boldsymbol{v}_0 = \boldsymbol{F}_0 - \boldsymbol{K} \cdot \boldsymbol{d}_0 \tag{4.48}$$

- **predictor:**

$$\tilde{\boldsymbol{d}}_{n+1} = \boldsymbol{d}_n + (1-\alpha)\Delta t \boldsymbol{v}_n \tag{4.49}$$

- **solution:**

$$(\boldsymbol{M} + \alpha \Delta t \boldsymbol{K})\boldsymbol{v}_{n+1} = \boldsymbol{F}_{n+1} - \boldsymbol{K}\tilde{\boldsymbol{d}}_{n+1} \tag{4.50}$$

- **corrector:**

$$\boldsymbol{d}_{n+1} = \tilde{\boldsymbol{d}}_{n+1} + \alpha \Delta t \boldsymbol{v}_{n+1} \tag{4.51}$$

- **stability:**

  – unconditional: $\alpha \geq 1/2$

  – conditional: $\alpha < 1/2$; $\Delta t < \frac{2}{(1-2\alpha)\lambda^h_{\max}}$ *for 1D heat transfer: $\lambda^h_{\max} = (\omega^h_{\max})^2$, $\omega^h_{\max} = \frac{2\sqrt{3}\sqrt{k}}{h}$, $k = \frac{\kappa}{\rho c}$
  *then, $\Delta t < \frac{h^2}{6(1-2\alpha)k}$
  *for 2D and 3D, this critical time step is approximate (and also for nonlinear problems)

4.12 Analogy to saturated groundwater flow

Early versions of ground water flow (rigid soil and rock) FE codes essentially used transient heat conduction codes and applied a change of variables and parameters. The **corresponding terms and equations** are,

heat conduction	groundwater flow
temperature θ (°C)	total head $h = \frac{p_w}{\gamma_w} + h_e$ (m)
thermal conductivity κ (W/(m °C))	hydraulic conductivity κ (m/s)
Fourier's law $\boldsymbol{q} = -\boldsymbol{\kappa} \cdot \boldsymbol{\nabla}\theta$	Darcy's law $\boldsymbol{v}^w = -\boldsymbol{\kappa} \cdot \boldsymbol{\nabla} h$
heat capacity ρc (J/(m^3 °C))	specific storage S_c (1/m)
heat source f (W/m^3)	fluid mass production η (kg/(s m^3))

where p_w is the pore water pressure, $\gamma_w = \rho_w g$ the unit weight of water ($\rho_w = 1000$ kg/m^3, $g = 9.8$m/s^2), h_e the elevation head, and $\boldsymbol{v}^w$ is the superficial (or Darcy) velocity of the water. Refer to Fig.4.14 for an illustration of Bernoulli's equation.

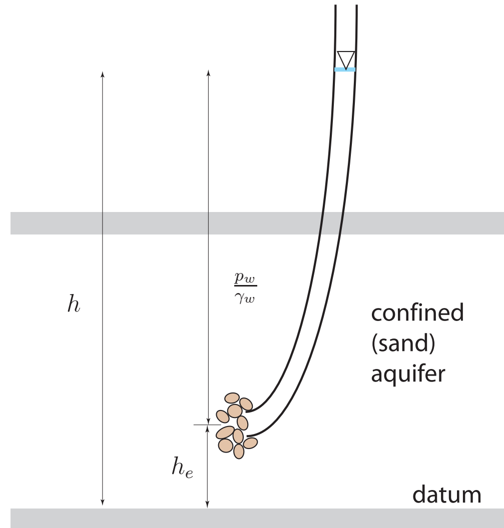

Figure 4.14. Illustration of Bernoulli's equation.

The Strong form is then written as,

$$(S)\begin{cases} \text{Find } h(x,y) : \bar{\Omega} \times [0,T] \mapsto \mathbb{R}, & \text{such that} \\ S_c h_{,t} + v^w_{i,i} = \frac{\eta}{\rho_w} & \in \Omega \times]0,T[\\ h = r & \text{on } \Gamma_r \times]0,T[\\ -v^w_i n_i = s & \text{on } \Gamma_s \times]0,T[\\ h(\boldsymbol{x},0) = h_0(\boldsymbol{x}) & \boldsymbol{x} \in \Omega \end{cases} \tag{4.52}$$

where r is the prescribed total head on Γ_r, s the prescribed fluid flux into the body across Γ_s, and h_0 the initial total head within the body.

For a steady-state analysis, consider the Concrete Gravity Dam (assumed rigid solid concrete skeleton) in Fig.4.15.

Or an embankment dam or levee (in Fig.4.16) with rising water level (again, assuming rigid solid skeleton, which is not valid here, but still used for estimating pore water pressures).

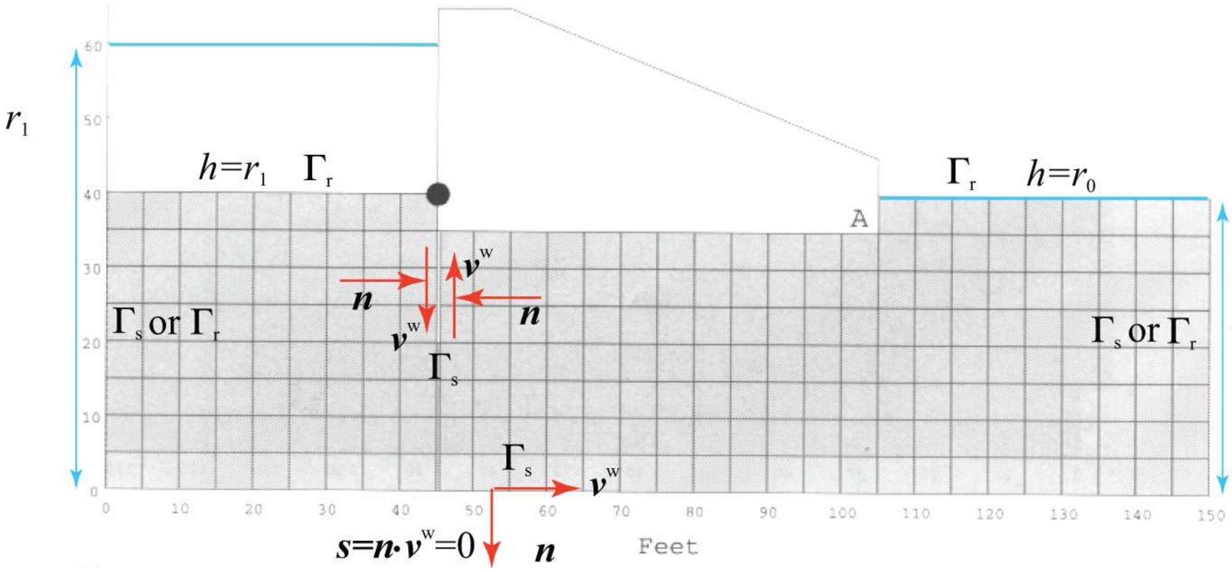

Figure 4.15. Concrete gravity dam analysis.

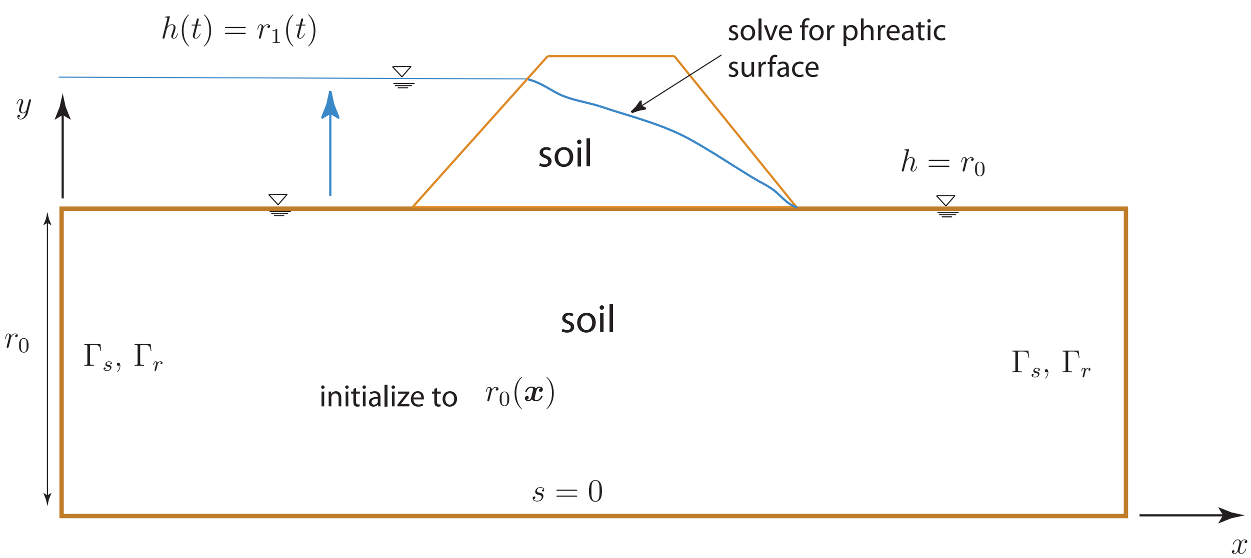

Figure 4.16. Embankment dam pore water flow analysis assuming soil is rigid.

4.13 Lagrange polynomials for higher order element formulation

A description of Lagrange polynomials used to formulate higher order polynomial-based finite elements is provided starting on pg.126 of Hughes. The **formula for a Lagrange polynomial** is,

$$\ell_a^{(n_{\text{en}}-1)}(\xi) = \frac{\prod_{b=1,b\neq a}^{n_{\text{en}}}(\xi - \xi_b)}{\prod_{b=1,b\neq a}^{n_{\text{en}}}(\xi_a - \xi_b)} \tag{4.53}$$

where,

$$\begin{aligned} n_{\text{en}} - 1 &= \text{order of polynomial} \\ a &= \text{node number} \\ \prod &= \text{product operator} \end{aligned}$$

such that for 1D, 2D, and 3D, we have,

$$\begin{aligned} 1D:\ N_a(\xi) &= \ell_a^{(n_{\text{en}}-1)}(\xi) \\ 2D:\ N_a(\xi,\eta) &= \ell_b^{(n_{\text{en}}-1)_\xi}(\xi)\ell_c^{(n_{\text{en}}-1)_\eta}(\eta) \\ 3D:\ N_a(\xi,\eta,\zeta) &= \ell_b^{(n_{\text{en}}-1)_\xi}(\xi)\ell_c^{(n_{\text{en}}-1)_\eta}(\eta)\ell_d^{(n_{\text{en}}-1)_\zeta}(\zeta) \end{aligned}$$

We consider some 1D examples. The 2-node, linear 1D element is formulated in Fig.4.17.

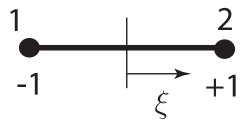

$n_{\text{en}} = 2 \Longrightarrow$
$n_{\text{en}} - 1 = 1$

$$\begin{aligned} N_1(\xi) &= \ell_1^1(\xi) = \frac{\xi-\xi_2}{\xi_1-\xi_2} = \frac{\xi-1}{-1-1} = (1-\xi)/2 \\ N_2(\xi) &= \ell_2^1(\xi) = \frac{\xi-\xi_1}{\xi_2-\xi_1} = \frac{\xi-(-1)}{1-(-1)} = (1+\xi)/2 \end{aligned}$$

Figure 4.17. 2-node, linear FE interpolation functions formulated from Lagrange polynomials.

The 3-node, quadratic 1D element is formulated in Fig.4.18.

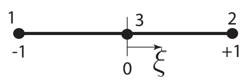

$n_{\text{en}} = 3 \Longrightarrow$
$n_{\text{en}} - 1 = 2$

$$\begin{aligned} N_1(\xi) &= \ell_1^2(\xi) = \frac{(\xi-\xi_2)(\xi-\xi_3)}{(\xi_1-\xi_2)(\xi_1-\xi_3)} = \frac{(\xi-1)\xi}{(-1-1)(-1)} = \xi(\xi-1)/2 \\ N_2(\xi) &= \ell_2^2(\xi) = \frac{(\xi-\xi_1)(\xi-\xi_3)}{(\xi_2-\xi_1)(\xi_2-\xi_3)} = \frac{(\xi-(-1))\xi}{(1-(-1))(1)} = \xi(\xi+1)/2 \\ N_3(\xi) &= \ell_3^2(\xi) = \frac{(\xi-\xi_1)(\xi-\xi_2)}{(\xi_3-\xi_1)(\xi_3-\xi_2)} = \frac{(\xi+1)(\xi-1)}{(1)(-1)} = 1-\xi^2 \end{aligned}$$

Figure 4.18. 3-node, quadratic FE interpolation functions formulated from Lagrange polynomials.

In two dimensions (2D), consider the **4 node, bilinear quadrilateral element** in Fig.4.19 with shape functions:

$$\begin{aligned} N_a(\xi,\eta) &= \ell_b^1(\xi)\ell_c^1(\eta) \\ N_1(\xi,\eta) &= \ell_1^1(\xi)\ell_1^1(\eta) = (1-\xi)/2(1-\eta)/2 = (1-\xi)(1-\eta)/4 \\ N_2(\xi,\eta) &= \ell_2^1(\xi)\ell_1^1(\eta) = (1+\xi)/2(1-\eta)/2 = (1+\xi)(1-\eta)/4 \\ N_3(\xi,\eta) &= \ell_2^1(\xi)\ell_2^1(\eta) = (1+\xi)/2(1+\eta)/2 = (1+\xi)(1+\eta)/4 \\ N_4(\xi,\eta) &= \ell_1^1(\xi)\ell_2^1(\eta) = (1-\xi)/2(1+\eta)/2 = (1-\xi)(1+\eta)/4 \end{aligned}$$

Consider the **9 node, bilquadratic quadrilateral element** in Fig.4.20 with shape func-

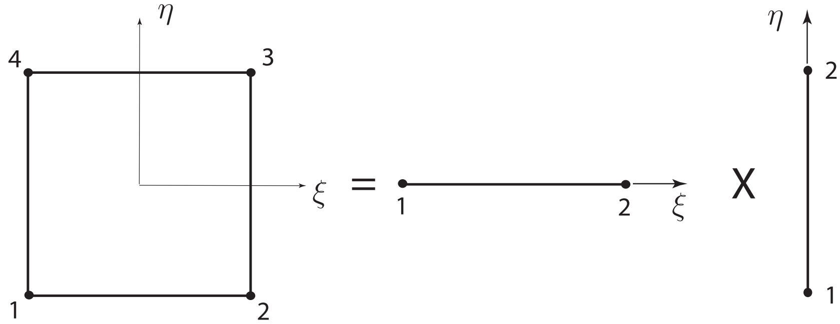

a	b	c
1	1	1
2	2	1
3	2	2
4	1	2

$$(n_{\text{en}})_\xi = 2, (n_{\text{en}})_\eta = 2 \Longrightarrow n_{\text{en}} - 1 = 1$$

Figure 4.19. 4-node, bilinear quadrilateral FE interpolation functions formulated from Lagrange polynomials.

tions:

$$\begin{aligned}
N_a(\xi,\eta) &= \ell_b^2(\xi)\ell_c^2(\eta) \\
\text{corner node } N_1(\xi,\eta) &= \ell_1^2(\xi)\ell_1^2(\eta) = \frac{1}{2}\xi(\xi-1)\frac{1}{2}\eta(\eta-1) = \frac{1}{4}\xi\eta(\xi-1)(\eta-1) \\
\text{midside node } N_5(\xi,\eta) &= \ell_3^2(\xi)\ell_1^2(\eta) = (1-\xi^2)\frac{1}{2}\eta(\eta-1) = \frac{1}{2}\eta(1-\xi^2)(\eta-1) \\
\text{middle node } N_9(\xi,\eta) &= \ell_3^2(\xi)\ell_3^2(\eta) = (1-\xi^2)(1-\eta^2)
\end{aligned}$$

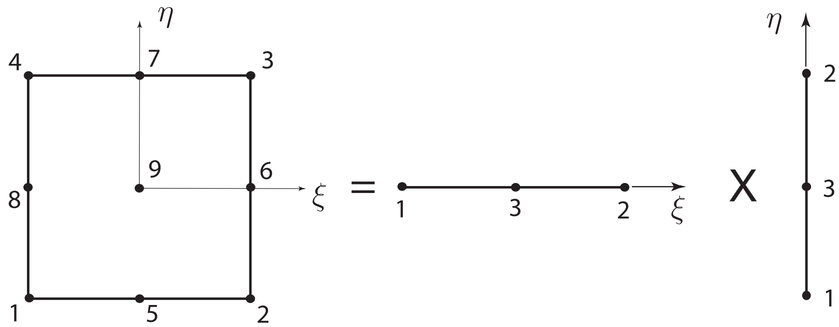

$(n_{\text{en}})_\xi = 3, (n_{\text{en}})_\eta = 3 \Longrightarrow n_{\text{en}} - 1 = 2$

a	b	c
1	1	1
2	2	1
3	2	2
4	1	2
5	3	1
6	2	3
7	3	2
8	1	3
9	3	3

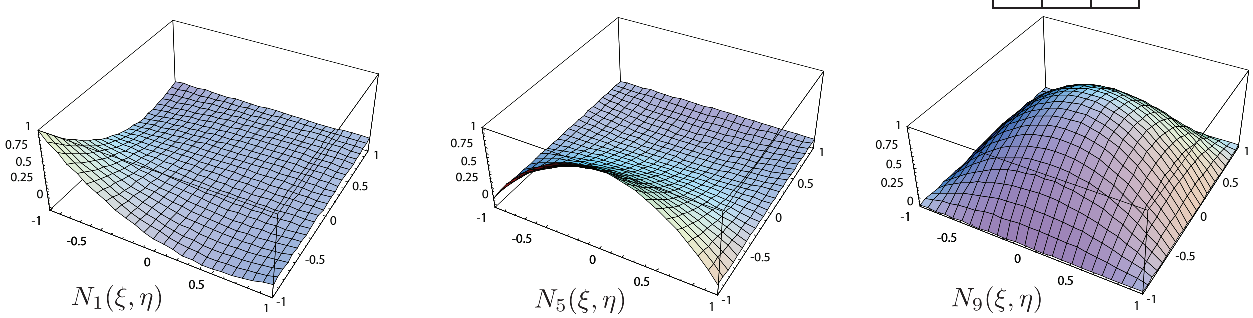

Figure 4.20. 9-node, biquadratic quadrilateral FE interpolation functions formulated from Lagrange polynomials.

Transition elements: Consider the mesh in Fig.4.21.

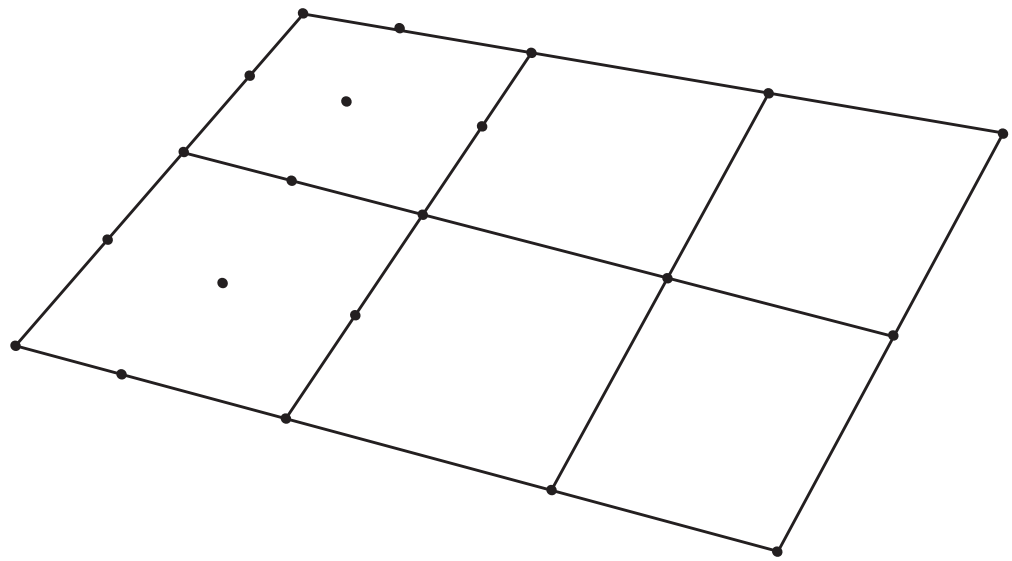

Figure 4.21. Linear to quadratic quadrilateral transition elements.

A 5-node quadrilateral transition element (Fig.4.22) may be formulated to address the proper compatibility requirement in the mesh in Fig.4.21. Start with the bilinear quadrilateral shape functions and introduce a 5th node along one of the element edges to make that edge have quadratic interpolation, while the 3 other edges have linear interpolation. Correction of adjacent nodal shape functions N_1 and N_2 is needed, as shown in Fig.4.22.

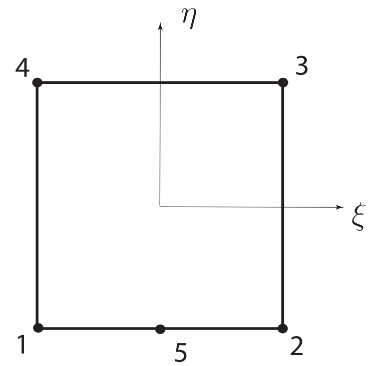

$$
\begin{aligned}
N_a(\xi,\eta) &= \frac{1}{4}(1+\xi_a\xi)(1+\eta_a\eta)\ ,\ a = 1, ..., 4 \\
N_5(\xi,\eta) &= \ell_3^2(\xi)\ell_1^1(\eta) = \frac{1}{2}(1-\xi^2)(1-\eta) \\
\text{need } N_5(\xi_a,\eta_a) &= \begin{cases} 1 & a = 5 \\ 0 & a \neq 5 \end{cases} \\
\text{correction } N_1 &= N_1 - \frac{1}{2}N_5 \\
N_2 &= N_2 - \frac{1}{2}N_5
\end{aligned}
$$

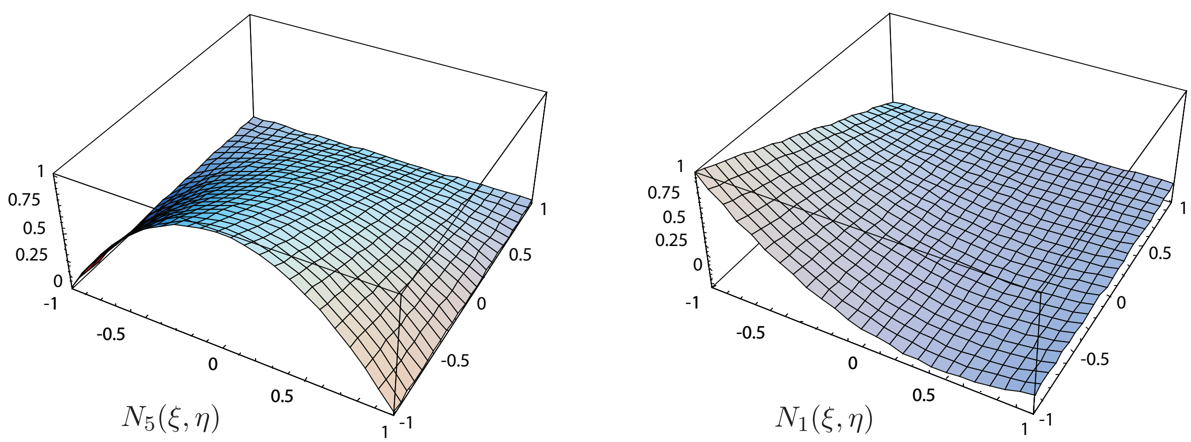

Figure 4.22. 5-node linear to quadratic interpolation transition quadrilateral element.

Chapter 5

3D Linear Elastostatics and Elastodynamics

For the 3D linear elastostatic and elastodynamic FEM, we assume linearity in the form of linear isotropic elasticity. These notes are drawn from Hughes [1987]. Topics covered in the remaining sections include the following:

(1) linear isotropic elasticity; small strains *and* small rotations (examples for small and finite); small strain versus large strain tensors;

(2) differential form and boundary conditions (BCs) to provide Strong Form (S) of 3D elastostatics;

(3) variational, Weak Form (W); re-write in vector-matrix form;

(4) review of plane elasticity: plane stress, plane strain, and axisymmetry;

(5) review of von Mises stress;

(6) discrete, Galerkin Form (G);

(7) Finite Element (FE), Matrix form in 3D;

(8) trilinear, hexhedral shape functions in natural coordinates (ξ, η, ζ) via Lagrange polynomials;

(9) 2D FE matrix form for linear elastostatics;

(10) element assembly to obtain Global Matrix form;

(11) convergence: (1) compatibility (satisfied by shape functions), and (2) completeness (consider an "engineering version" called the *Patch Test*);

(12) incompressibility constraint and mesh-locking; mixed formulation, selective reduced integration;

(13) linear elastodynamics.

5.1 3D linear isotropic elasticity

We assume linearity in the form of **small strains and rotations** (geometric, deformation) as,

$$\boldsymbol{\epsilon} = \frac{1}{2}\left(\boldsymbol{\nabla u} + (\boldsymbol{\nabla u})^T\right) \tag{5.1}$$

$$\epsilon_{ij} = \frac{1}{2}\left(\frac{\partial u_i}{\partial x_j} + \frac{\partial u_j}{\partial x_i}\right) \tag{5.2}$$

and **linear isotropic elasticity** (material, constitutive equation) as,

$$\boldsymbol{\sigma} = \boldsymbol{c} : \boldsymbol{\epsilon} \tag{5.3}$$

$$\sigma_{ij} = c_{ijkl}\epsilon_{kl} \tag{5.4}$$

where the fourth order isotropic elasticity tensor c_{ijkl} has two types of symmetry:

(i) major: $c_{ijkl} = c_{klij}$,

(ii) minor: $c_{ijkl} = c_{jikl} = c_{jilk} = c_{ijlk}$.

We can write as,

$$\boldsymbol{c} = \lambda \mathbf{1} \otimes \mathbf{1} + 2\mu \boldsymbol{I} \tag{5.5}$$

$$c_{ijkl} = \lambda \delta_{ij}\delta_{kl} + 2\mu I_{ijkl} \tag{5.6}$$

$$I_{ijkl} = \frac{1}{2}(\delta_{ik}\delta_{jl} + \delta_{il}\delta_{jk}) \tag{5.7}$$

The **Lamé parameters** are,

$$\mu = \frac{E}{2(1+\nu)}\ , \quad \lambda = \frac{2\mu\nu}{1-2\nu} \tag{5.8}$$

with **bulk modulus** $K = \lambda + \frac{2}{3}\mu = \frac{E}{3(1-2\nu)}$. For **incompressible elasticity** (e.g., rubber materials), then $\nu \to 0.5 \implies K \to \infty$ where **thermodynamically admissible values of Poisson's ratio** are $-1 < \nu < 0.5$.

5.2 Examples of small and finite strain and rotations

An example of both **small strain and rotation** is an I-beam experiencing design live and dead loads as in Fig.5.1.

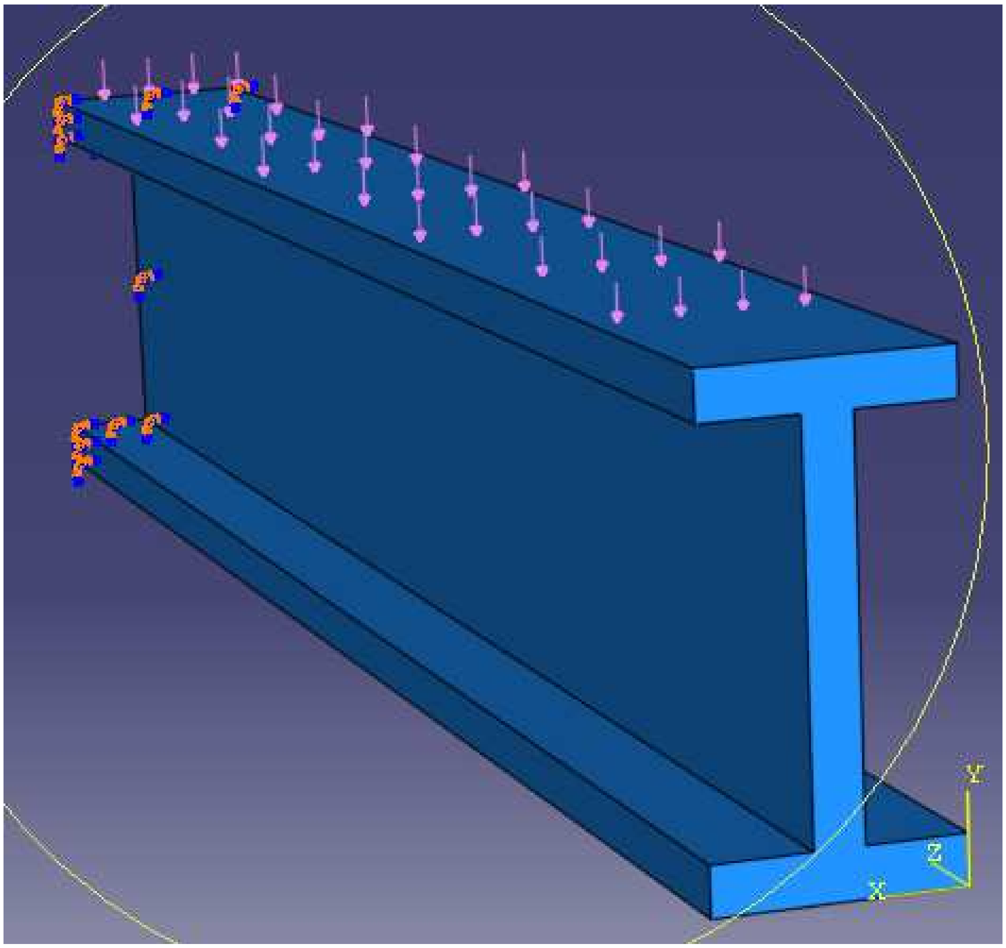

Figure 5.1. An I-beam experiencing design live and dead loads, and thus small strains and small rotations.

An example of **large strain with small rotation** is a car tire at constant angular velocity (no rotation of deformed part with respect to reference frame) as shown in Fig.5.2.

Figure 5.2. A car tire under constant angular velocity, and thus no rotation of deformed part with respect to reference frame (simulia.com).

An example of **large strain and large rotation** is a slope stability failure simulation as shown in Fig.5.3.

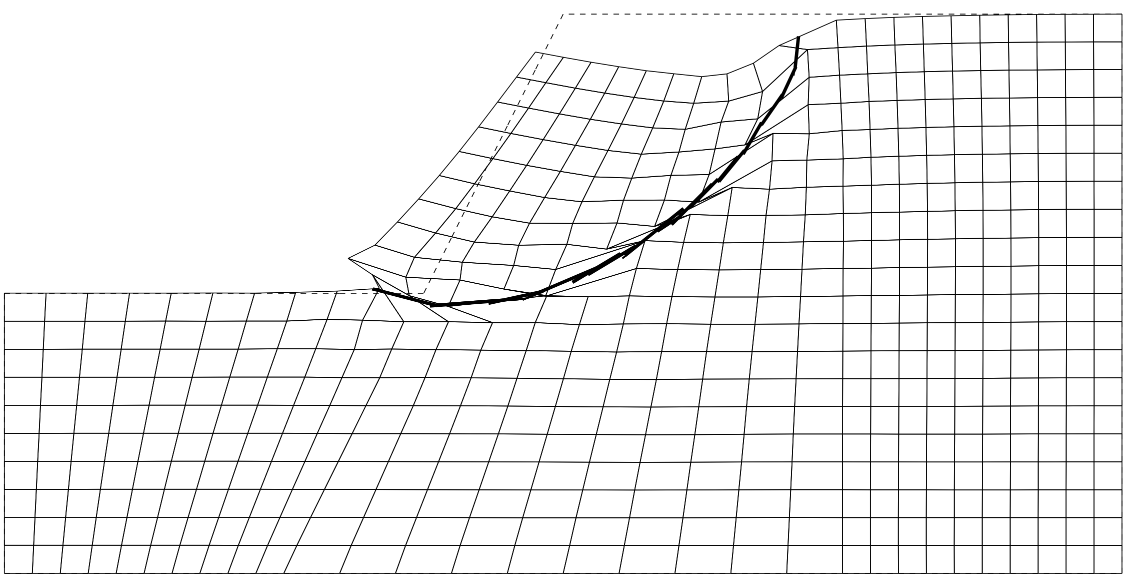

Figure 5.3. FEA simulation of slope failure, demonstrating large strain and large rotation.

For comparison of small strain and finite strain (Lagrangian) tensors, refer to pg.17 of Lubliner [1990].

Consider a **finite rotation** θ and **small shear strain** $|\gamma| \ll 1$ as shown in Fig.5.4.

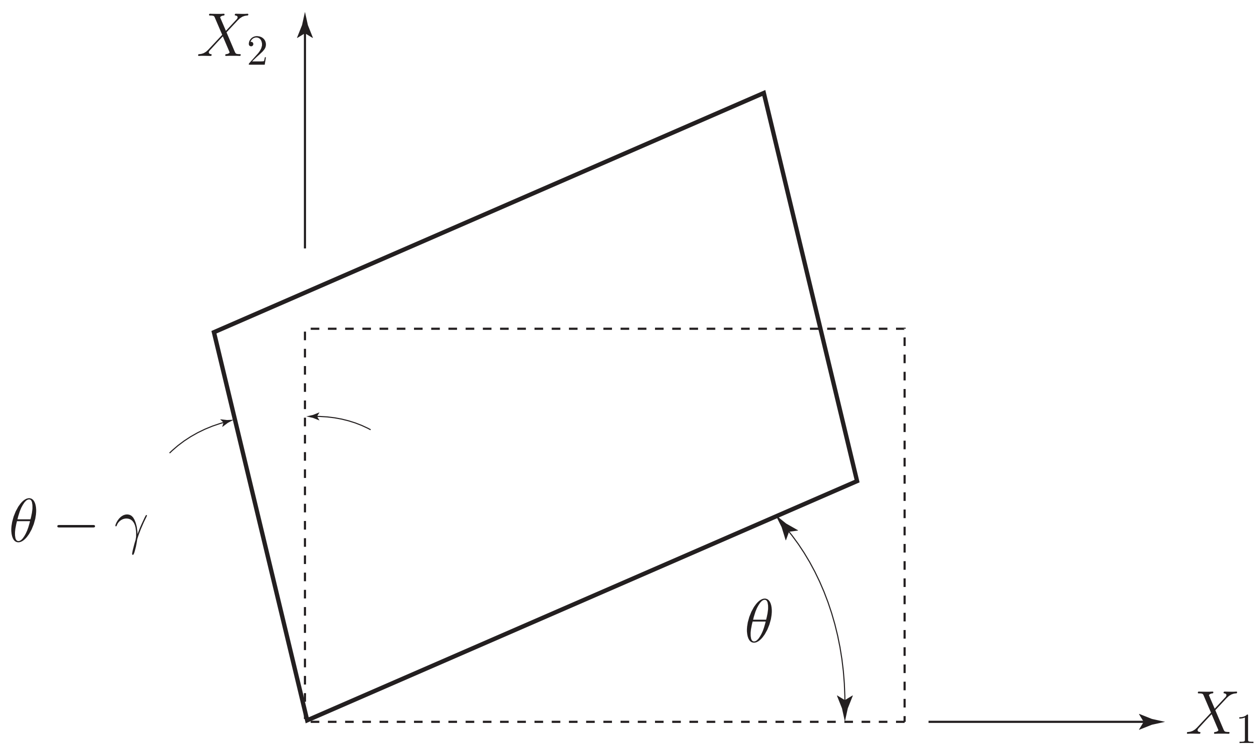

Figure 5.4. Block undergoing small shear strain γ and large rotation θ.

Assuming homogeneous deformation, we can write the displacements as,

$$u_1 = (\cos\theta - 1)X_1 - (\sin\theta - \gamma\cos\theta)X_2 \tag{5.9}$$

$$u_2 = \sin\theta X_1 - (1 - \cos\theta - \gamma\sin\theta)X_2 \tag{5.10}$$

where we can **evaluate the small strain tensor** (assume $x_i = X_I$) as,

$$\epsilon_{11} = \frac{\partial u_1}{\partial x_1} = \cos\theta - 1 \tag{5.11}$$

$$\epsilon_{22} = \frac{\partial u_2}{\partial x_2} = \cos\theta + \gamma \sin\theta - 1 \tag{5.12}$$

$$\epsilon_{12} = \epsilon_{21} = \frac{1}{2}\left(\frac{\partial u_1}{\partial x_2} + \frac{\partial u_2}{\partial x_1}\right) = \frac{1}{2}\gamma\cos\theta \tag{5.13}$$

$$\boldsymbol{\epsilon} = \begin{bmatrix} \cos\theta - 1 & \frac{1}{2}\gamma\cos\theta & 0 \\ \frac{1}{2}\gamma\cos\theta & \cos\theta + \gamma\sin\theta - 1 & 0 \\ 0 & 0 & 0 \end{bmatrix} \tag{5.14}$$

But strain should be independent of rotation θ, correct? If $\theta \approx 0$, then $\boldsymbol{\epsilon}$ yields the simple shear, small strain tensor we expect, but here θ is finite, so what do we do?

Consider the **Lagrangian finite strain tensor** $\boldsymbol{E}$ (there are more than one finite strain tensor, but only one small strain tensor) as,

$$E_{IJ} = \frac{1}{2}\left(\frac{\partial u_I}{\partial X_J} + \frac{\partial u_J}{\partial X_I} + \frac{\partial u_i}{\partial X_I}\frac{\partial u_i}{\partial X_J}\right) \tag{5.15}$$

and evaluate ($x_i \neq X_I$) as,

$$E_{11} = \frac{1}{2}\left(2\frac{\partial u_1}{\partial X_1} + \frac{\partial u_i}{\partial X_1}\frac{\partial u_i}{\partial X_1}\right) = \cos\theta - 1 + 1 - \cos\theta = 0 \tag{5.16}$$

$$E_{22} = \frac{1}{2}\left(2\frac{\partial u_2}{\partial X_2} + \frac{\partial u_i}{\partial X_2}\frac{\partial u_i}{\partial X_2}\right) = \frac{1}{2}\gamma^2 \approx 0 \tag{5.17}$$

$$E_{12} = E_{21} = \frac{1}{2}\left(\frac{\partial u_1}{\partial X_2} + \frac{\partial u_2}{\partial X_1} + \frac{\partial u_i}{\partial X_1}\frac{\partial u_i}{\partial X_2}\right) = \frac{1}{2}\gamma \tag{5.18}$$

$$\boldsymbol{E} = \begin{bmatrix} 0 & \frac{1}{2}\gamma & 0 \\ \frac{1}{2}\gamma & 0 & 0 \\ 0 & 0 & 0 \end{bmatrix} \tag{5.19}$$

Thus, the Lagrangian strain tensor is independent of rotation θ, showing simple shear, small strain tensor as we expected, even for finite rotation θ.

5.3 Strong form for 3D elastostatics

For **3D elastostatics**, the second order Cauchy stress tensor $\boldsymbol{\sigma}$ (Pa), body force vector $\boldsymbol{f}$ (N/m^3), prescribed displacement vector $\boldsymbol{g}^u$ (m) on Γ_u, prescribed traction vector $\boldsymbol{t}^\sigma$ on Γ_t with unit normal vector $\boldsymbol{n}$, $\bar{\Omega} = \Omega \cup \Gamma_u \cup \Gamma_t$ are shown in Fig.5.5.

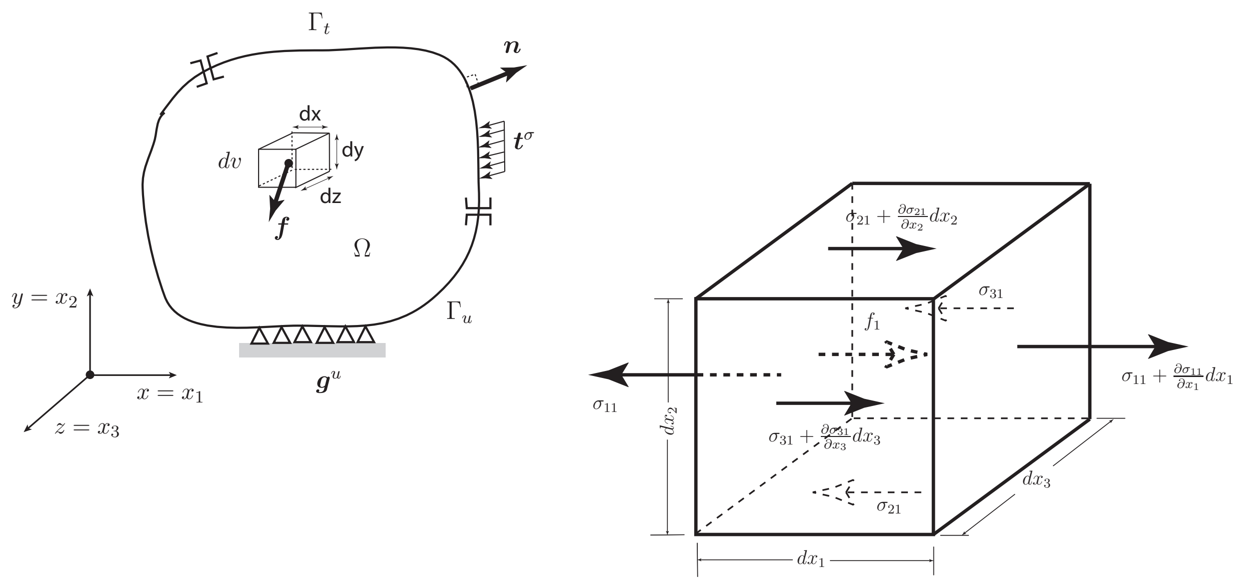

Figure 5.5. The body Ω with BCs, and differential volume dv for satisfying balance of linear momentum.

The sum of the forces in the x_1 direction for static equilibrium,

$$\begin{aligned} & \left(\sigma_{21} + \frac{\partial \sigma_{21}}{\partial x_2} dx_2\right) dx_1 dx_3 - \sigma_{21} dx_1 dx_3 \\ + & \left(\sigma_{31} + \frac{\partial \sigma_{31}}{\partial x_3} dx_3\right) dx_1 dx_2 - \sigma_{31} dx_1 dx_2 \\ + & \left(\sigma_{11} + \frac{\partial \sigma_{11}}{\partial x_1} dx_1\right) dx_2 dx_3 - \sigma_{11} dx_2 dx_3 \\ + & f_1 dx_1 dx_2 dx_3 = 0 \end{aligned} \tag{5.20}$$

Divide by $dv = dx_1 dx_2 dx_3$ to obtain the balance of linear momentum in the x_1 direction,

$$\frac{\partial \sigma_{11}}{\partial x_1} + \frac{\partial \sigma_{21}}{\partial x_2} + \frac{\partial \sigma_{31}}{\partial x_3} + f_1 = 0 \tag{5.21}$$

We do the same in x_2 and x_3 directions, such that,

$$\frac{\partial \sigma_{12}}{\partial x_1} + \frac{\partial \sigma_{22}}{\partial x_2} + \frac{\partial \sigma_{32}}{\partial x_3} + f_2 = 0 \tag{5.22}$$

$$\frac{\partial \sigma_{13}}{\partial x_1} + \frac{\partial \sigma_{23}}{\partial x_2} + \frac{\partial \sigma_{33}}{\partial x_3} + f_3 = 0 \tag{5.23}$$

For **non-polar materials (i.e., no couple stresses), the balance of angular momentum leads to a symmetric stress tensor**: $\sigma_{ij} = \sigma_{ji}$, thus we may write the **balance of linear momentum** in compact, index notation as,

$$\frac{\partial \sigma_{ij}}{\partial x_j} + f_i = 0 \tag{5.24}$$

$$\sigma_{ij,j} + f_i = 0 \tag{5.25}$$

Thus, the Strong form is written as,

$$(S) \begin{cases} \text{Find } u_i(\boldsymbol{x}) : \bar{\Omega} \mapsto \mathbb{R}^{n_{\mathrm{sd}}}, & \text{such that} \\ \sigma_{ij,j} + f_i = 0 & \in \Omega \\ u_i = g_i^u & \text{on } \Gamma_u \\ \sigma_{ij} n_j = t_i^\sigma & \text{on } \Gamma_t \end{cases} \tag{5.26}$$

where

- $u_i(\boldsymbol{x}) : \bar{\Omega} \mapsto \mathbb{R}^{n_{\mathrm{sd}}}$ reads "with $\boldsymbol{x}$ in $\bar{\Omega}$, u_i maps to the real number space $\mathbb{R}^{n_{\mathrm{sd}}}$ of number of spatial dimensions n_{sd}"

- for 3D, $n_{\mathrm{sd}} = 3$, and for 2D, $n_{\mathrm{sd}} = 2$

- body force vector $f_i(\boldsymbol{x})$

- traction vector t_i^σ is natural, or Neumann, BC

- prescribed displacement vector g_i^u is essential, or Dirichlet, BC

5.4 Weak form for 3D elastostatics

We apply the **Method of Weighted Residuals** to derive the Weak Form of the balance of linear momentum. The weighting function w_i, which if a variational principle can be established (which it can for elastostatics), can be thought of as a "variation of displacement" $w_i = \delta u_i$. We write the balance equation in residual form, multiply by w_i, and then integrate over domain Ω, such that,

$$\int_\Omega w_i(\sigma_{ij,j} + f_i)dv = 0 \tag{5.27}$$

We apply the chain rule as,

$$\frac{\partial}{\partial x_j}(w_i\sigma_{ij}) = \frac{\partial w_i}{\partial x_j}\sigma_{ij} + w_i\frac{\partial \sigma_{ij}}{\partial x_j} \tag{5.28}$$

Then,

$$\int_\Omega w_i\sigma_{ij,j}dv = \int_\Omega \left[(w_i\sigma_{ij})_{,j} - w_{i,j}\sigma_{ij}\right] dv \tag{5.29}$$

Applying the divergence theorem,

$$\int_\Omega (w_i\sigma_{ij})_{,j}dv = \int_\Gamma (w_i\sigma_{ij})n_j da \tag{5.30}$$

and recall that $w_i = 0$ on Γ_u, and $\sigma_{ij}n_j = t_i^\sigma$ on Γ_t, such that,

$$\begin{aligned}\int_\Gamma (w_i\sigma_{ij})n_j da &= \int_{\Gamma_u} (w_i\sigma_{ij})n_j da + \int_{\Gamma_t} (w_i\sigma_{ij})n_j da \\ &= \end{aligned}$$

Substitute to obtain,

$$\int_\Omega w_{i,j}\sigma_{ij} dv = \int_\Omega w_i f_i dv + \int_{\Gamma_t} w_i t_i^\sigma da \tag{5.31}$$

Using linear isotropic elasticity (and its minor symmetry) ($\sigma_{ij} = c_{ijkl}\epsilon_{kl} = c_{ijkl}u_{k,l}$), state Weak form (W) as,

$$(W)\begin{cases}\text{Find } u_i(\boldsymbol{x}) \in \mathscr{S} = \{u_i : \Omega \mapsto \mathbb{R}^{n_{\text{sd}}}, u_i \in H^1, u_i = g_i^u \text{ on } \Gamma_u\}, \text{such that} \\ \int_\Omega w_{i,j}c_{ijkl}u_{k,l}dv = \int_\Omega w_i f_i dv + \int_{\Gamma_t} w_i t_i^\sigma da \\ \text{holds } \forall w_i(\boldsymbol{x}) \in \mathscr{V} = \{w_i : \Omega \mapsto \mathbb{R}^{n_{\text{sd}}}, w_i \in H^1, w_i = 0 \text{ on } \Gamma_u\}\end{cases} \tag{5.32}$$

where

- $\forall$ reads "for all"
- $\mathscr{S}$ is the space of admissible trial functions
- $\mathscr{V}$ is the space of weighting functions
- H^1 is the first Sobolev space, such that the H^1 norm is finite:
  i.e., $\|\boldsymbol{u}\|_1 = \left[\int_\Omega (u_i u_i + u_{i,j}u_{i,j})dx\right]^{1/2} < \infty$
- $\|\boldsymbol{u}\|_1$ is called the natural norm
- $u_i \in H^1$ essentially says that first spatial derivatives $u_{i,j}$ CANNOT be Dirac Delta functions, but can be Heaviside functions (discontinuous)
- ... leads to a "C^0 theory" for linear elastostatics (as we had for the 1D axially-loaded bar and 2D linear heat conduction)

Now, we rewrite the variational, weak form in vector-matrix form. Consider the potential energy term in the weak form where,

$$\begin{aligned}
\int_\Omega w_{i,j} c_{ijkl} u_{k,l} dv &= \int_\Omega \{w_{i,j}\}_I \left[c_{ijkl}\right]_{IJ} \{u_{k,l}\}_J \, dv \\
&= \int_\Omega \epsilon_I(\boldsymbol{w}) D_{IJ} \epsilon_J(\boldsymbol{u}) dv \\
&= \int_\Omega \boldsymbol{\epsilon}^T(\boldsymbol{w}) \cdot \boldsymbol{D} \cdot \boldsymbol{\epsilon}(\boldsymbol{u}) dv
\end{aligned}$$

By accounting for major and minor symmetries of c_{ijkl}, and for $n_{\text{sd}} = 3$, $I, J = 1, \ldots, 6$, we can write,

$$\epsilon_I(\boldsymbol{w}) = \{w_{i,j}\}_I = \left\{ \begin{matrix} w_{1,1} \\ w_{2,2} \\ w_{3,3} \\ w_{2,3} + w_{3,2} \\ w_{1,3} + w_{3,1} \\ w_{1,2} + w_{2,1} \end{matrix} \right\}, \quad \epsilon_J(\boldsymbol{u}) = \{u_{i,j}\}_J = \left\{ \begin{matrix} u_{1,1} \\ u_{2,2} \\ u_{3,3} \\ u_{2,3} + u_{3,2} \\ u_{1,3} + u_{3,1} \\ u_{1,2} + u_{2,1} \end{matrix} \right\} \tag{5.33}$$

And for the isotropic elasticity matrix,

$$D_{IJ} = \left[c_{ijkl}\right]_{IJ} = \begin{bmatrix} 2\mu + \lambda & \lambda & \lambda & 0 & 0 & 0 \\ \lambda & 2\mu + \lambda & \lambda & 0 & 0 & 0 \\ \lambda & \lambda & 2\mu + \lambda & 0 & 0 & 0 \\ 0 & 0 & 0 & \mu & 0 & 0 \\ 0 & 0 & 0 & 0 & \mu & 0 \\ 0 & 0 & 0 & 0 & 0 & \mu \end{bmatrix} \tag{5.34}$$

It is possible to generate tables to make this rewrite more transparent for 3D as,

I/J	i/k	j/l
1	1	1
2	2	2
3	3	3
4	2	3
4	3	2
5	1	3
5	3	1
6	1	2
6	2	1

such that,

$$D_{11} = c_{1111}$$

$$D_{14} = c_{1123} = c_{1132}$$

$$D_{55} = c_{1313} = c_{1331} = c_{3131} = c_{3113}$$

5.5 Review of plane elasticity: plane stress, plane strain, and axisymmetric

For **plane stress**, consider a thin plate or beam in Fig.5.6.

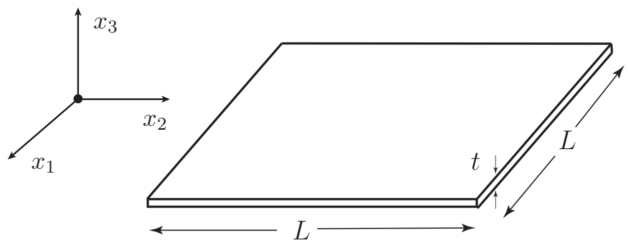

- $t \ll L$
- $\sigma_{33} \approx 0$, $\sigma_{13} \approx 0$, $\sigma_{23} \approx 0$

Figure 5.6. Plane stress elasticity.

The linear isotropic elasticity equation is then written as,

$$\boldsymbol{\sigma} = \boldsymbol{D} \cdot \boldsymbol{\epsilon} \tag{5.35}$$

$$\begin{bmatrix} \sigma_{11} \\ \sigma_{22} \\ \sigma_{12} \end{bmatrix} = \frac{E}{1-\nu^2} \begin{bmatrix} 1 & \nu & 0 \\ \nu & 1 & 0 \\ 0 & 0 & \frac{1}{2}(1-\nu) \end{bmatrix} \begin{bmatrix} \epsilon_{11} \\ \epsilon_{22} \\ 2\epsilon_{12} \end{bmatrix} \tag{5.36}$$

For **plane strain**, consider a long, thick solid like a retaining wall loaded in plane as in Fig.5.7.

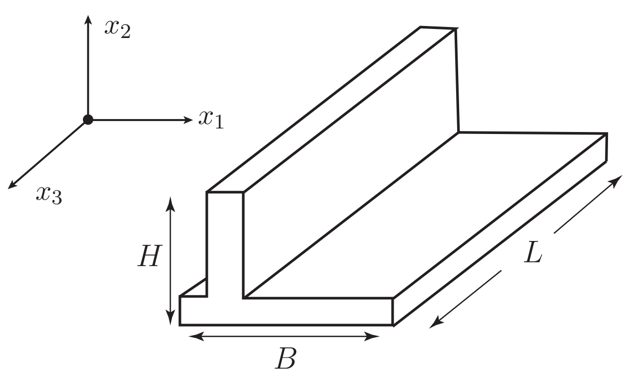

- $B, H \ll L$
- $\epsilon_{33} \approx 0$, $\epsilon_{13} \approx 0$, $\epsilon_{23} \approx 0$
- $\sigma_{33} \neq 0$, $\sigma_{13} \approx 0$, $\sigma_{23} \approx 0$

Figure 5.7. Plane strain elasticity.

The linear isotropic elastic constitutive relation becomes,

$$\begin{bmatrix} \sigma_{11} \\ \sigma_{22} \\ \sigma_{12} \end{bmatrix} = \begin{bmatrix} \lambda+2\mu & \lambda & 0 \\ \lambda & \lambda+2\mu & 0 \\ 0 & 0 & \mu \end{bmatrix} \begin{bmatrix} \epsilon_{11} \\ \epsilon_{22} \\ 2\epsilon_{12} \end{bmatrix} \tag{5.37}$$

$$\sigma_{33} = \lambda(\epsilon_{11} + \epsilon_{22}) \tag{5.38}$$

For torsionless, column compression with centric loading, in cylindrical coordinates, we have **axisymmetric elasticity** as shown in Fig.5.8.

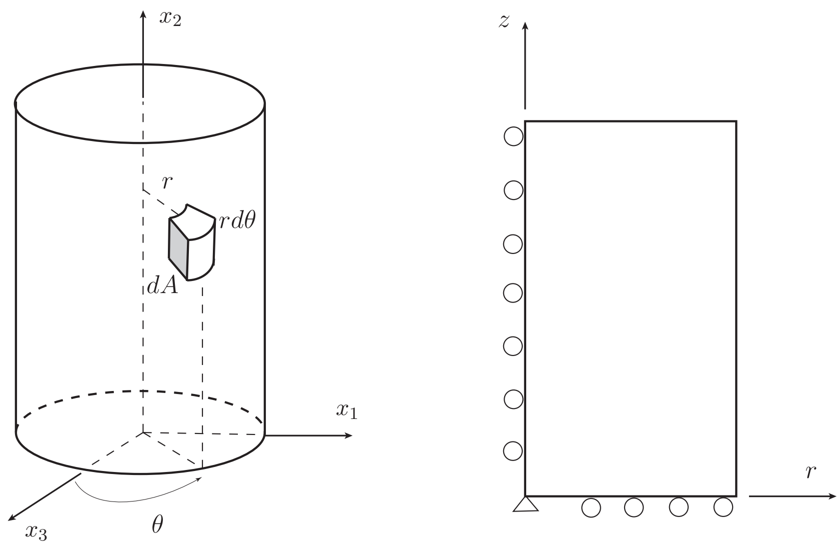

- independent of θ
- coordinates:
  radial r
  axial z
  circumferential θ

Figure 5.8. Linear isotropic, axisymmetric elasticity.

For spatial integration, $dv = rd\theta dA = rd\theta drdz$, where,

$$\int_\Omega (\bullet)dv = \int_0^{2\pi} \int_A (\bullet) r dA d\theta = 2\pi \int_A (\bullet) r dr dz \tag{5.39}$$

The displacements are radial u_r, axial u_z, circumferential u_θ. For strain, assume $u_\theta = 0$, such that $\epsilon_{r\theta} = \epsilon_{z\theta} = 0$, but there is hoop strain due to radial displacement $\epsilon_{\theta\theta} = \frac{u_r}{r}$.

For stresses, $\sigma_{r\theta} = \sigma_{z\theta} = 0$; hoop stress $\sigma_{\theta\theta} \neq 0$, such that the linear isotropic elastic, axisymmetric stress-strain relation is,

$$\begin{bmatrix} \sigma_{rr} \\ \sigma_{zz} \\ \sigma_{rz} \\ \sigma_{\theta\theta} \end{bmatrix} = \begin{bmatrix} \lambda + 2\mu & \lambda & 0 & \lambda \\ \lambda & \lambda + 2\mu & 0 & \lambda \\ 0 & 0 & \mu & 0 \\ \lambda & \lambda & 0 & \lambda + 2\mu \end{bmatrix} \begin{bmatrix} \epsilon_{rr} \\ \epsilon_{zz} \\ 2\epsilon_{rz} \\ \epsilon_{\theta\theta} \end{bmatrix} \tag{5.40}$$

5.6 von Mises stress

The definition of the **von Mises (VM) stress** is $= \sqrt{\frac{3}{2}J_2}$, where the second invariant of the deviatoric stress $J_2 = s_{ij}s_{ij}$. The deviatoric stress $s_{ij} = \sigma_{ij} - \frac{1}{3}\sigma_{kk}\delta_{ij}$ (it is traceless).

Consider a compression or tension specimen loaded axially, with potential confining stress if geomaterial (soil, rock, concrete) such that,

$$\boldsymbol{\sigma} = \begin{bmatrix} \sigma_a & 0 & 0 \\ 0 & \sigma_r & 0 \\ 0 & 0 & \sigma_r \end{bmatrix} \tag{5.41}$$

$$\boldsymbol{s} = \boldsymbol{\sigma} - \frac{1}{3}\sigma_{ii}\mathbf{1} \tag{5.42}$$

$$= (\sigma_a - \sigma_r)/3 \begin{bmatrix} 2 & 0 & 0 \\ 0 & -1 & 0 \\ 0 & 0 & -1 \end{bmatrix} \tag{5.43}$$

Then, $J_2 = \frac{2}{3}(\sigma_a - \sigma_r)^2$, and VM $= \sqrt{\frac{3}{2}J_2} = |\sigma_a - \sigma_r|$ ($= q$ in soil mechanics). For zero radial stress, $\sigma_r = 0$, then VM $= |\sigma_a|$, which can be determined experimentally and compared the VM value when conducting a 3D FEA for elasticity, even if you do not invoke a nonlinear constitutive relation like elastoplasticity.

5.7 Discrete, Galerkin form (G)

Find the approximate solution $u_i^h(\boldsymbol{x}) \approx u_i(\boldsymbol{x})$, where h is the discretization parameter, or characteristic length of the mesh. Consider the 3D solid body with domain Ω, and discretize with 'elements' of characteristic length h (may not all be equal), such as in Fig.5.9.

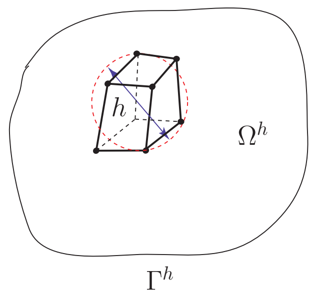

- $\Omega^h \subset \Omega$, $\bar{\Omega}^h = \Omega^h \cup \Gamma^h$

Figure 5.9. Discretization of domain Ω into 'mesh' Ω^h.

We may rewrite the Weak form in discrete, Galerkin form as,

$$(G)\begin{cases} \text{Find } u_i^h(\boldsymbol{x}) \in \mathscr{S}^h = \{u_i^h : \Omega^h \mapsto \mathbb{R}^{n_{\mathrm{sd}}}, u_i^h \in H^1, u_i^h = g_i^u \text{ on } \Gamma_u^h\}, \text{such that} \\ \int_{\Omega^h} w_{i,j}^h c_{ijkl} u_{k,l}^h dv = \int_{\Omega^h} w_i^h f_i dv + \int_{\Gamma_t^h} w_i^h t_i^\sigma da \\ \text{holds } \forall w_i^h(\boldsymbol{x}) \in \mathscr{V}^h = \{w_i^h : \Omega^h \mapsto \mathbb{R}^{n_{\mathrm{sd}}}, w_i^h \in H^1, w_i^h = 0 \text{ on } \Gamma_u^h\} \end{cases} \tag{5.44}$$

where

- $\mathscr{S}^h \subset \mathscr{S}$ is the discrete space of admissible trial functions
- $\mathscr{V}^h \subset \mathscr{V}$ is the discrete space of weighting functions
- $(G) \approx (W)$: note that even though u_i^h and w_i^h are discrete approximations to u_i and w_i, respectively, they must still satisfy restrictions on the spaces (in order to ensure convergence: i.e., $\lim_{h \to 0} u_i^h(\boldsymbol{x}) = u_i(\boldsymbol{x})$)

5.8 Finite Element (FE) Matrix form

Discretize the 3D body into n_{el} elements. For the **global perspective**, consider Fig.5.10.

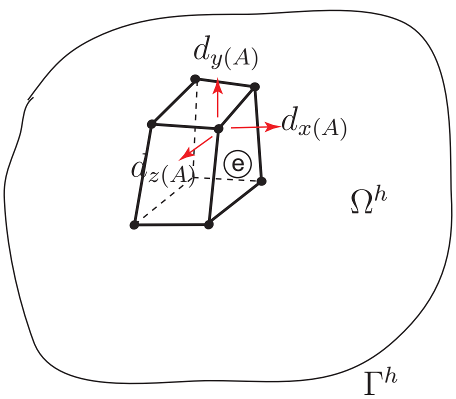

- $u_i^h(\boldsymbol{x}) = \sum_{A=1}^{n_{\text{np}}} N_A(\boldsymbol{x}) d_{i(A)}$
- global dofs: $d_1 = d_{x(A)}$, $d_2 = d_{y(A)}$, $d_3 = d_{z(A)}$, ...
- n_{np} is the number of nodal points
- $N_A(\boldsymbol{x})$ is the shape function at global node A

Figure 5.10. Global perspective

For the **element perspective**, consider an element e in Fig.5.11.

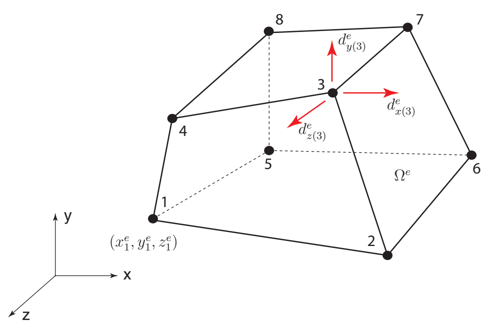

- local element nodal dof $d^e_{i(a)} = u_i^h(x_a^e, y_a^e, z_a^e)$
- element domain Ω^e
- discrete domain $\Omega^h = \mathbf{A}_{e=1}^{n_{\text{el}}} \Omega^e$
- $\mathbf{A}_{e=1}^{n_{\text{el}}}$ is the element assembly operator

Figure 5.11. Element perspective.

Discretize the Galerkin integral equation into finite elements, such that,

$$\mathbf{A}_{e=1}^{n_{\text{el}}} \left[\int_{\Omega^e} w_{i,j}^{h^e} c_{ijkl} u_{k,l}^{h^e} dv = \int_{\Omega^e} w_i^{h^e} f_i dv + \int_{\Gamma_t^e} w_i^{h^e} t_i^{\sigma} da \right] \tag{5.45}$$

and write the interpolations as,

$$u_k^{h^e}(\boldsymbol{x}) = \sum_{a=1}^{n_{\text{en}}} N_a(\boldsymbol{x}) d_{k(a)}^e = \left\{ \underbrace{\boldsymbol{N}^e}_{n_{\text{sd}}\times(n_{\text{en}}*n_{\text{sd}})} \cdot \underbrace{\boldsymbol{d}^e}_{(n_{\text{en}}*n_{\text{sd}})\times 1} \right\}_k \tag{5.46}$$

$$\boldsymbol{N}_a = \begin{bmatrix} N_a & 0 & 0 \\ 0 & N_a & 0 \\ 0 & 0 & N_a \end{bmatrix} \tag{5.47}$$

$$\boldsymbol{u}^{h^e} = \begin{bmatrix} \boldsymbol{N}_1 & \boldsymbol{N}_2 & \dots & \boldsymbol{N}_{n_{\text{en}}} \end{bmatrix} \begin{bmatrix} \boldsymbol{d}_1^e \\ \boldsymbol{d}_2^e \\ \vdots \\ \boldsymbol{d}_{n_{\text{en}}}^e \end{bmatrix} = \boldsymbol{N}^e \cdot \boldsymbol{d}^e \tag{5.48}$$

$$w_i^{h^e}(\boldsymbol{x}) = \sum_{a=1}^{n_{\text{en}}} N_a(\boldsymbol{x}) c_{i(a)}^e = \{\boldsymbol{N}^e \cdot \boldsymbol{c}^e\}_i \tag{5.49}$$

where n_{en} is number of element nodes, $n_{\text{sd}} = 3$ is number of spatial dimensions for 3D.

Their spatial derivatives are written as,

$$u_{k,l}^{h^e}(\boldsymbol{x}) = \sum_{a=1}^{n_{\text{en}}} \frac{\partial N_a(\boldsymbol{x})}{\partial x_l} d_{k(a)}^e \tag{5.50}$$

$$w_{i,j}^{h^e}(\boldsymbol{x}) = \sum_{a=1}^{n_{\text{en}}} \frac{\partial N_a(\boldsymbol{x})}{\partial x_j} c_{i(a)}^e \tag{5.51}$$

Recall that we re-wrote in matrix-vector form, such that for strain $\boldsymbol{\epsilon}^{h^e}(\boldsymbol{u}) = \boldsymbol{B}^e \cdot \boldsymbol{d}^e$:

$$
\begin{aligned}
\boldsymbol{\epsilon}^{h^e}(\boldsymbol{u}) &= \left\{ \begin{array}{c} u^{h^e}_{1,1} \\ u^{h^e}_{2,2} \\ u^{h^e}_{3,3} \\ u^{h^e}_{2,3} + u^{h^e}_{3,2} \\ u^{h^e}_{1,3} + u^{h^e}_{3,1} \\ u^{h^e}_{1,2} + u^{h^e}_{2,1} \end{array} \right\} = \sum_{a=1}^{n_{\text{en}}} \begin{bmatrix} N_{a,1} & 0 & 0 \\ 0 & N_{a,2} & 0 \\ 0 & 0 & N_{a,3} \\ 0 & N_{a,3} & N_{a,2} \\ N_{a,3} & 0 & N_{a,1} \\ N_{a,2} & N_{a,1} & 0 \end{bmatrix} \left\{ \begin{array}{c} d^e_{1(a)} \\ d^e_{2(a)} \\ d^e_{3(a)} \end{array} \right\} \\
&= \sum_{a=1}^{n_{\text{en}}} \boldsymbol{B}_a \cdot \boldsymbol{d}^e_a = \begin{bmatrix} \boldsymbol{B}_1 & \boldsymbol{B}_2 & \ldots & \boldsymbol{B}_{n_{\text{en}}} \end{bmatrix} \begin{bmatrix} \boldsymbol{d}^e_1 \\ \boldsymbol{d}^e_2 \\ \vdots \\ \boldsymbol{d}^e_{n_{\text{en}}} \end{bmatrix} \\
&= \underbrace{\boldsymbol{B}^e}_{6\times(n_{\text{en}}*n_{\text{sd}})} \cdot \underbrace{\boldsymbol{d}^e}_{(n_{\text{en}}*n_{\text{sd}})\times 1}
\end{aligned} \tag{5.52}
$$

Recall the coordinate transformation and use of the Jacobian:

$$
\begin{aligned}
\frac{\partial N_a}{\partial \boldsymbol{x}} &= \frac{\partial N_a}{\partial \boldsymbol{\xi}} \cdot \frac{\partial \boldsymbol{\xi}}{\partial \boldsymbol{x}} = \begin{bmatrix} \frac{\partial N_a}{\partial \xi} & \frac{\partial N_a}{\partial \eta} & \frac{\partial N_a}{\partial \zeta} \end{bmatrix} \begin{bmatrix} \frac{\partial \xi}{\partial x} & \frac{\partial \xi}{\partial y} & \frac{\partial \xi}{\partial z} \\ \frac{\partial \eta}{\partial x} & \frac{\partial \eta}{\partial y} & \frac{\partial \eta}{\partial z} \\ \frac{\partial \zeta}{\partial x} & \frac{\partial \zeta}{\partial y} & \frac{\partial \zeta}{\partial z} \end{bmatrix} \\
&= \frac{\partial N_a}{\partial \boldsymbol{\xi}} \cdot (\boldsymbol{J}^e)^{-1}
\end{aligned}
$$

and map (x, y, z) to (ξ, η, ζ).

Let $\boldsymbol{D}$ be the matrix form of the 4th order elastic modulus tensor, and then,

$$
\mathop{\mathbf{A}}_{e=1}^{n_{\text{el}}} (\boldsymbol{c}^e)^T \cdot \left[\underbrace{\left(\int_{\Omega^e} (\boldsymbol{B}^e)^T \cdot \boldsymbol{D} \cdot \boldsymbol{B}^e dv \right)}_{\boldsymbol{k}^e} \cdot \boldsymbol{d}^e = \underbrace{\int_{\Omega^e} (\boldsymbol{N}^e)^T \cdot \boldsymbol{f} dv}_{\boldsymbol{f}^e_f} + \underbrace{\int_{\Gamma^e_t} (\boldsymbol{N}^e)^T \cdot \boldsymbol{t}^\sigma da}_{\boldsymbol{f}^e_t} \right] \tag{5.53}
$$

and,

$$\mathop{\mathsf{A}}_{e=1}^{n_{\mathrm{el}}} (\boldsymbol{c}^e)^T \cdot \left[\boldsymbol{k}^e \cdot \boldsymbol{d}^e = \boldsymbol{f}_f^e + \boldsymbol{f}_t^e\right] \tag{5.54}$$

After element assembly, we have,

$$\boldsymbol{K} \cdot \boldsymbol{d} = \boldsymbol{F}_f + \boldsymbol{F}_t + \boldsymbol{F}_g \tag{5.55}$$

But before assembling, let's introduce the trilinear, hexahedral element in natural coordinates.

5.9 Trilinear hexahedral element

Refer to pg.123 of Hughes [1987]. For coordinate mapping, refer to Fig.5.12.

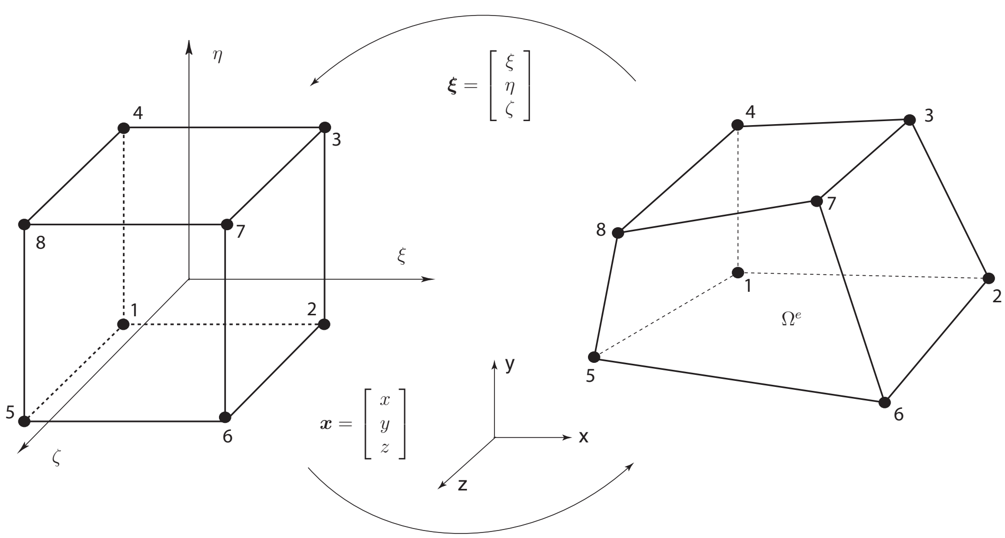

Figure 5.12. Trilinear hexahedral element in natural coordinates.

Recall the isoparametric mapping, $\boldsymbol{x}^{h^e}(\boldsymbol{\xi}) = \sum_{a=1}^{8} N_a(\boldsymbol{\xi}) \boldsymbol{x}_a^e$, and trilinear shape functions,

$N_a(\xi,\eta,\zeta) = \frac{1}{8}(1+\xi_a\xi)(1+\eta_a\eta)(1+\zeta_a\zeta)$. We then interpolate in terms of $\boldsymbol{\xi}$ as,

$$u_i^{h^e}(\boldsymbol{\xi}) = \sum_{a=1}^{8} N_a(\boldsymbol{\xi}) d_{i(a)}^e \tag{5.56}$$

$$w_i^{h^e}(\boldsymbol{\xi}) = \sum_{a=1}^{8} N_a(\boldsymbol{\xi}) c_{i(a)}^e \tag{5.57}$$

Then, we can evaluate the stiffness matrix and body force vector in the parent domain using Gaussian quadrature as,

$$\boldsymbol{k}^e = \int_{-1}^{1}\int_{-1}^{1}\int_{-1}^{1} [\boldsymbol{B}^e(\boldsymbol{\xi})]^T \cdot \boldsymbol{D} \cdot \boldsymbol{B}^e(\boldsymbol{\xi}) j^e d\xi d\eta d\zeta \tag{5.58}$$

$$\boldsymbol{f}_f^e = \int_{-1}^{1}\int_{-1}^{1}\int_{-1}^{1} [\boldsymbol{N}^e(\boldsymbol{\xi})]^T \hat{f}(\boldsymbol{\xi}) j^e d\xi d\eta d\zeta \tag{5.59}$$

Similar to the heat flux BC in 2D, the traction vector BC at the element boundary Γ^e (if the element is on the boundary Γ_t^h) needs to be evaluated,

$$\boldsymbol{f}_t^e = \int_{\Gamma_t^e} (\boldsymbol{N}^e)^T \cdot \boldsymbol{t}^\sigma da \tag{5.60}$$

This evaluation is more involved in 3D, and will not be covered here.

5.10 Element assembly process

Refer to pg.92 of Hughes [1987].

- use IEN and ID "arrays" to obtain LM
- **element nodes array**, $\text{IEN}(a, e) = A$, where a is the local element node number, e the element number, and A the global node number

- the **ID array** relates global node numbers A and local dofs i to global equation numbers (dofs)

- the **location matrix (LM)** can then be determined from the IEN and ID as LM(i, a, e) =ID$(i$, IEN$(a, e))$ to return the global dof given local element nodal dof i, node number a and element number e

Consider the example from pg.92 of Hughes [1987] in Fig.5.13,5.14.

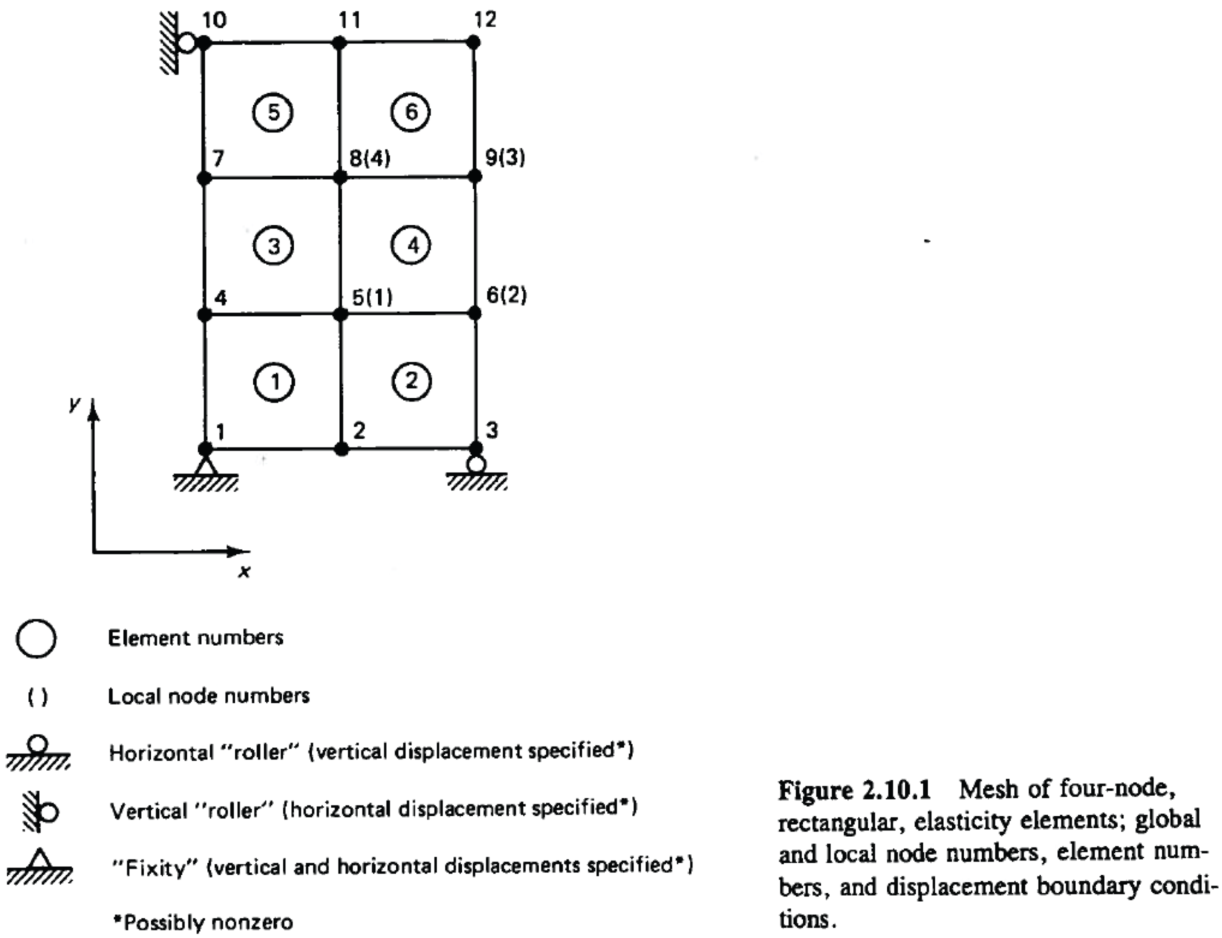

Figure 5.13. Element assembly example [Hughes, 1987].

ID array:

Global node numbers (A) ($n_{np} = 12$)

Global degrees of freedom (i)	1	2	3	4	5	6	7	8	9	10	11	12
1	0*	1	3	4	6	8	10	12	14	0	17	19
2	0	2	0	5	7	9	11	13	15	16	18	20

($n_{dof} = 2$) $P = \mathrm{ID}(i, A)$ ($n_{eq} = 20$)

IEN array:

Element numbers (e) ($n_{el} = 6$)

Local node numbers (a)	1	2	3	4	5	6
1	1	2	4	5	7	8
2	2	3	5	6	8	9
3	5	6	8	9	11	12
4	4	5	7	8	10	11

($n_{en} = 4$)

$A = \mathrm{IEN}(a, e)$

LM array:

Element numbers (e) ($n_{el} = 6$)

p	a	i	1	2	3	4	5	6
1	1	1	0*	1	4	6	10	12
2	1	2	0	2	5	7	11	13
3	2	1	1	3	6	8	12	14
4	2	2	2	0	7	9	13	15
5	3	1	6	8	12	14	17	19
6	3	2	7	9	13	15	18	20
7	4	1	4	6	10	12	0	17
8	4	2	5	7	11	13	16	18

($n_{ee} = 8$)

Element degree of freedom numbers (i, where $1 \leq i \leq n_{ed}$ and here $n_{ed} = 2$)
Local node numbers (a)
Local equation numbers ($p = n_{ed}(a - 1) + i$)

$$P = \mathrm{LM}(p, e) = \mathrm{LM}(i, a, e) = \mathrm{ID}(i, \mathrm{IEN}(a, e))$$

*Displacement boundary conditions are denoted by zeros.

Figure 5.14. Element assembly example [Hughes, 1987].

5.11 Patch test

The patch test is an **engineering version of the completeness condition**, and is a good check to see that a new finite element has been implemented correctly (with regard to verification). We require an arbitrary patch of elements to satisfy *exactly* the following: (1) rigid body motion without strain, and (2) constant strain in x and y directions (for 2D).

Consider the example in Fig.5.15: prescribe displacements at the boundary nodes, and solve for displacement at node 5. The patch test passes if (1) the solution at node 5 is exact (takes on values in the table), and (2) stresses and strains are exact at the Gauss points.

node	x	y
1	0	0
2	1	0
3	2	0
4	0	0.75
5	1.2	1.25
6	2	1
7	0	2
8	0.8	2
9	2	2

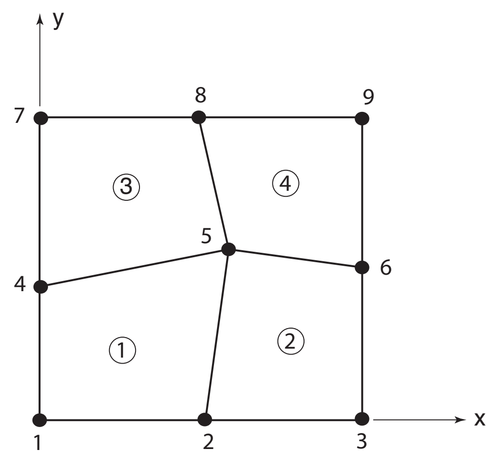

patch tests

test	$d^e_{x(a)}$	$d^e_{y(a)}$
1	1	0
2	0	1
3	x^e_a	0
4	0	x^e_a
5	y^e_a	0
6	0	y^e_a

Figure 5.15. Patch test.

5.12 Incompressibility Constraint

Refer to Chapter 4 of Hughes [1987].

(I) **incompressible linear elasticity**, $\nu \rightarrow 0.5$ (rubber-like materials).

$$\sigma_{ij} = c_{ijkl}\epsilon_{kl} = \lambda\epsilon_{kk}\delta_{ij} + 2\mu\epsilon_{ij}$$

where the mean stress p related to bulk modulus K is,

$$p = \frac{1}{3}\sigma_{ii} = K\epsilon_{vol} \quad ; \qquad K = \lambda + \frac{2}{3}\mu = \frac{E}{3(1-2\nu)}$$

To maintain constant pressure p for nearly incompressible elastic material, volumetric strain $\epsilon_{ii} = 0$ as,

$$\nu \to 0.5\ , \quad K \to \infty \quad \Longrightarrow \epsilon_{vol} = \epsilon_{ii} = 0$$

(II) **metal plasticity**, it is typically incompressible (isochoric) even with compressible elasticity (e.g., $\nu = 0.3$). The large isochoric plastic deformation can dominate the response and lead to mesh locking in FE solutions.

(III) **undrained, saturated soil plasticity**: in soil with low hydraulic conductivity (permeability), for transient loading (during and immediately after construction), soil can behave in an undrained condition, such that its plasticity is isochoric for a total stress analysis. Then this becomes the same problem as metal plasticity for FE solutions (total stress analysis).

Consider the example on pg.207 of Hughes [1987].

As an example of **mesh locking** in Fig.5.16, consider the mesh composed of constant strain triangles, where $u^h_{i,i} = \epsilon^h_{ii} = 0$ holds pointwise since interpolation is linear.

For **element 1**: $e = 1$, $\boldsymbol{d}^e_2 = \boldsymbol{d}^e_3 = \boldsymbol{0}$,

$$\begin{aligned}
\epsilon^h_{vol} &= u^h_{x,x} + u^h_{y,y} = N_{1,x}d^e_{x(1)} + N_{1,y}d^e_{y(1)} \\
&= \frac{1}{2(Area)}\left[(y^e_2 - y^e_3)d^e_{x(1)} + (x^e_3 - x^e_2)d^e_{y(1)}\right] \\
\Longrightarrow\ & d^e_{y(1)} = 0
\end{aligned}$$

Thus, $d^e_{x(1)}$, or $d_{x(A)}$, is the free dof, and $d_{y(A)} = 0$.

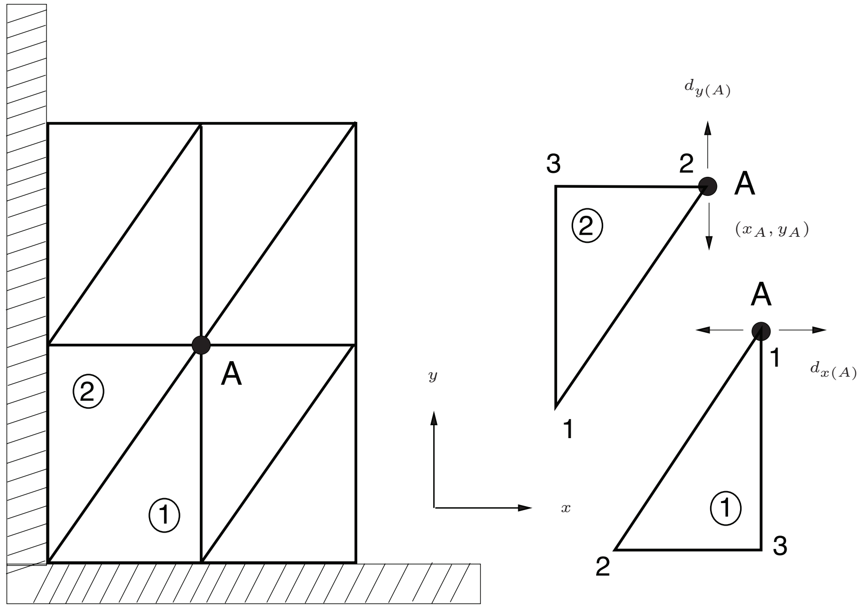

$$\frac{dN_1}{d\boldsymbol{x}} = \frac{1}{2(Area)} \left[\begin{array}{cc} y_2^e - y_3^e & x_3^e - x_2^e \end{array} \right] \; ; \quad \frac{dN_2}{d\boldsymbol{x}} = \frac{1}{2(Area)} \left[\begin{array}{cc} y_3^e - y_1^e & x_1^e - x_3^e \end{array} \right]$$

$$\frac{dN_3}{d\boldsymbol{x}} = \frac{1}{2(Area)} \left[\begin{array}{cc} y_1^e - y_2^e & x_2^e - x_1^e \end{array} \right]$$

Figure 5.16. Example of mesh locking.

For **element 2**: $e = 2$, $\boldsymbol{d}_1^e = \boldsymbol{d}_3^e = \boldsymbol{0}$,

$$\begin{aligned} \epsilon_{vol}^h &= u_{x,x}^h + u_{y,y}^h = N_{2,x} d_{x(2)}^e + N_{2,y} d_{y(2)}^e \\ &= \frac{1}{2(Area)} \left[(y_3^e - y_1^e) d_{x(2)}^e + (x_1^e - x_3^e) d_{y(2)}^e \right] \\ &\Longrightarrow d_{x(2)}^e = 0 \end{aligned}$$

Thus, $d_{y(2)}^e$, or $d_{y(A)}$, is the free dof, and $d_{x(A)} = 0$. Therefore, there are no dofs at node A: $d_{x(A)} = d_{y(A)} = 0$; so the mesh will lock! There is NO meaningful approximation ability of this mesh using this element type (linear triangle). The linear triangle is a particularly poor element to use for elastostatics, but there are better elements and methods to handle the incompressiblity constraint:

- *Reduced and Selective Integration*: 'Soften' stiffness matrix by underintegrating. Full reduced integration leads to rank deficient stiffness matrix (i.e., singular) and thus instability, whereas selective reduced integration only underintegrates the dilatational part of stiffness matrix and maintains stability, *Hughes 1987*.

- *Mixed Methods*: Introduce pressure degrees of freedom to solve compressible and incompressible problems, *Hughes 1987*. Passing the Babuška-Brezzi (LBB) condition ensures convergence, *Oden & Carey 1983*.

- $\bar{B}$*-method*: Split strain-displacement matrix $\boldsymbol{B}$ into deviatoric and dilatational parts, then relax the incompressibility constraint on the dilatational part. For finite deformations does NOT pass the LBB condition, *Hughes 1980*. Can be classified as an *Assumed Enhanced Strain Method*.

- *Assumed Enhanced Strain Method*: Formulate variational equations of equilibrium with enhanced strain or enhanced deformation gradient to relax the incompressibility constraint, and embed this enhancement within the individual finite element domain for efficient numerical solutions, *Simo & Hughes 1986, Simo & Rifai 1990, Simo et al. 1993*.

- *Hourglass Control*: Uniform strain hexahedral element with additional nodal 'hourglass' forces applied to control spurious hourglass modes which result from full reduced integration, *Flanagan & Belytschko 1981*.

Recall for plane strain,

$$\boldsymbol{D} = \begin{bmatrix} \lambda + 2\mu & \lambda & 0 \\ \lambda & \lambda + 2\mu & 0 \\ 0 & 0 & \mu \end{bmatrix} = \bar{\boldsymbol{D}} + \bar{\bar{\boldsymbol{D}}} \tag{5.61}$$

$$\bar{\boldsymbol{D}} = \begin{bmatrix} 2\mu & 0 & 0 \\ 0 & 2\mu & 0 \\ 0 & 0 & \mu \end{bmatrix} \quad ; \quad \bar{\bar{\boldsymbol{D}}} = \begin{bmatrix} \lambda & \lambda & 0 \\ \lambda & \lambda & 0 \\ 0 & 0 & 0 \end{bmatrix} \tag{5.62}$$

and the stiffness matrix:

$$\boldsymbol{k}^e = \int_{\Omega^e} [\boldsymbol{B}^e]^T \cdot \boldsymbol{D} \cdot \boldsymbol{B}^e da = \int_{\Omega^e} [\boldsymbol{B}^e]^T \cdot (\bar{\boldsymbol{D}} + \bar{\bar{\boldsymbol{D}}}) \cdot \boldsymbol{B}^e da \tag{5.63}$$

$$= \bar{\boldsymbol{k}}^e + \bar{\bar{\boldsymbol{k}}}^e \tag{5.64}$$

We use normal Gauss integration for shear stiffness matrix $\bar{\boldsymbol{k}}^e$, and reduced integration for volumetric stiffness $\bar{\bar{\boldsymbol{k}}}^e$. This is called "selective reduced integration" to keep the stiffness matrix invertible. Note that selective reduced integration is limited to isotropy; for anisotropy (and nonlinear formulations) we need something different, such as (1) $\bar{B}$-method (small strain), (2) mixed formulation, or (3) enhanced strain elements.

The LBB condition must be satisfied for convergence; in Fig.5.17 are discontinuous pressure elements as examples.

With analogy with selective reduced integration schemes for small strain in Fig.5.18.

For continuous pressure elements, consider Fig.5.19.

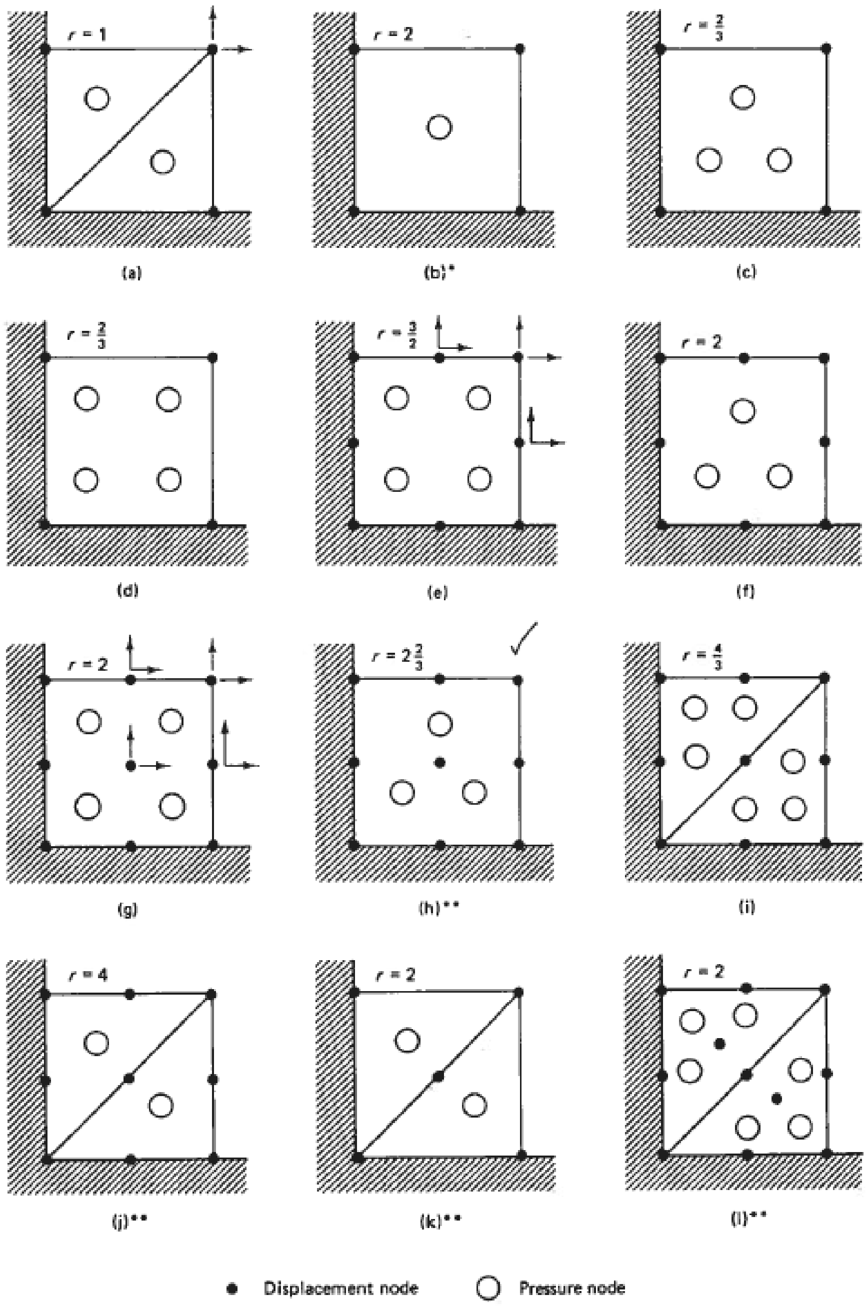

Figure 5.17. Examples of discontinuous pressure elements [Hughes, 1987].

	Mixed element		Equivalent selective integration element	
	Displacement interpolation	Pressure interpolation	Normal Gaussian quadrature* ($\bar{k}$)	Reduced Gaussian quadrature ($\bar{\bar{k}}$)
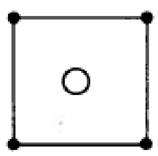	Bilinear	Constant	2 X 2	One-point
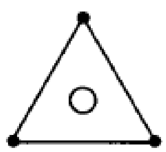	Linear	Constant	One-point	One-point
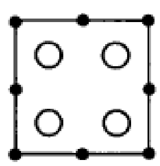	Serendipity	Bilinear	3 X 3	2 X 2
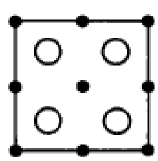	Biquadratic	Bilinear	3 X 3	2 X 2
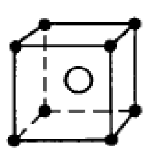	Trilinear	Constant	2 X 2 X 2	One-point

*Also used on all terms of mixed formulation.

Figure 5.18. Analogy between selective reduced integration and mixed formulations [Hughes, 1987].

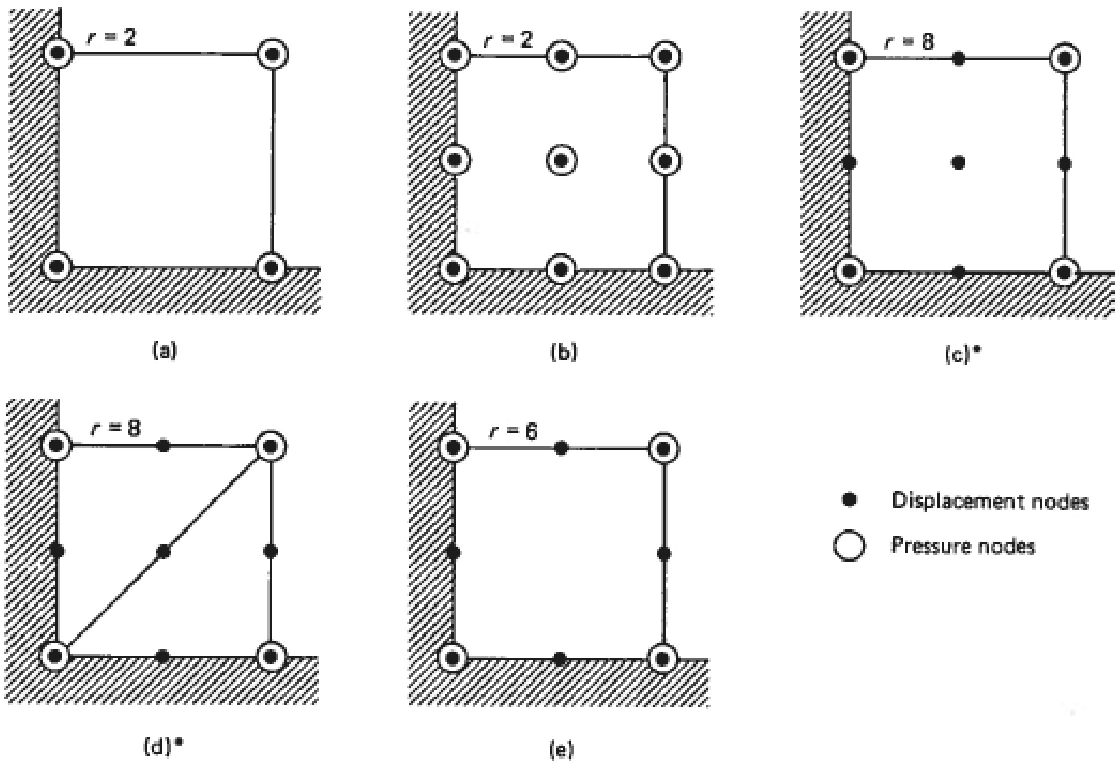

* These elements satisfy the Babuška-Brezzi condition. The convergence rate is 2. The elements in (a) and (b) violate the Babuška-Brezzi condition, whereas the issue is still open regarding the element in (e).

Figure 5.19. Continuous pressure mixed formulation element [Hughes, 1987].

5.13 Linear Elastodynamics

Refer to pg.423 of Hughes [1987]. Similar to the elastodynamic bar problem, ignoring damping for now, the Strong Form is,

$$
(S)\left\{\begin{array}{lcll}
\text{Find } u_i(\boldsymbol{x},t) : \bar{\Omega}\times[0,T]\mapsto\mathbb{R}^{n_{\mathrm{sd}}}, & & \text{such that} & \\
\rho u_{i,tt}-\sigma_{ij,j} & = & f_i & \boldsymbol{x}\in\Omega\times]0,T[\\
u_i(\boldsymbol{x},t) & = & g_i^u(t) & \boldsymbol{x}\in\Gamma_u\times]0,T[\\
\sigma_{ij}(\boldsymbol{x},t)n_j(\boldsymbol{x}) & = & t_i^\sigma(t) & \boldsymbol{x}\in\Gamma_t\times]0,T[\\
u_i(\boldsymbol{x},0) & = & u_{0i}(\boldsymbol{x}) & \boldsymbol{x}\in\Omega \\
u_{i,t}(\boldsymbol{x},0) & = & u_{0i,t}(\boldsymbol{x}) & \boldsymbol{x}\in\Omega
\end{array}\right. \tag{5.65}
$$

with initial displacement $u_{0i}(\boldsymbol{x})$ and velocity $u_{0i,t}(\boldsymbol{x})$.

The Weak Form (derivation excluded) may be written as,

$$
(W)\left\{\begin{array}{l}
\text{Find } u_i(\boldsymbol{x},t)\in\mathscr{S}, \text{such that} \\
\mathscr{S}=\{u_i:\Omega\mapsto\mathbb{R}^{n_{\mathrm{sd}}}, t\in[0,T], u_i\in H^1, u_i(t)=g_i^u(t) \text{ on } \Gamma_u\times]0,T[\} \\
\int_\Omega(\rho w_i u_{i,tt}+w_{i,j}c_{ijkl}u_{k,l})\,dv=\int_\Omega w_i f_i dv+\int_{\Gamma_t}w_i t_i^\sigma da \\
\int_\Omega w_i u_i(\boldsymbol{x},0)dv=\int_\Omega w_i u_{0i}(\boldsymbol{x})dv \\
\int_\Omega w_i u_{i,t}(\boldsymbol{x},0)dv=\int_\Omega w_i u_{0i,t}(\boldsymbol{x})dv \\
\text{holds } \forall w_i(\boldsymbol{x})\in\mathscr{V}=\{w_i:\Omega\mapsto\mathbb{R}^{n_{\mathrm{sd}}}, w_i\in H^1, w_i=0 \text{ on } \Gamma_u\}
\end{array}\right. \tag{5.66}
$$

where the weak form is written for initial conditions, in case the initial displacement or velocity is some function over the domain (i.e., not homogeneous).

Assume for the Galerkin form, $(G)=(W^h)$.

For the **Finite Element Matrix Form**, the isoparametric formulation is,

$$x_i^{h^e}(\boldsymbol{x}) = \sum_{a=1}^{n_{\text{en}}} N_a(\boldsymbol{x}) x_{i(a)}^e \tag{5.67}$$

$$u_i^{h^e}(\boldsymbol{x},t) = \sum_{a=1}^{n_{\text{en}}} N_a(\boldsymbol{x}) d_{i(a)}^e(t) = \{\boldsymbol{N}^e \cdot \boldsymbol{d}^e\}_i \tag{5.68}$$

$$u_{i,t}^{h^e}(\boldsymbol{x},t) = \sum_{a=1}^{n_{\text{en}}} N_a(\boldsymbol{x}) \dot{d}_{i(a)}^e(t) = \left\{\boldsymbol{N}^e \cdot \dot{\boldsymbol{d}}^e\right\}_i \tag{5.69}$$

$$u_{i,tt}^{h^e}(\boldsymbol{x},t) = \sum_{a=1}^{n_{\text{en}}} N_a(\boldsymbol{x}) \ddot{d}_{i(a)}^e(t) = \left\{\boldsymbol{N}^e \cdot \ddot{\boldsymbol{d}}^e\right\}_i \tag{5.70}$$

$$w_i^{h^e}(\boldsymbol{x}) = \sum_{a=1}^{n_{\text{en}}} N_a(\boldsymbol{x}) c_{i(a)}^e = \{\boldsymbol{N}^e \cdot \boldsymbol{c}^e\}_i \tag{5.71}$$

Then, the element form is,

$$\mathop{\mathbf{A}}_{e=1}^{n_{\text{el}}} (\boldsymbol{c}^e)^T \cdot \left[\underbrace{\left(\int_{\Omega^e} \rho (\boldsymbol{N}^e)^T \cdot \boldsymbol{N}^e dv\right)}_{\boldsymbol{m}^e} \cdot \ddot{\boldsymbol{d}}^e + \underbrace{\left(\int_{\Omega^e} (\boldsymbol{B}^e)^T \cdot \boldsymbol{D} \cdot \boldsymbol{B}^e dv\right)}_{\boldsymbol{k}^e} \cdot \boldsymbol{d}^e \right.$$

$$\left. = \underbrace{\int_{\Omega^e} (\boldsymbol{N}^e)^T \cdot \boldsymbol{f} dv}_{\boldsymbol{f}_f^e} + \underbrace{\int_{\Gamma_t^e} (\boldsymbol{N}^e)^T \cdot \boldsymbol{t}^\sigma da}_{\boldsymbol{f}_t^e} \right] \tag{5.72}$$

and

$$\mathop{\mathbf{A}}_{e=1}^{n_{\text{el}}} (\boldsymbol{c}^e)^T \cdot \left[\underbrace{\left(\int_{\Omega^e} (\boldsymbol{N}^e)^T \cdot \boldsymbol{N}^e dv\right)}_{\boldsymbol{m}^e/\rho} \cdot \boldsymbol{d}^e(0) = \underbrace{\left(\int_{\Omega^e} (\boldsymbol{N}^e)^T \cdot \boldsymbol{u}_0(\boldsymbol{x}) dv\right)}_{\boldsymbol{u}_0^e} \right] \tag{5.73}$$

$$\mathop{\mathbf{A}}_{e=1}^{n_{\text{el}}} (\boldsymbol{c}^e)^T \cdot \left[\underbrace{\left(\int_{\Omega^e} (\boldsymbol{N}^e)^T \cdot \boldsymbol{N}^e dv\right)}_{\boldsymbol{m}^e/\rho} \cdot \dot{\boldsymbol{d}}^e(0) = \underbrace{\left(\int_{\Omega^e} (\boldsymbol{N}^e)^T \cdot \dot{\boldsymbol{u}}_0(\boldsymbol{x}) dv\right)}_{\dot{\boldsymbol{u}}_0^e} \right] \tag{5.74}$$

and

$$\mathop{\mathbf{A}}_{e=1}^{n_{\text{el}}} (\boldsymbol{c}^e)^T \cdot \left[\boldsymbol{m}^e \cdot \ddot{\boldsymbol{d}}^e + \boldsymbol{k}^e \cdot \boldsymbol{d}^e = \boldsymbol{f}_f^e + \boldsymbol{f}_t^e \right] \tag{5.75}$$

$$\mathop{\mathsf{A}}_{e=1}^{n_{\mathrm{el}}} (\boldsymbol{c}^e)^T \cdot \left[\frac{1}{\rho}\boldsymbol{m}^e \cdot \boldsymbol{d}^e(0) = \boldsymbol{u}_0^e\right] \tag{5.76}$$

$$\mathop{\mathsf{A}}_{e=1}^{n_{\mathrm{el}}} (\boldsymbol{c}^e)^T \cdot \left[\frac{1}{\rho}\boldsymbol{m}^e \cdot \dot{\boldsymbol{d}}^e(0) = \dot{\boldsymbol{u}}_0^e\right] \tag{5.77}$$

After element assembly, and accounting for essential BCs, we have,

$$\boldsymbol{M} \cdot \ddot{\boldsymbol{d}} + \boldsymbol{K} \cdot \boldsymbol{d} = \boldsymbol{F}_f + \boldsymbol{F}_t + \boldsymbol{F}_g \tag{5.78}$$

$$\boldsymbol{d}(0) = \rho \boldsymbol{M}^{-1} \cdot \boldsymbol{U}_0 \tag{5.79}$$

$$\dot{\boldsymbol{d}}(0) = \rho \boldsymbol{M}^{-1} \cdot \dot{\boldsymbol{U}}_0 \tag{5.80}$$

Assume Rayleigh (proportional) damping as $\boldsymbol{C} = a\boldsymbol{M} + b\boldsymbol{K}$, such that after assembly,

$$\boldsymbol{M} \cdot \ddot{\boldsymbol{d}} + \boldsymbol{C} \cdot \dot{\boldsymbol{d}} + \boldsymbol{K} \cdot \boldsymbol{d} = \boldsymbol{F}_f + \boldsymbol{F}_t + \boldsymbol{F}_g \tag{5.81}$$

Use the Newmark family of time integration schemes to integrate the hyperbolic ODE, as we did before for the 1D elastodynamic bar.

This page intentionally left blank.

Bibliography

I. Babuska and J.T. Oden. Verification and validation in computational engineering and science: basic concepts. *Comp. Meth. App. Mech. Engr.*, 193:4057–66, 2004.

T. J. R. Hughes. *The Finite Element Method*. Prentice-Hall: New Jersey, 1987.

C. Lanczos. *The Variational Principles of Mechanics*. Dover Pub. Inc., New York, 4 edition, 1949.

J. Lubliner. *Plasticity Theory*. Macmillan Pub., NY, 1990.

W.L. Oberkampf, T.G. Trucano, and C. Hirsch. Verification, validation, and predictive capability in computational engineering and physics. *App. Mech. Rev.*, 57:345–84, 2004.

P.M. Pinsky. Finite Element Structural Analysis. unpublished course notes, Stanford University, 2001.

L.E. Schwer. An overview of the PTC 60/V and V 10: Guide for verification and validation in computational solid mechanics. *Engineering with Computers*, 23(4):245 – 252, 2007.

I. Vardoulakis and M. Goldschieder. Biaxial apparatus for testing shear bands in soils. In *Soil Mechanics and Foundation Engineering*, pages 819–824. A.A. Balkema, 1981.

I. Vardoulakis, M. Goldschieder, and G. Gudehus. Formation of shear bands in sand bodies as a bifurcation problem. *Int. J. Numer. Anal. Methods Geomech.*, 2:99–128, 1978.

K. Washizu. *Variational Methods in Elasticity and Plasticity*. Pergamon Press, 3 edition, 1982.